Edited by Charlotte Bengtsson, Carl-Johan Johansson

GIROD – Glued in Rods for Timber Structures

SMT4-CT97-2199

Postal address:
Box 857,
SE-501 15 BORÅS, Sweden
Telephone: +46 33 16 50 00
Telex: 36252 Testing S
Telefax: +46 33 13 55 02
E-mail: info@sp.se

Contents

Preface

The GIROD project was launched as a pre-normative research project in the beginning of 1998 with a three year schedule. The financial supports from the European Commission, SMT4-CT97-2199, and the Swedish Agency for Innovation Systems (VINNOVA) are gratefully acknowledged.

The project has been carried out in collaboration between five research partners. Swedish National Testing and Research Institute (SP, coordinator), University of Lund (Sweden), TRADA Technology Ltd (UK), University of Karlsruhe (Germany) and FMPA in Stuttgart (Germany). The different workpackages with responsible partners are given below.

- WP 1 – Development of a calculation model, University of Lund (Per-Johan Gustafsson and Erik Serrano).
- WP 2 – Test Methods for adhesives, SP (Carl-Johan Johansson and Charlotte Bengtsson (she replaced Martin Kemmsies 1999)).
- WP 3 - Effect of distance between rods and between rods and timber edge on the axial strength, University of Karlsruhe (Hans Blass, Rainer Görlacher and Bernd Laskewitz).
- WP 4 – Effect of moisture conditions, FMPA (Simon Aicher).
- WP 5 – Duration of load test on full-sized glued-in rod specimens, FMPA (Simon Aicher).
- WP 6 – Effect of fatigue, TRADA (Rob Bainbridge and Christopher Mettem).
- WP 7 – Test methods for production control, SP (Carl-Johan Johansson and Charlotte Bengtsson).
- WP 8 – Draft design rules for Eurocode 5, TRADA (Rob Bainbridge and Christopher Mettem).
- WP 9 – Project coordination, SP (Carl-Johan Johansson).

In this report, the chapter for each WP was written by the responsible partner. Introductory chapters and conclusions were written at SP.

Valuable help from the industry were given to the project from following industries:
Moelven Töreboda Limträ AB, Sweden
Casco Products AB, Sweden
Studiengemeinschaft Holzleimbau, Germany
UK Glued Laminated Timber Association, UK
Klebchemie M.G. Becker GmbH & Co., Germany
Wevo-Chemie Becker GmbH & Co., Germany

Charlotte Bengtsson and Carl-Johan Johansson
Borås, August 2002

Summary

Background

Glued-in rods have been used for a number of years in several of the EU Member States which are active in timber engineering. They are an economically, architecturally and industrially attractive means of transferring forces within a structure, and of providing local reinforcement to critical zones of timber members. They also provide an important technology for the repair and upgrading of historically important timber structures which exist throughout Europe. Not withstanding their importance, internationally acknowledged design rules for glued-in rods do not exist. The lack of standards and design rules within the field of glued-in rods lead to this project being initiated.

Objectives

The objective of this project was to provide the information required to prepare standards and design rules that will allow an increased, more advanced and more reliable use of glued-in rods in timber structures.

Work programme

The project included following three parts:

1. Development of a calculation model. The work included effects of rod spacing and edge distances, effects of varying temperature and moisture conditions, effect of fatigue and drafting of design rules for Eurocode 5. (Input to CEN/TC250/SC5).
2. Development of test methods for assessment of adhesives. (Input to CEN/TC193/SC1).
3. Development of production control methods. (Input to CEN/TC124).

The project included comprehensive experimental studies and theoretical analysis/modelling. Three different adhesive types were studied.

Results and achievements

1. Design rules for Eurocode 5. A calculation model based on Volkersen theory and fracture mechanics gave good prediction of the pullout strength for adhesives that bond to the rod such as polyurethane (PUR) and epoxy (EP). It was proposed to CEN/TC250/SC5 to determine the parameters in the design formula from EP and PUR data obtained within this project. Proposals for suitable distances between rods and edge distances were made. The effect of moisture depends on the adhesive type and must be handled by correction factors in EC 5 or by requirements on the adhesives. Three different alternatives were given for handling the difficult issue with duration of load effects in design rules for glued-in rods. It was demonstrated that fatigue may limit the use of glued-in rods in certain applications.
2. Two test methods for adhesives for glued-in rods were developed. One, which is capable of ranking adhesives from a durability point of view and one which determines the creep-rupture behaviour of small glued-in rod specimens.
3. A proof-loading test method for production control of glued-in rod connections was developed. The method was shown to be capable of detecting production defects that may occur.

1. Description of the project

1.1 Objectives

The objective of this project is to provide the information required to prepare standards that will allow an increased, more advanced and more reliable use of glued-in rods in timber structures. The steps involved in reaching this objective are as follows:

1. Perform theoretical and experimental work leading to a calculation model for axially loaded glued-in rods based on the adhesive bond properties as well as the wood and rod material properties. This must take into account the effect of varying climatic and loading conditions as well as fatigue. This step will give information required by CEN/TC250/SC5 in the preparation of Eurocode 5 - Design of Timber Structures.

2. Develop test methods for the evaluation of adhesives for glued-in rods with respect to strength, durability, creep and creep rupture behaviour under different climatic conditions. This will support the work of CEN/TC193/SC1.

3. Derive test methods for the production control of structural glued-in rod connections. This will support the work of CEN/TC124.

The project structure is summarized below:

1. Development of calculation model
- Theoretical model based on non-linear fracture mechanics
- Testing of adhesive bond properties
- Verification of the model by testing of full sized glued-in rods

Effect of rod spacing and end and edge distances. Under what conditions is the calculation model valid?

Effect of varying temperature and moisture conditions.
- Calculation and testing of the effect of moisture conditions
- Duration of load tests on full sized glued-in rods

To what extent are corrections of the calculation model necessary?

Drafting **design rules for Eurocode 5**

Effect of fatigue. In what situations does it have to be considered?

2. Development of test methods for assessment of adhesives
- Durability of adhesives
- Creep and creep rupture

3. Development of production control test methods
- Proof-loading method
- Destructive test

1.2 Background

Glued-in rods have been used for a number of years in several of the EU Member States which are active in timber engineering. They are an economically, architecturally and industrially attractive means of transferring forces within a structure, and of providing local reinforcement to critical zones of timber members. They also provide an important technology for the repair and upgrading of historically important timber structures which exist throughout Europe.

Not withstanding their importance, internationally acknowledged design rules for glued-in rods do not exist. A proposal was presented to CIB W18 (International Council for Building

Research Studies and Documentation - Working Commission W18 - Timber Structures) at a meeting in Parksville, Vancouver Island, Canada, 1988. This proposal is the basis of STEP lecture C14 (Structural Timber Education Programme, Johansson 1995). STEP was published in 1995 and it is closely linked with Eurocode 5. The design rules given here are, however, limited to steel rods and to two types of adhesives, one brittle and one ductile.

Work presented at the CIB meeting in Copenhagen 1995, shows that the axial strength of glued-in rods depends, in addition to the glued-in length, upon the adhesive bond properties (shear strength and fracture energy), as well as the modulus of elasticity of the wood and of the rod material. This implies that the design rules proposed to CIB W18 do not necessarily apply to combinations other than steel rods and the two adhesive types. If the wood and the rod material respond differently to temperature and moisture changes, which is certainly the case with steel rods, this is likely to cause in-service shear stress changes in the adhesive bond, as has been demonstrated in a government funded research project in Germany. Research in Germany also indicates that the minimum distances between rods in the CIB proposal should be reconsidered.

Advanced use of glued-in rods in, for instance, timber bridges, requires that considerable temperature and moisture changes must be accommodated for satisfactory performance. Consequently if tests show that this influence is not negligible, then it will have to be provided for in design rules. Experience in the use of glued-in rods in rotor blades of wind turbines in Denmark shows that fatigue may be a problem. For glued-in rods in certain designs of timber bridges therefore, fatigue may also be a significant issue, thus requiring design rules.

Adhesives for glued-in rods, in addition to good durability, must have acceptable creep and creep rupture properties. Common adhesive types used with glued-in rods are phenol-resorcinol formaldehyde (PRF), two-component polyurethane (2 comp. PUR) and epoxy systems. The existing standards for adhesives for load bearing timber structures EN301 (Requirements) and EN 302 (Test methods), however, cover only the phenol-resorcinol type adhesives, which have well established creep and creep rupture properties and extremely good durability. It is a considerable problem that a corresponding system of standards does not exist for other adhesive types. It is probable that the EN 301/EN 302 system may continue to be used, but methods and requirements regarding durability and creep rupture must be added for adhesives other than phenol-resorcinol.

Systems for production control only exist to a limited extent, and are mainly aimed at ensuring that sufficient adhesive is applied. However, further controls are required. The finished product, including the glued-in rods after hardening of the adhesive bond, must be tested. Destructive testing is normally not possible. Non-destructive methods are unlikely to be an industrially viable alternative at present. Experience from the Swedish glued laminated timber industry indicates that proof-loading may be a solution.

This project concerns the generic development of standardisation related to concealed connections within timber structures. The key innovation is that glued-in rods of steel or other high-strength materials are used to replace technically disadvantageous external steel plates and brackets, which require attachment using separate, mechanically-driven fasteners.

In the new technology, the bonded-in fixings are completely concealed within the connection. This provides major advantages for the design team and for the end-user. Key amongst these

are that the concealment provides optimal aesthetic quality, producing structures of the best possible appearance. This is in keeping with the strong tactile and "warmth" appeal of the expressed glulam (glued laminated timber) or LVL (Laminated Veneer Lumber) frame itself, an aspect of great importance to architects and clients.

Glued-in rod connections also generate high-strength, rigid and structurally efficient nodes. The technology is capable of rapid and accurate fabrication, with equipment which is readily available to timber structure manufacturers. Factory fabricated, and site assembled versions of bonded rod connections are possible, answering the need for simple, accurate and waste-free construction procedures. Further advantages of concealed glued-in connections include excellent fire resistance, and the elimination of wood-related problems such as splitting due to stresses perpendicular to the grain.

2. Description of the role of different partners

The project has been carried out by a consortium consisting of the following 11 partners. Partners 1 to 5 are Contractors, partners 6 to 11 are Associated Contractors:

Partner 1:   Swedish National Testing and Research Institute (SP), from Sweden, is GIROD's coordinator and responsible for WP 2, WP 7 and WP 9.

Partner 2:   University of Lund (ULUND), from Sweden, is the responsible partner for WP 1, as well as participating in WP 4 and WP 5.

Partner 3:   Forschungs- und Materialprüfungsanstalt Baden-Württemberg (FMPA), from Germany, is responsible for WP 4 and WP 5, and participates in WP 1 as well.

Partner 4:   TRADA Technology Limited (TTL), from the UK, is responsible for WP 6 and WP 8, as well as participating in WP 4 and WP 5.

Partner 5:   Universität Karlsruhe (UKLIB), from Germany, is responsible for WP 3.

Partner 6:   Moelven Töreboda Limträ AB (MOELVEN), from Sweden, is an associated partner in WP 1, WP 4, WP 5 and WP 7. Moelven produced the major part of the full sized glued-in rod specimens containing glued laminated timber to be used in WP 1, WP 4, WP 5 and WP 7.

Partner 7:   Casco Products AB (CASCO), from Sweden, is an associated partner in WP 2 and WP 7. Casco supplied adhesive for some of the specimens in WP1, WP 2 and WP 7.

Partner 8:   Studiengemeinschaft Holzleimbau e.V. (HOLZLEIMBAU), from Germany, is an associated partner in WP 4 and WP 5. Holzleimbau and it's members provided glulam specimen material for WP 4 and WP 5, expert advice on production of glued-in rods and financial subsidies for the experimental work of partners 3 and 5.

Partner 9:   UK Glued laminated Timber Association (GLTA), from the UK, is an associated partner in WP 4, WP 5, WP 6 and WP 8. Supplier of glulam specimens in WP 4, WP 5, WP 6 and WP 8.

Partner 10:   Klebchemie M.G. Becker GmbH & Co. KG (KLEIBERIT), from Germany, is an associated partner in WP 1, WP 2 and WP 5. Supplier of adhesives in the work packages WP1, WP2 and WP5.

Partner 11:   Wevo-Chemie GmbH & Co. KG (WEVO), from Germany, is an associated partner in WP 1, WP 2 and WP 5. Supplier of adhesives in work packages WP 1, WP 2 and WP 5.

3. Description of the work carried out in the different WP:s

Each partner responsible for a WP has written the description of the work carried out. The material has been edited at SP (coordinator). The summarizing conclusions are written at SP.

3.1 WP 1 – Development of a calculation model

The objective of Work Package 1, WP 1, was to establish a calculation model for the basic pull-out strength, that can be used as a basis for establishing design rules for glued-in rods and for creating a better understanding of the mechanical behaviour of glued-in rods. WP 1 was organised in four parts:

- WP 1.1 Theoretical work on models for stress and strength analysis
- WP 1.2 Bond line tests of mechanical properties
- WP 1.3 Full scale joint test for calibration and verification
- WP 1.4 Verification of model and design equation proposal

3.1.1 WP 1.1 – Theoretical work

Strength calculation models can be purely empirical or rational. The presented work has focused on rational, theoretical models. In such models a strength equation or calculation algorithm is developed by means of fundamentals such as equilibrium, geometrical compatibility of deformations and some mathematical descriptions of the performance of the materials. The free parameters may be identified as parameters that define geometry, loading conditions and material properties. The material parameters may be determined by material property tests or by fitting of theoretical strength results to experimental strength data. Five models were dealt with. Models 1 and 2 are both special cases of model 3, which in turn is a special case of model 4. Model 5 is a non-linear finite element (FE) model. Models 1-4 are analytical.

Bar shear lag fracture model (Model 3)

This model is a combination of the Volkersen model and fracture mechanics (Gustafsson 1987). The rod and the wood are assumed to perform as linear elastic bars and the bond layer as an elastic shear lag layer. The governing differential equation for the bar shear lag analysis is:

$$\tau_3'' - \omega^2 \tau_3 = -QG_3/(t_3E_2), \quad \omega^2 = (G_3/t_3)(2\pi r)(1/(E_2A_2) + 1/(E_1A_1)) \tag{3.1.1}$$

where

τ_3 is the bond line shear stress, E_2A_2 and E_1A_1 the normal bar stiffness of the wood and rod, respectively, $2r=d$ the rod diameter, and G_3 and t_3 the adhesive shear stiffness and the bond line thickness, respetively. Q is a volume load acting on the wood. The two constants in the general solution of this equation are determined from the loads at the ends of the joint parts.

Direct application of the linear elastic bar shear lag theory for stress analysis is not of very great interest for wood adhesive joints since the elastic shear stiffness of wood and glue is of a similar magnitude. The theory is however of interest in relation to calculation of joint strength. Success of joint strength analysis is by correct representation of the local failure stress of the bond line and the fracture energy of the bond line. In conventional stress based joint strength analysis only the local failure stress of the bond line is represented. The bond line fracture energy, G_f, at linearised representation of the shear stress to slip performance, $\tau(\delta)$, is:

$$G_f = (1/2)\,\tau_f\,\delta_f = (1/2)\,\tau_f\,\tau_f/(G_3/t_3) \tag{3.1.2}$$

where

τ_f is the local shear strength of the bond layer and δ_f the corresponding shear slip. G_f and τ_f

are regarded as the basic bond parameters for the analysis of the pull-out load carrying capacity of the glued-in rods. In terms of these parameters the shear stiffness is:

$(G_3/t_3) = \tau_f^2/(2G_f)$ (3.1.3)

Having calculated the shear stress distribution, the joint pull-out strength is obtained by the criterion

$\tau_{max} = \tau_f$ (3.1.4)

or by $G = G_f$, due to the substitution (3.1.3) giving the same joint strength prediction.

Explicit expressions for the shear stress distribution and the pull-out strength was derived for five loading cases: "pull-pull", "pull-compression", "pull of rod", "pull of wood" and "pull distributed". Cases 3 and 4 may be used for analysis of eigen-loading due temperature and moisture induced strains. Case 5 in combination with other cases can be useful for approximate analysis of rods glued-in perpendicular to a beam. In Figure 3.1.1 failure loads are shown for: E_1=200000 N/mm^2, E_2=10000 N/mm^2, G_f=2 Nmm/mm^2, τ_f=8 N/mm^2, r=8 mm, A_1=200 mm^2 and A_2=10000 mm^2. The values of G_f and τ_f correspond to G_3=8 N/mm^2 if t_3=0.5 mm.

Pull-out strength according to ideal plastic model (Model 1)

In this simple model it is assumed that the adhesive layer has the ability to perform in an ideal plastic manner and carry a constant shear stress, τ_f, at any magnitude of the shear deformation of the bond layer. This means that the shear stress is constant along the rod, for load cases 1 (pull-pull), 2 (pull-compression) and 5 (pull distributed) giving:

$P_f/(2\pi r l \tau_f) = 1.0$ (3.1.5)

For load cases 3 (pull of the rod) and 4 (pull of the wood) no failure is predicted.

Pull-out strength according to linear elastic fracture mechanics (Model 2)

In this model the joint failure and material properties are assumed in accordance with linear elastic fracture mechanics: failure is assumed to take place as crack propagation along the rod, the fracture process region is small, the fracture energy is $G_c = G_f$, the shear strength τ_f is infinite and the deformation capacity, $\tau_f/(G_3/t_3)$, of the bond layer is zero. The corresponding strength equations are found by letting the dimensionless number ωl approach infinity.

Timoshenko beam shear lag fracture model (Model 4)

The shear strains in the wood part of the axi-symmetric lap joint are in this model taken into account in a way similar to the shear strain consideration in the Timoshenko theory for beams. This results in a 4:th order differential equation:

$\tau_3'''' + S\tau_3'' + T\tau_3 = 0$ (3.1.6)

where the coefficients S and T can be determined from geometry and material parameters that define the joint. The four integration constants in the general solution of the equation can be determined from the normal forces, i.e. the load, and the bending moments or the shear forces acting on the wood or from the corresponding kinematical conditions. Development of the boundary condition equations and calculation of the constants is much more laborious than for the above models 1, 2 and 3.

Several stress and strength analyses were made, including studies of the influence of boundary conditions and the wood shear stiffness. Model 4 calculations give information also about shear strain in the wood and normal stress acting perpendicular to the bound line.
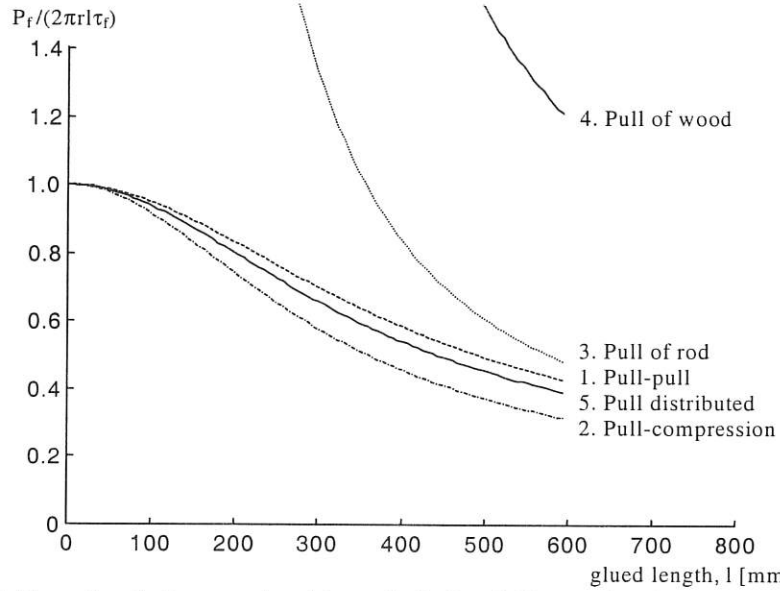
Figure 3.1.1 Failure load, P_f, vs. glued length, l, for different loads according to model 3.

Finite element analysis (Model 5)

In the FE-simulations the 3D geometry of glued-in rod joints were taken into account as well as non-linear gradual fracture softening, or damage, of the bond layer. Five parameter studies were made:

I.   Analysis of the pull-out strength with regard to the influence of various geometry and material property parameters. The loading case "pull-pull" was studied.

II.   Analysis of the stresses in the wood and the effect on pull-out strength of varying stiffness properties within the wood.

III. Analysis of the pull-out strength at loading "pull-compression" versus the strength at "pull-pull". The effect of support arrangements was studied.

IV.   Analysis of the pull-out strength for different load-to-grain angles. Both pull-pull and three-point bending loading was examined.

V.   Analysis of rods glued-in at various grain to rod angles

The wood was treated as an orthotropic linear elastic continuum, the steel as a linear elastic continuum and the bond layer as a layer in which the components of stress are non-linear functions of the relative shear and normal displacements across the layer. The bond layer model used is a 3D extension of the model developed by Wernersson 1994. Four parameters define the properties of the bond layer: the strength and fracture energy for pure shear and for pure tension, denoted τ_f, $G_{f,s}$, σ_f and $G_{f,n}$. An example of a typical finite element subdivision used for the calculations is shown in Figure 3.1.2.

In particular study I was comprehensive, comprising non-linear 3D analysis of 22 joints. The studies I-V were all successful, showing how the variables investigated are predicted to affect the fracture performance and the load bearing capacity of a joint.
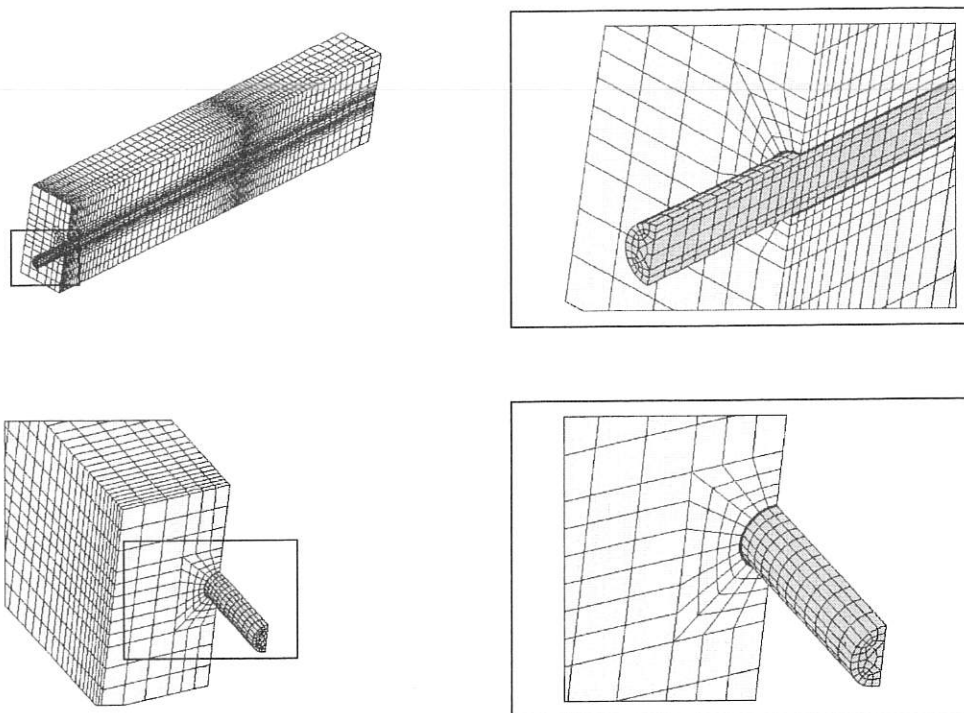
Figure 3.1.2 Finite element subdivision used in many of the simulations.

3.1.2 WP 1.2 – Bond line tests

In WP 1.2 tests were made on small specimens to determine the shear stress versus shear slip performance of bond lines. The complete curves, including the descending damage branch of the stress-slip relation, were tested. Such testing is difficult and there is no tradition on how to make the testing. Having recorded the complete curve, the local shear strength and the fracture energy parameters are also known. Two pre-test series were made to determine a good testing method, then a main set of test series were made.

All samples were prepared using wood pieces cut from glulam beams taken from the same shipment as all of the glulam used in GIROD. The glulam beams were stored in standard climate 20°C, 65%RH. The gluing and curing as well as the storing of the finished specimens was also done in this climate. All specimens were cured for at least 7 days prior to testing. For the main series short rods and wood pieces as shown in Figure 3.1.3 were used. The test specimens were placed on a self-aligning plate which in turn was fitted into the lower hydraulic grips of the testing machine. The self-aligning plate was used in order to achieve a more uniform stress distribution at the contact surface. The length of the bond line was only 8 mm, partly to achieve a uniform stress distribution along the bond line. The initial speed of the loading was set to 0.003 mm/s (cross-head speed). After a 40% load drop after peak load the loading speed was gradually increased so that each test was completed after 7-10 minutes. The final speed was set to be 0.03 mm/s.

In addition to the original plan, including five nominally equal tests for every material combination, it was decided to investigate the characteristics at unloading after peak stress for one specimen in each test series. Here, unloading means decreasing deformation. The unloading was set to take place after a 20% load drop.

14
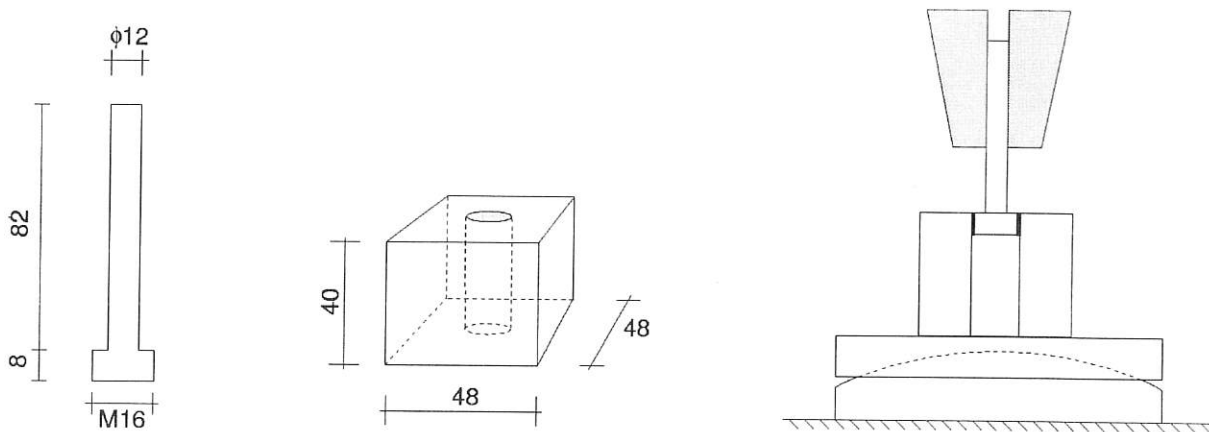
Figure 3.1.3 Specimens and set-up used in the main test series.

For each of the 10 series of nominally equal materials and grain orientation, 5 replicates were performed. In addition, for each material combination, one test was performed with unloading of the specimen. The most important test results are shown in Figures 3.1.4 and 3.1.5. Test series with two classes of wood, C24 and C35, showed no significant difference. The failure modes obtained in the main test series are of three types, each typical for one type of adhesive:

1. Failure in the adhesive at the threading of the bolt. This failure mode was obtained only for the PRF adhesive at about 75-100% of the fracture area. The remaining fracture area showed a wood interface failure.

2. Failure in the adhesive close to the wood. This failure was obtained only for the PUR specimens at 100% of the fracture area.

3. Failure in the wood in the vicinity of the adhesive. Note that this wood failure is not characterised by a large plug being pushed out, but rather by a wood interface failure due to a weak boundary layer. This failure type was obtained only for the EPX specimens. For the 0° load to grain angle tests there was a fairly large amount of wood fibres visible on the adhesive after failure. For the other load to grain angles the fracture surface was almost free from fibres.
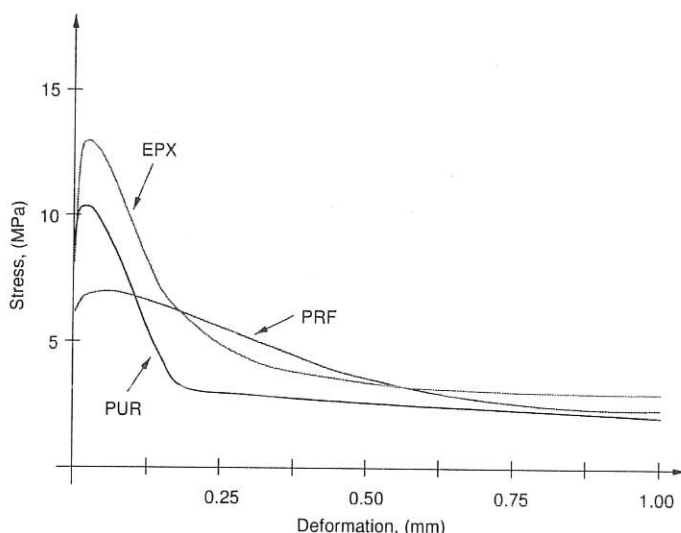
Figure 3.1.4 Mean stress-displacement curves showing influence of adhesive type.

15
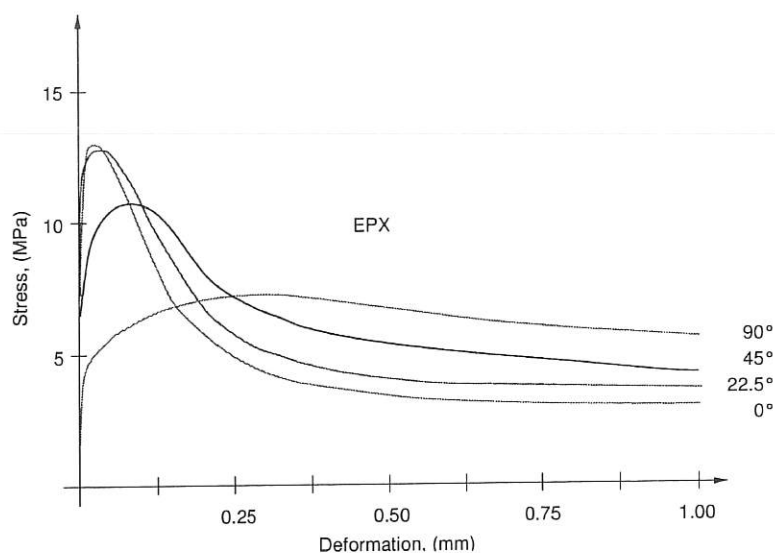
Figure.3.1.5 Mean stress-displacement curves showing influence of grain orientation.

3.1.3 WP 1.3 – Full scale joint tests

WP 1.3 concerns short term ramp loading tests of glued-in rods conditioned at 65%RH. Some tests of WP 1.3 are common with reference tests of WP 4 and WP 5. Many of the tests results of WP 7, obtained by partner SP, are used together with the test results of WP 1.3 for verification and calibration purposes. Project partner FMPA has co-ordinated the work of WP 1.3 and a detailed reporting of WP 1.3 is provided by partner FMPA as a Technical Report (Aicher 2001a), including i.a. recorded load-displacement curves. Partner FMPA has, moreover, recently carried out a large number of additional tests outside the GIROD project, but very closely related to the GIROD tests (Aicher 2001b).

The dimensions of the glulam specimens are indicated in Table 3.1.1, where l_g is the glued-in length. The centric tensile load applied to the rod was for the specimens loaded parallel to the grain counteracted by a tensile loading of a rod glued-into the opposite end of the specimen. The counteracting rod had a glued-in length of 1.2 l_g and its diameter was 1.5 times the diameter of the tested rod. The rods were glued in the centre of the specimens.

In Table 3.1.2 the characteristics of the specimens are given together with mean and standard deviation of the pull-out strengths. Please note that the nominal shear strengths are calculated as $P_f/(\pi d l_g)$. They could alternatively be calculated for a cylinder with the diameter of the hole, i.e. for the diameter d+1mm. The number of tests in each series was 7. Table 3.1.2 shows for the 0 degree specimens also the density of the wood in the lamella, or in the two lamella, in which the rod was placed. The density was determined for a piece of length 1.2 l_g, cut after the ramp load testing from the middle of the specimen. In case of a finger joint in the test piece, its length was reduced so that the joint became excluded. The mean moisture content was 11.7% and the standard deviation of the moisture content was 0.7%.

16

Table 3.1.1 Dimensions of glulam.

Specimens	Dimensions of glulam, b*h*l, mm³	Number of lamella	Thickness of lamella, mm
φ= 8mm, rod angel 0^0	70*70*3.6lg	2	35+35
φ= 16mm, rod angel 0^0	120*120*3.6lg	3	37.5+45+37.5
φ= 30mm, rod angel 0^0	210*210*3.6lg	5	37.5+3*45+37.5
Rod to grain angle > 0^0	120*450*2400	10	10*45

Table 3.1.2 Results of WP 1.3. Pull-out strength test results obtained at ramp loading of specimens conditioned at 65%RH.

Series	Partner that did the testing	d mm	l_g mm	Glue	Wood	Density ρ_{12} kg/m³	Rod	Angle	P_f kN	$\tau_{bond}=P_f/(\pi d l_g)$, N/mm² Average	COV %
2.1/r	SP	16	320	PRF	C35	-	ste	22.5	94.5±7.8	5.88	8.3
2.2/r	TTL	16	320	PRF	C35	-	ste	45	103.6±7.3	6.44	7.0
2.3/r	TTL	16	320	PRF	C35	-	ste	90	103.4±5.1	6.43	4.9
2.4/r	TTL	16	160	PRF	C35	-	ste	90	50.9±6.3	6.33	12.4
2.5/r	FMPA	8	80	PRF	C35	483±27	ste	0	12.7±1.7	6.32	13.4
2.6/r	FMPA	8	160	PRF	C35	447±12	ste	0	31.3±1.6	7.78	5.1
2.7/r	FMPA	8	320	PRF	C35	476±22	ste	0	40.5±1.5	5.04	3.7
2.8/r	FMPA	16	80	PRF	C35	451±13	ste	0	24.1±2.4	5.99	10.0
2.9/r	FMPA	16	160	PRF	C35	468±37	ste	0	55.3±2.8	6.88	5.1
2.10/r	FMPA	16	320	PRF	C35	470±17	ste	0	101.7±5.1	6.32	5.0
2.11/r	FMPA	16	640	PRF	C35	473±59	ste	0	144.1±10.9	4.48	7.6
2.12/r	FMPA	30	150	PRF	C35	446±25	ste	0	60.5±4.6	4.28	7.6
2.13/r	FMPA	30	300	PRF	C35	451±56	ste	0	142.3±20.2	5.03	14.2
2.14/r	FMPA	30	600	PRF	C35	427±52	ste	0	280.4±17.1	4.96	6.1
2.15/r	FMPA	16	320	PUR	C35	511±41	ste	0	92.7±5.8	5.76	6.3
2.16/r	FMPA	16	320	EP	C35	517±40	ste	0	103.6±11.7	6.44	11.3
2.17/r	FMPA	16	320	PRF	C24	487±28	ste	0	102.3±8.2	6.36	8.0
2.18/r	FMPA	16	320	PUR	C24	492±34	ste	0	93.3±22.5	5.80	24.1
2.19/r	FMPA	16	320	EP	C24	520±28	ste	0	96.6±9.8	6.01	10.1
2.20/r	TTL	16	160	PUR	C35	-	gla	0	-		
2.21/r	TTL	16	160	PUR	C35	-	ste	90	63.9±2.9	7.95	4.5
2.22/r	FMPA	16	160	PUR	C35	488±45	ste	0	68.3±6.5	8.49	9.5
2.23/r	FMPA	8	160	PUR	C35	480±23	ste	0	31.4±3.4	7.81	10.8
2.24/r	FMPA	16	160	EP	C35	437±37	ste	0	57.3±10.8	7.12	18.8
2.25/r	FMPA	8	160	EP	C35	478±21	ste	0	28.5±2.9	7.09	10.2

3.1.4 WP 1.4 – Verification analysis and a design equation
Design equation proposal
The idea before proposal of a strength design method for the basic pull-out strength at short time ramp loading at constant climate was to find a method such that:

- The method is both general and simple, preferably just one or a few explicit equations.
- The equations should have a rational theoretical and physical basis.
- The method should give reasonably accurate strength predictions, on the average and in general give predictions on the safe side.

The combined Volkersen-Fracture mechanics theory, i.e. model 3, is used as the basis. The pull-out strength is according this theory determined by the geometry of the joint and by two bond line and material property parameters. It is proposed that these two parameters are determined by testing the pull-out strength of two sets of full-scale joints with different geometry (length and/or diameter) and loaded in "pull-compression". Given the two material parameters, the equation for the "pull-compression" loading is used also for "pull-pull" and "pull-distributed". This gives a single and simple design equation, which according to theory gives "exact" predictions for the first type of loading and predictions on the safe side for the other two types of loading.

The above proposal is intended for adhesives that bonds to both substrates, i.e. also to the rod. For adhesives with no bond to the rod (i.e. the PRF tested in the GIROD-project) no equation that fulfils the above basic goals has yet been found. For such adhesives it is proposed that testing is made as for the common adhesives, but no design equation is proposed, only a design rule saying that the load bearing capacity of joints with greater or equal rod diameter, greater or equal length, and at all three types of loading may be assigned the same load bearing capacity as the tested joint.

For the loading case pull-compression:

$$\frac{P_f}{\pi d l} = \tau_f \frac{\tanh \varpi}{\varpi} \qquad \text{where} \qquad \varpi = \sqrt{\frac{l_{geo}}{l_m}} \tag{3.1.7}$$

where
l_{geo} is a length parameter defined by the geometry of the joint and the rod to wood ratio for modulus of elasticity:

$$l_{geo} = \frac{\pi d l^2}{2} \left(\frac{1}{A_r} + \frac{E_r / E_w}{A_w} \right) \tag{3.1.8}$$

and l_m is a material property length parameter, which can be expressed as:

$$l_m = \frac{E_r G_f}{\tau_f^2} \tag{3.1.9}$$

The ratio E_r/E_w can be estimated in an approximate manner. The two parameters to be determined from tests are then τ_f and l_m. (It is thus not necessary to separate l_m into E_r, G_f and τ_f, although this in general is simple since E_r in general is known).

For a square shaped cross section with a centric location of the rod A_w is taken as a^2, where a is the side length of the square. For other geometry $A_w = a^2$, where $a/2$ is the shortest distance from the center of the rod to an edge of the cross section. This shortest edge distance, $a/2$, may not be less than a distance determined in WP 3, presumably $4d_r$.

$P_f /(\pi dl)$ for arbitrary inclination, α, of the rod relative to grain may be determined by interpolation between the results for rods along grain and perpendicular to grain according to the Hankinson equation. The two material parameters must be determined for both rod to grain orientations.

Test results on the pull-out strength at pull-compression loading are presented by project partner SP (Johansson 2000). Parameters τ_f and l_m (and G_f) were determined from these test results for the three adhesives investigated by use of the method described above. This evaluation is indicated in Table 3.1.3. The tests refer to loading along the grain and the ratio E_r/E_w was therefore set equal to 18.

Table 3.1.3 Test results for determination of material property parameters τ_f and l_m.

Adhesive	d mm	l mm	a mm	l_{geo} mm	Failure load, P_f kN	$P_f /(\pi d\,l)$ N/mm^2	τ_f N/mm^2	l_m mm	G_f [1] Nmm/ mm^2
EPOXY	16	160	115	4070	62.61	7.79	10.5	3600	1.89
	16	320	115	16300	77.36	4.81			
PRF	16	160	115	4070	63.83	7.94	8.9	11000	4.15
	16	320	115	16300	98.43	6.12			
PUR	16	160	115	4070	58.98	7.33	9.7	3960	1.77
	16	320	115	16300	74.09	4.61			

1) G_f calculated from l_m with the assumption E_r=205000 N/mm^2.

The material combinations for which the material parameters were determined have been tested in several other joints, with other geometry and other type of loading. In Figures 3.1.6, 3.1.7 and 3.1.8 are the design equation compared with those other test results. Each mark in the diagrams represent mean values obtained in series with 6-10 tests in each series. The diagrams include the tests at SP of pull-pull loading and pull-compression loading. The diagram also includes the tests made at FMPA at pull-pull of joints of varying size and shape. Both the results for timber strength class C35 and the three series with timber of strength class C24 are included. For epoxy and PUR are in addition three previous series by Aicher and Herr and a test series of Deng, Moss and Buchanan, see Aicher et al. 1999.

For the PRF, the test results do not only comply with the theoretical curve, but the diagram also shows a scattered picture, indicating that $P_f/(\pi dl)$ may hardly be described as a function of l_{geo}. (l_{geo} is in most cases very close to being proportional to l^2/d.) The results found for PUR and epoxy are more appealing: the design equation gives reasonable predictions and the predictions are in most cases on the safe side.

The different results found for the three adhesives are most probably related to the different ways in which the bondlines act. For PUR and epoxy there can in the critical region be tensile stress (and very small deformation) normal to the bond area. For the PRF there may be compressive stress (and significant deformation) normal to the bond area. Above one single design proposal has been discussed. Possible modifications giving alternative, yet similar, proposals include:

- No consideration of grain to rod angle. Testing and all design made as for parallel orientation.

- No consideration of different loading conditions (pull-pull, pull-compression, pull perp. to beam). Testing and all design made as for pull-pull. Eq (3.1.7) replaced by the corresponding equation for pull-pull.

In August 2002 a simplified and in some respects improved version of the design equation discussed above was submitted to CEN/TC250/SC5 – Eurocode 5. This equation is reported in Gustafsson and Serrano 2002.
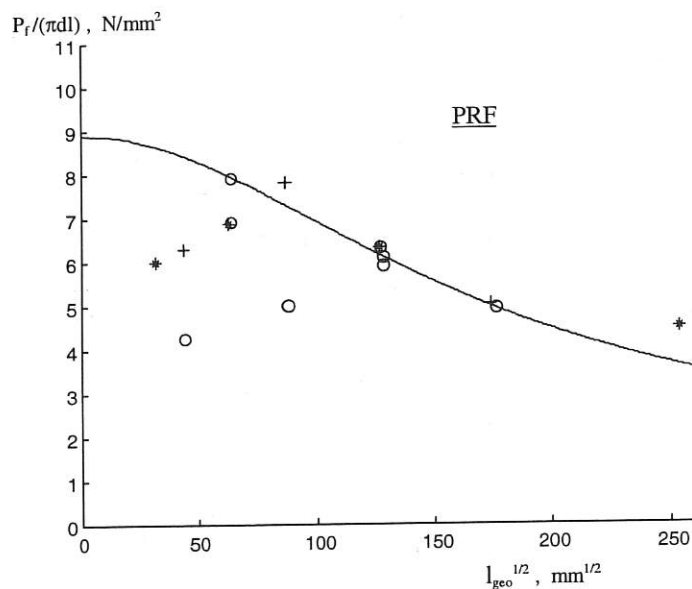
Figure 3.1.6 PRF: $P_f/(\pi dl)$, N/mm^2, versus square root of l_{geo}, $l_{geo}^{1/2}$, mm$^{1/2}$.
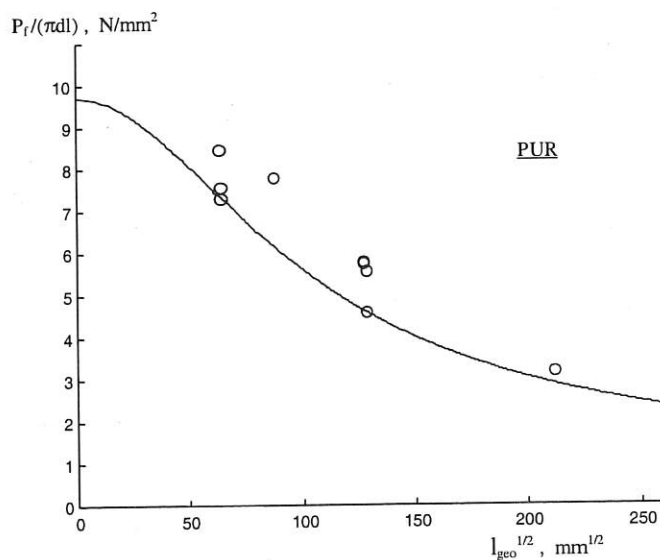
Figure 3.1.7 PUR: $P_f/(\pi dl)$, N/mm^2, versus square root of l_{geo}, $l_{geo}^{1/2}$, mm$^{1/2}$.
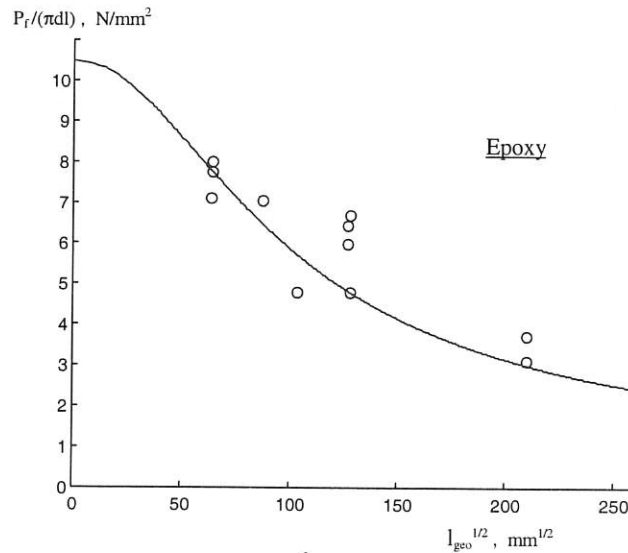
Figure 3.1.8 Epoxy: $P_f/(\pi dl)$, N/mm^2, versus square root of l_{geo}, $l_{geo}^{1/2}$, mm$^{1/2}$.

Finite element verification analyses.

The FE verification analyses comprised FE simulations of the test set-up used in the small specimen tests (WP 1.2) and the test set-up used in the full-size specimen tests (pull-pull). Analysis of the small bond line specimens showed that the assumptions made during evaluation of the bond line properties from the test recordings appear to be good: evaluation of theoretically simulated test results gave with a reasonable accuracy back the input data used for the simulations.

The tests used for verification of the full sized joint analysis by FEM are from WP 1.3 and WP 7. All test results and FE-simulations are for steel rods with d=16 mm loaded in pull-pull. The input values for the bondline constitutive model are from the small scale bond line tests. The results of the predictions of full scaled joint strength from the small bond line test results are given in Table 3.1.4. The agreement between the predictions and the test results is quite good except for the epoxy glued joint with 160 mm length.

Table 3.1.4 Simulated and tested pull-out loads.

	PRF			PUR		EPX	
Glued-in length (mm)	160	320	640	160	320	160	320
Pull-out load, test (kN)	55.3	101.7	144.1	64.4	91.0	61.6	106.3
Pull-out load, FEM (kN)	53.9	104.1	151.6	67.1	93.8	89.2	118.7

Also the load versus versus displacement curves were compared. Again the simulations showed a good correlation to the tests, although the initial elastic stiffness of the joints was overestimated. In Figure 3.1.9, finally, a comparison between FE strength predictions and predictions of the analytical models is shown.

21
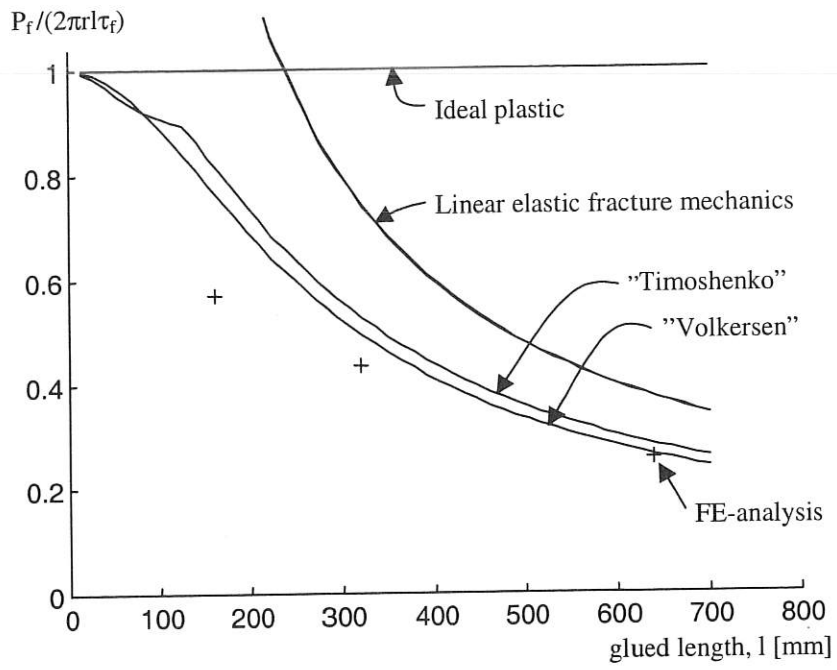
Figure 3.1.9 Comparison of different models.

3.2 WP 2 - Test methods for adhesives

WP 2 within the GIROD project deals with test methods for adhesives which are to be used in glued-in rod connections. Structural members, and the components thereof, are by their definition required to adequately resist the effects of actions applied to them throughout their design life. The objective is to develop test methods to evaluate the durability and creep-rupture properties of adhesives for glued-in rods. Details of the work carried out within this WP can be found in the Technical report (Bengtsson 2001).

3.2.1 WP 2.1 - Durability of the adhesive

A method which enables testing of the durability of wood to rod material adhesive bonds was developed using EN302-Part 1 (Determination of bond strength in longitudinal shear) as a basis. The beech tensile shear specimen was exchanged for a small glued-in rod specimen, with the geometry shown in Figure 3.2.1a. The type and duration of treatment prior to shear testing was kept the same as in EN302-Part 1. The adhesives mainly studied in the GIROD-project were epoxy (EP), phenol-resorcinol (PRF), and a two- component polyurethane (2K PUR). Only the treatments A4 and A5 of EN301-Part 1 were used. Comparisons were made with EN302-Part 1 with pure beech specimens, so as to allow the requirements in EN301 to be applicable to glued-in rods. The rod material was steel and glass fibre, respectively.

3.2.2 Results WP 2.1

Test procedure

Instead of the wood to wood tensile shear specimens in EN 302-1, small pieces of threaded steel rods bonded into beech blocks were used. Initially, 240 specimens with different rod diameters and different beech wood thicknesses were tested. Based on these results, it was decided to perform further tests by using 16 mm threaded rods bonded into 20 mm thick wooden blocks with a cross section of 40 x 40 mm, see Figure 3.2.1 a. The hole diameter was 17 mm. This shaping of the test specimens was chosen to simplify the manufacture of the specimens and for making it relatively easy to centre the rod into the beech wood. Also the test set-up was modified for the further tests. A compression test set-up was designed instead of tension tests (according to EN 302-1), see Figure 3.2.1 b.

The specimens were treated according to A4 (6 hours in boiling water, 2 hours in 20°C water, then testing in the wet state) and A5 in EN 302-1 (6 hours in boiling water, 2 hours in 20°C water, then the specimens were conditioned in 20°C and 65% relative humidity back to 12% moisture content of the wood before the testing). Additionally, a control test series was performed (tested after 7 days in 20°C and 65% relative humidity).

To the three adhesives mainly studied within the GIROD-project, EP, 2K PUR and PRF, four other adhesives were added. These were: melamine-urea-formaldehyde (MUF), one component polyurethane (1K PUR), emulsion-polymer-isocyanate (EPI) and a modified silyl-epoxy (MS). In this way, the suggested test method was applied for a large spectrum of adhesives with differing mechanical and durability properties. For each treatment and adhesive ten specimens were tested, which gave a total amount of 210 specimens.
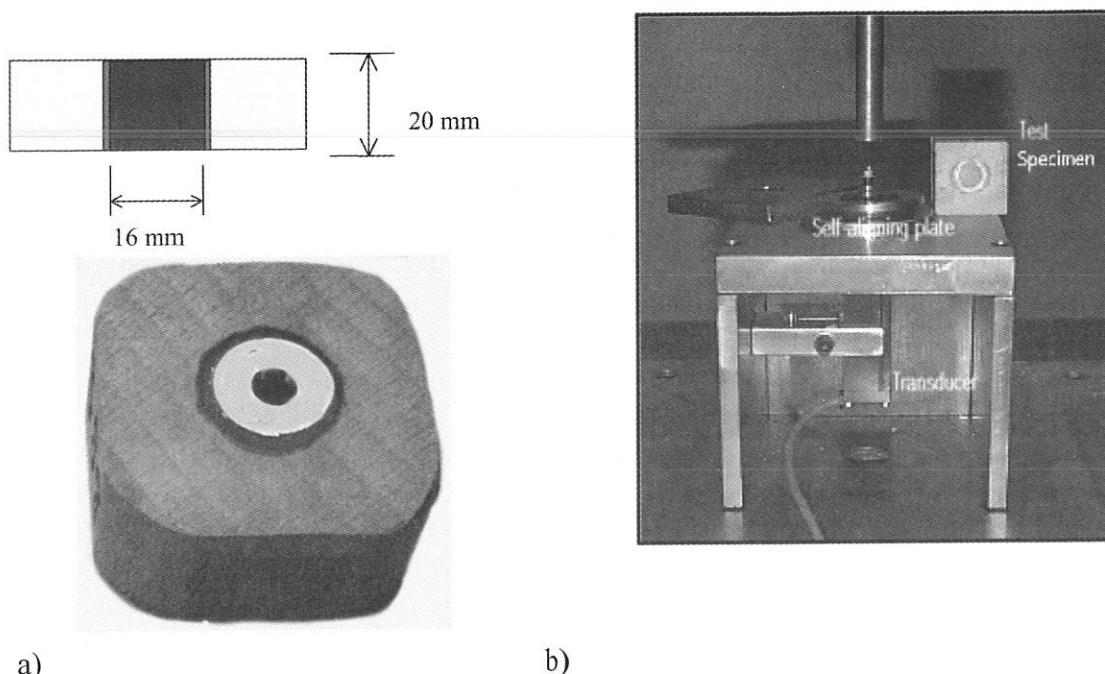
Figure 3.2.1 a) Geometry of the chosen test specimen. b) Test set-up for loading in compression.

The purpose of basing the new test method for durability of the adhesive on EN 302 was to allow comparison with wood-to-wood bonds (pure beech specimens), tested according to this standard, and to apply the requirements (for type I adhesives) set in EN 301 also to glued-in rods. The shear strength requirements according to EN 301 are for thin glue lines: Control: 10 MPa, A4 treatment: 6 MPa, A5 treatment: 8 MPa. For thick glue lines the required values are 80% of the values for thin glue lines. However, the chosen test specimen is very different from standard test pieces according to EN 302. Both the geometry and the thickness of the glue-line differ and the comparison with the requirements according to EN 301 is therefore questionable.

Test results

Figures 3.2.2-3.2.3 and Table 3.2.1 show the results of the shear strength tests obtained by the suggested test method. Anyway, if the requirements according to EN 301 (for thin or thick glue lines) are applied for the glued-in rods tested here only the EP adhesive passes. Whether that is a reasonable result can not be based just on these tests. The A4 treatment (cooking and then testing in wet state) gives very low shear strength values. This verifies that water and high temperatures put strong requirements on the adhesive bonds.

Both treatments, A4 and A5, seem to classify the adhesives in the same order. The shear strength was lower after the A4 treatment as the specimens were tested in the wet state. The EP-bonded specimens clearly display the highest shear strength values. Then, 2K PUR and PRF can be classified as one group. The MUF and 1K PUR control specimens display similar shear strength but MUF-bonded specimens are less cooking resistant. Also the shear strength of EPI-bonded specimens drops dramatically after cooking.

Table 3.2.1 Mean shear strength, standard deviation and coefficient of variation (CoV) for each group of ten tested specimens. (The EPI bonded specimens treated according to A4 were not possible to test).

	Control			A4			A5		
	Mean shear [N/mm^2]	St. dev.	CoV [%]	Mean shear [N/mm^2]	St. dev.	CoV [%]	Mean shear [N/mm^2]	St. dev.	CoV [%]
EP	13.57	1.47	11	5.34	1.66	31	11.29	2.41	21
2K PUR	8.97	2.09	23	2.28	0.76	33	7.54	1.57	21
PRF	8.55	0.99	12	1.57	0.36	23	6.26	0.54	9
MUF	7.03	1.38	20	0.76	0.25	33	2.21	0.61	28
1K PUR	6.81	0.56	8	1.54	0.24	15	4.44	0.31	7
EPI	4.27	1.46	34	0	0	0	0.77	0.28	37
MS	1.75	0.2	11	0.37	0.04	12	0.82	0.27	33
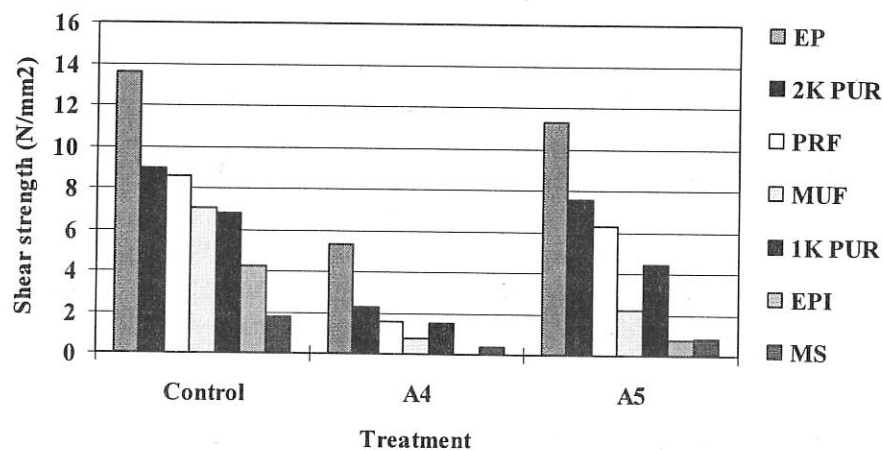
Figure 3.2.2 Shear strength (tested in compression). The shown values are average values of the ten specimens in each group.
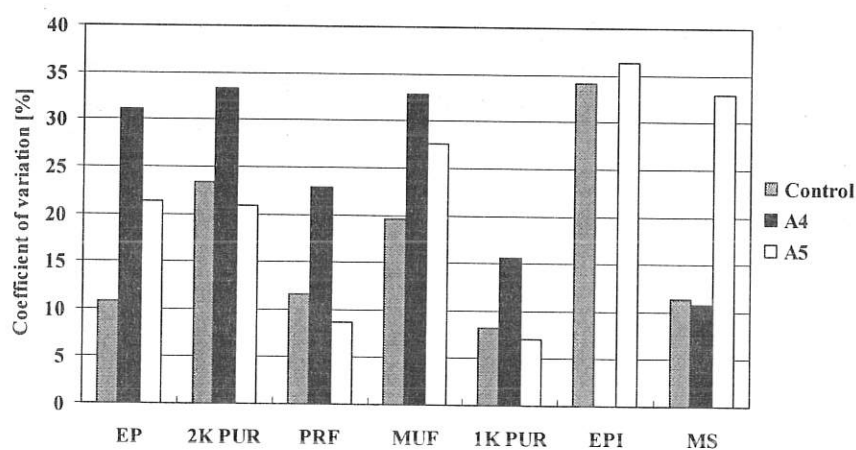
Figure 3.2.3 Coefficient of variation for shear strength.

There were large variations (large CoV) in the shear strength test results, see Figure 3.2.3. One possible reason for this behaviour can be variation in the beech material. Therefore, all specimens were examined visually. This visual inspection did not point out any clear reasons

for the variability in the test results. The different groups of specimens seemed to be similar. However, it appeared that badly centred bolts could be one explanation to the large variation in the test results. The magnitudes of the coefficients of variation were similar for the initial 240 tests as for the here presented tests.

The coefficients of variation are in most cases highest after the A4 treatment. This is probably due to the testing of wet specimens. It is worth to note that also for pure beech specimens tested according to EN 302, the variability in the shear strength test results usually is of the same order as obtained in present tests.

To try to minimise the variability in the test results some more tests, using EP, 2K PUR and PRF were performed. For these new specimens the variability in the beech material was minimised and the rods were carefully centred. This extra test series was performed with three adhesives (the first three in the list used before), EP, PUR and PRF. Control specimens and specimens treated according to "A4" and "A5" were tested in compression as described above. Each group consisted of 10 specimens which gave a total amount of 90 specimens.

The shear test results after treatments are summarised in Table 3.2.2 and in Figure 3.2.4. It can be seen that the shear strength specially of the EP- and PUR-bonded control specimens were higher compared to the previous test results. Among the treated specimens the difference between the previous test results and the extra tests was smaller. The test results of the different adhesive types appeared in the same order with one another as expected. The variability in the test results was strongly reduced for the extra tests, see Tables 3.2.1 and 3.2.2. The coefficients of variation were decreased in all cases and in most cases strongly decreased. Also the failure modes for the different adhesives were the same as described above.

It can be concluded that by preparing the specimens in a careful way the variability in the test results can be reduced.

Table 3.2.2 Shear strength test results for the 90 "extra tests".

	Control			A4			Modified A5		
	Mean shear [N/mm^2]	St. dev.	CoV [%]	Mean shear [N/mm^2]	St. dev.	CoV [%]	Mean shear [N/mm^2]	St. dev.	CoV [%]
EP	16.91	1.08	6.37	6.56	0.62	9.44	14.60	0.87	5.94
2K PUR	15.85	0.67	4.18	3.67	0.32	8.63	8.39	1.32	15.66
PRF	8.10	0.50	6.14	1.66	0.22	13.18	5.16	0.16	2.99
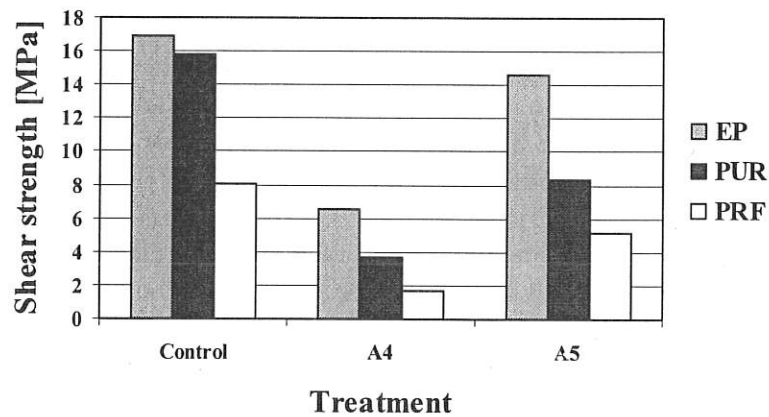
Figure 3.2.4 Shear strength for the extra tests. Mean values are shown above the bars.

Durability tests were performed also for a few specimens with bonded-in FRP rods. The shaping of the specimens was the same as for steel rods. This test series was performed with three adhesives, EP, PUR and PRF. The FRP pieces were cleaned with ethanol before the gluing. Control specimens and specimens treated according to "A4" and "A5" were tested in compression as described above. Each group consisted of only 3 specimens which gave a total amount of 27 specimens. The test results are summarised in Table 3.2.3 and in Figure 3.2.5. Only average values are shown as each group of specimens was very small.

The adhesion to the FRP rod was generally poor for all three adhesives. There was a large variation in the test results. This variation is most probably caused by the varying adhesion to the rods. In a few cases there was adhesion to the rods which gave "high" shear strength values and in some cases it was the other way around.
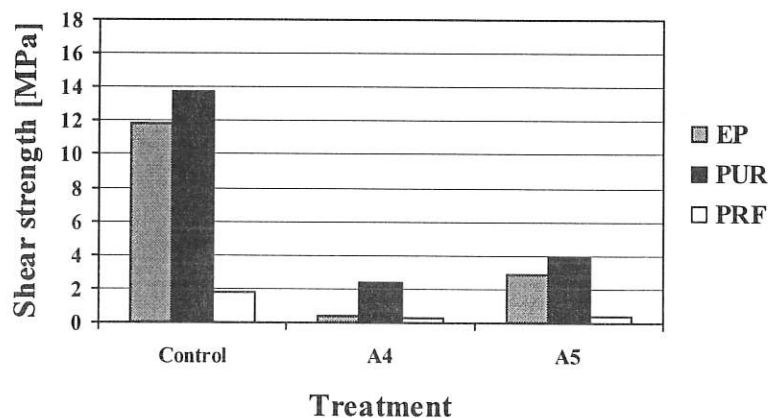
Figure 3.2.5 Shear strength for FRP-bonded rods.

Table 3.2.3 Shear strength of bonded in FRP-rods.

	Mean shear [N/mm²]		
	Control	A4	A5
EP	11.81	0.40	2.89
PUR	13.68	2.34	3.87
PRF	1.83	0.33	0.39

27

3.2.3 Conclusions WP 2.1

A test method for the durability of the adhesive for glued-in rods was developed. 40 x 40 x 20 mm beech blocks with glued-in 16 mm threaded rods are used. The specimens are treated according to EN 301 and tested in compression. The method has been tested for adhesives with a wide range in properties. To achieve small variability in the test results, careful preparation of the specimens is required.

The results above show that EP-bonded rods have a shear strength similar to the shear strength of the beech wood. This is reasonable as in this case the failure was a wood failure. For the other adhesives no clear wood failures occurred and the shear strength was lower. It seems like the suggested method is able to test the adhesive in a proper way.

3.2.4 WP 2.2 - Creep and creep-rupture

A method for testing the creep and creep- rupture properties of adhesives was developed. The glued-in rod specimen described above in WP 2.1 was used. The test was performed at three different climatic conditions at 20°C/65 % RH; 50°C/30%RH; and at 20°C/85 % RH. For each adhesive type the short term strength (failure within 1 minute) was determined. Constant load was then applied to specimens at 80, 60 and sometimes 40 % of the short term load, and the time to failure was recorded.

3.2.5 Results WP 2.2

Test procedure

Creep-rupture (time-to-failure) data provides a measure of the ultimate load-carrying ability of an adhesive bond as a function of time at various levels of stress, temperature and relative humidity. Thus, creep-rupture properties need to be tested for different load levels and for different climatic conditions. The different climates include high humidities and high temperatures. With respect to these demands it was decided to use the same test principle as in ASTM D 4680 for the creep-rupture tests of glued-in rods. This method allows loaded specimens to be placed in different climates. Static loads are applied and maintained by spring-loading, as shown in Figure 3.2.6a. The spring should be designed with a particular load capacity, and must be corrosion-resistant. An automatic time-recorder equipped with a micro-switch records the time-to-failure. The testing device according to ASTM D 4680 is shown in Figure 3.2.6.
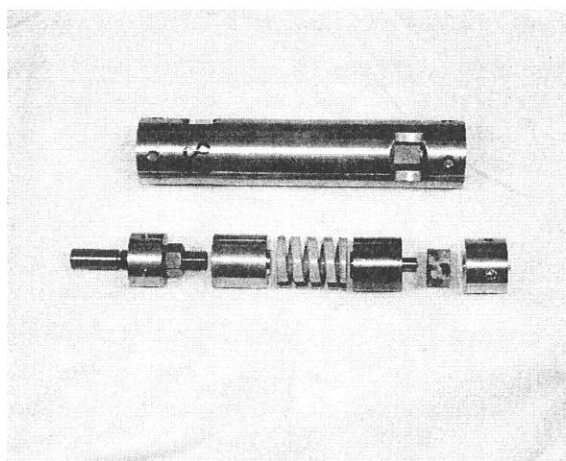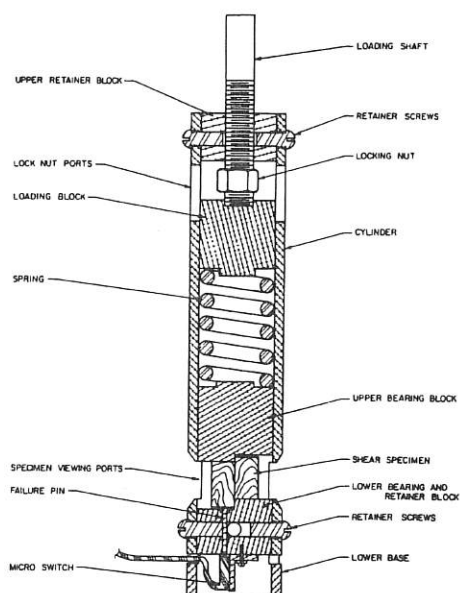
a)   b)

Figure 3.2.6 a) Testing device according to ASTM 4680. The shear specimen is replaced with a small glued-in rod specimen. b) Creep-rupture testing device.

The shear specimen is for the glued-in rod application replaced with the specimen shown in Figure 3.2.1 a (the same test specimen as for the durability tests). The upper and lower bearing blocks were exchanged and adjusted to fit the glued-in rod test specimen. The maximum load which was possible to apply by using this spring is 14 kN. The spring constant for this spring was calculated to 0.78 kN/mm. The switch registering time to failure released when the deformation was approximately two mm. Spring loading of the test specimens has one big disadvantage. The creep deformation, before the failure occurs, leads to relaxation of the spring and consequently a decrease in the applied load. One specimen bonded with each adhesive was unloaded after approximately six months under load to check that no creep deformation in the glue line had occurred. However, for the checked specimens no creep deformation was visible.

The performance of the loading tubes was tested with a load cell placed within the upper bearing block. This evaluation showed that when applying the load to the specimens in a tube the load decreased with approximately 5% when the locking nut was tightened.

Creep-rupture tests were planned to be carried out for:
- Three adhesives, EP, PUR and PRF
- Three load levels, 40%, 60% and 80% of the assumed maximum load
- Three climates, 20°/65% relative humidity (RH), 20°/85% RH and 50°/30% RH

Table 3.2.4 summarises the number of specimens tested. A total amount of 360 specimens was used in this study.

Table 3.2.4 Summary of the number of test specimens used for the creep-rupture tests. 120 specimens were tested for each climate which gave a total amount of 360 specimens tested.

20°/65% RH, 20°/85% RH, 50°/30% RH	Load levels			
	Controls	40%	60%	80%
EP	10	10	10	10
PUR	10	10	10	10
PRF	10	10	10	10

The control specimens were tested at equilibrium moisture content in the three climates. They were loaded so that failure occurred within one minute. The supports were arranged to be equal to the conditions within the creep-rupture tubes.

Table 3.2.5 Failure loads for the control test specimens.

	20°/65% RH			20°/85% RH			50°/30% RH		
	Mean [kN]	St. dev.	CoV [%]	Mean [kN]	St. dev.	CoV [%]	Mean [kN]	St. dev.	CoV [%]
EP	17.44	1.01	6	13.97	0.88	6	19.84	1.71	9
PUR	14.32	1.85	13	10.96	1.63	15	16.15	0.92	6
PRF	8.62	0.36	4	6.32	0.39	6	9.34	0.88	9

The loads for the creep rupture tests were based on the failure loads for the control test specimens. The loads are shown in Table 3.2.6. The maximum possible load for the springs was 14 kN. Therefore, the 80% load level was not possible to reach for two EP bonded groups of specimens (*-marked in Table 3.2.6). The EP-bonded specimens in climate 20°/65% RH reached 76% load level and the EP-bonded specimens in climate 50°/30% RH reached 67% load level. The specimens were conditioned in the actual climates before loading. The loading to reach the desired load level took one minute.

Table 3.2.6 Loads [kN] for the creep rupture tests.

	20°/65% RH			20°/85% RH			50°/30% RH		
	40%	60%	80%	40%	60%	80%	40%	60%	80%
EP	7.32	10.99	14.65*	5.87	8.80	11.73	8.33	12.50	16.67*
PUR	6.01	9.02	12.03	4.60	6.90	9.21	6.78	10.17	13.57
PRF	3.62	5.43	7.24	2.65	3.98	5.31	3.92	5.88	7.85

*) These specimens did not reach the 80% load level.

Test results

Figures 3.2.7a, b and c show shear stress versus median time to failure (logarithmic scale) for all three adhesives in all three climates. Within the project period it was not possible to get results from all the planned test series as the time to failure was longer than expected. This means that the tests loaded to 40% load level and some tests loaded to 60% load level were not finished. However, enough results are available to decide whether the method is useful or not.

The creep-rupture curves at 20°/65% RH (Figure 3.2.7 a) for PUR and PRF are very conservative. For PRF all ten specimens survived 5500 hours. At that time the test was interrupted to be able to test other specimens. The PUR and PRF curves at 20°/85% RH are also conservative. Some of the specimens loaded to 60% load level are still under load.

20/65%

Conservative estimate, value after 15.5 months of loading (still 5 specimens left)

At this point all ten specimens survived and the test series was interrupted.

a)

20/85%

Conservative estimates for PRF and PUR.
PRF: all specimens left, the value after 8.5 months of loading is given.
PUR: value after 14.5 months of loading (still 5 specimens left)

b)

50/30%

Conservative estimate for PRF. The value after one year of loading when 7 specimens are left are given.

c)

Figure 3.2.7 Shear stress versus median time (hours) to failure in logarithmic scale for the three tested adhesives. a) 20°C/65% relative humidity b) 20°C/85% relative humidity c) 50°C/30% relative humidity

The PRF-curve at 50°/30% RH is conservative. The reason for the poor creep-rupture behaviour for EP and PUR at high temperatures is probably that these two adhesives have a

glass transition temperature of 45°-50°C. At these temperatures the properties of the adhesives change drastically.

The method for testing "Strength and durability of the adhesive", described above, ranked the adhesives in strength order, EP, PUR and PRF. This order seems to apply also for creep-rupture tests at 20°/65% RH and at 20°C/85% RH up to a time to failure of approximately 10000 hours.

3.2.6 Comparison with results obtained from full-sized glued-in rod connections

The test methods described above are developed for testing the durability and the creep-rupture behaviour of the adhesives. The test methods are of course most useful if the results are directly comparable to results obtained for full-sized connections. Within the GIROD-project strength (in different climates) and creep-rupture behaviour (DOL) was tested for steel rods with a diameter of 16 mm bonded into glulam with an anchorage length of 160 mm (WP5).

Table 3.2.7 shows the results of short-term pull-out tests for full-sized connections. The values shown are mean values of seven specimens relative to the pull-out strength at 20°/65% RH. Corresponding values for small specimens (mean value of ten specimens) are shown within brackets in Table 3.2.7. For PRF and PUR the decrease in strength at the high humidity obtained for full-sized connections are comparable with the strength decrease for the small specimens. For full-sized EP-bonded specimens the strength increased at high humidity compared to the strength at 20°C/65% RH. That was not the case for the small specimens. One possible explanation for this difference is the ductile behaviour that is obtained for the full-sized connection. At high temperature the full-sized connections and the small specimens displayed different results. One part of the explanation can be that the climatic conditions were different and especially PUR and EP are sensible to temperatures in excess of 50°C.

Table 3.2.7 Mean bond shear strength at different climatic conditions versus the value at 20°C/65% RH. Values for full-sized connections and small specimens (within brackets) are shown.

Climate	PRF	PUR	EP
20°C/65% RH	1 (1)	1 (1)	1 (1)
20°C/85% RH	0.85 (0.73)	0.85 (0.76)	1.03 (0.80)
50°C	0.77 (1.08)	0.87 (1.13)	1.05 (1.14)

Duration of load tests on full-sized glued-in rod connections showed that at high humidity (85% RH) EP-bonded specimens were most favourable (longest time to failure at 70% and 80% stress level), see Aicher 2001c. The behaviour of these specimens was comparable to the Madison curve. At high humidity the full-sized PUR- and PRF bonded specimens behaved similarly (approximately the same time to failure). The creep-rupture behaviour of the small specimens presented here seem to indicate that at high humidity PRF-bonded specimens are preferable. The analysis has, so far, not revealed any differences in failure modes between the small specimens and the full-sized connections.

It can be concluded that the comparison between test results obtained for small glued-in rod specimens are usually not directly transferable to results from full-sized glued-in rod connections. Presently, the results obtained for small specimens in this study should be used for assessment of the adhesive and not for assessment of the full-sized connection.

32

3.2.7 Conclusions WP 2.2

A test method for creep-rupture testing of small glued-in rod specimens was developed. The method is based on ASTM D 4680. The specimens for this test method are of the same type as for the strength and durability tests. Three load levels, 40%, 60% and 80% of the ultimate load, in three climates, 20°C/65% RH, 20°C/85% RH and 50°C/30% are studied. The three adhesives tested are very different.

Some examples show that the relationship between the behaviour of small glued-in rod specimens and behaviour of full-sized glued-in rod connections is not simple. Presently, the results obtained for small specimens in this study should be used for assessment of the adhesive and not for assessment of the full-sized connection.

3.3 WP 3 - Effect of distance between rods and between rods and timber edge on the axial strength

The objective of the third work package of GIROD was to study and to quantify the effect of the spacing between rods and the distance to the timber edges on the axial and lateral load-carrying capacity. Furthermore, some theoretical investigations were carried out to describe the behaviour of glued-in rods depending on spacings and distances of rods.

3.3.1 Rods glued-in parallel to the grain and loaded axially
Tests to determine the minimum edge distance
Glued laminated timber made of lamellas of strength class C35 was used. The timber was conditioned to a moisture content of 12 %. The threaded rods corresponded to strength class 8.8 and they were zinc-coated (galvanised) and not degreased. The diameter of the rods was 16 mm. The rods were glued into oversized holes of 17 mm diameter drilled parallel to the grain. The adhesives (used in the GIROD project) were a Casco PRF, Kleiberit Plastic-Mastic 573.8, a PUR, and WEVO Spezialharz, an Epoxy (EP). Also, some tests with different rod diameters were carried out.

The rods were glued-in parallel to the grain and loaded axially. The distances of the rods from the edge of the timber were varied to determine the minimum edge distance without causing shear block failure. That means if the distance of the rod to the edge is too small, a part of the timber including the rod breaks away.
Table 3.3.1 shows the test program. The definitions of spacings and distances are given in Figure 3.3.1.

Table 3.3.1 Test program for rods glued-in parallel to the grain and loaded axially.

Test series	Type of glue	Length of specimen/ Diameter of rod [mm]	Glued-in length [mm]	Spacing a_1 [mm]	Edge distance a_2 [mm]	Number of rods per test and side	Number of tests
GI-1	PRF	1088/16	320	101.8	24	2	5
GI-2	PRF	1088/16	320	79.2	32	2	5
GI-3	PRF	1088/16	320	56.6	40	2	5
GI-4	PRF	1088/16	320	33.9	48	2	5
GI-5	PRF	1088/16	320	-	60	1	5
GI-6	PUR	1088/16	320	-	60	1	3
GI-7	Epoxy	1088/16	320	-	60	1	3
GI-8	PRF	1360/20	400	-	60	1	5
GI-9	PRF	816/12	240	-	60	1	5
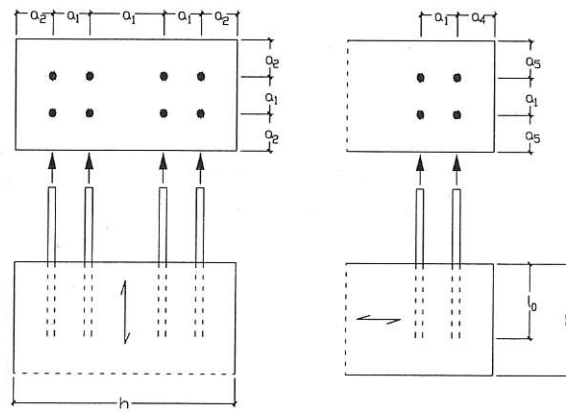
Figure 3.3.1 Definitions of spacings and distances.

Test results

Figure 3.3.2 presents all test results with 16 mm diameter rods in one diagram. The failure that occurred in most tests with a rod-to-edge distance of 24 to 48 mm was splitting of the wood. However, some test specimens failed because of pulling-out of the rod. The tests with one rod in the middle always failed due to rod pulling-out. The shear strength shown is defined as the failure load divided by the surface of a cylinder with a height equal to the glued-in length and a diameter equal to the outer diameter of the rod.

According to Figure 3.3.2 the load-carrying capacity increases with an increasing edge distance. The test results with an edge distance of 48 mm do not follow the general trend. An explanation of this behaviour could be that the rod spacing is getting an increasing influence and the influence of the timber edge distance is becoming smaller.
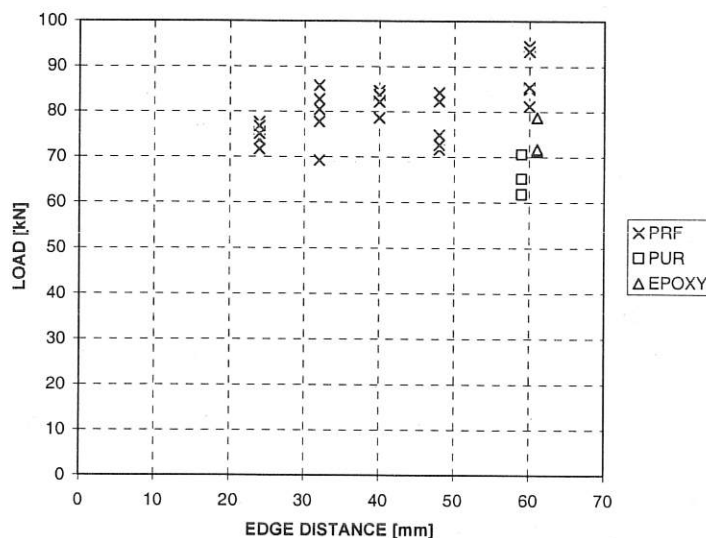
Figure 3.3.2 Failure load depending on edge distance and type of adhesive.

Tests to determine the minimum spacing

The materials, dimensions and other details are given in above. More details of these tests can be found in Table 3.3.2.

35

Table 3.3.2 Test program to determine the minimum spacing.

Test series	Type of glue	Glued-in length [mm]	Diameter of rod [mm]	Spacing a_1 [mm]	Number of rods per test and side	Number of tests
GI3-1	PRF	320	16	32	3	5
GI3-2	PRF	320	16	40	3	5
GI3-3	PRF	320	16	48	3	5
GI3-4	PRF	320	16	60	3	3

Test Results

Figure 3.3.3 shows the results of the tests to determine the minimum rod-to-rod distance without any significant influence on the load-carrying capacity.
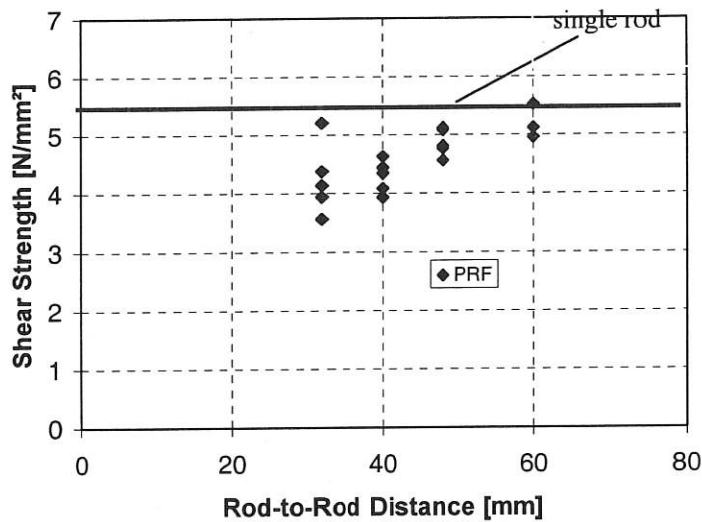
Figure 3.3.3 Shear strength versus rod-to-rod distance.

The edge distance of the rods was 40 mm, respectively 2.5 times of the rod's diameter. Regarding the results it can be seen that like in the previous tests the load-carrying capacity is increasing with the rod spacing. As a comparison the values of the tests with one rod in the middle of the cross-section were added to the diagram. The expected failure, namely splitting off the wood, occurred.

Theoretical investigations

Combining all tests (Blaß and Laskewitz 1999) where PRF was used, those to determine the minimum edge distance as well as those to establish the minimum rod spacing, leads to the diagram presented in Figure 3.3.4. The distance a on the abscissa is defined as follows: for the tests to determine the minimum edge distance, the distance a is the minimum of either half of the spacing or the edge distance. For the tests to establish the minimum rod spacing the distance a is defined as half of the rod spacing. A linear regression analysis leads to the following relation between mean shear strength and distance a [mm] to rod diameter d [mm] for a rod diameter of 16 mm:

36

$$\tau = 0.7 \cdot \frac{a}{d} + 3.7 \quad [\text{N/mm}^2]. \qquad (R^2 = 0.30) \qquad (3.3.1)$$

with $\qquad 1 \le \dfrac{a}{d} \le 2.5$

The horizontal straight line represents the mean value of the comparative tests with one rod in the centre of the cross-section. The point of intersection is situated close to a distance of 40 mm, or 2.5 times of the rod diameter. Consequently, a spacing of 80 mm or an edge distance of 40 mm does not cause a decrease of the load-carrying capacity compared to single rods with a diameter of 16 mm.

Therefore a rod-to-edge distance of 2.5 times of the rod diameter and a spacing of 5 times of the rod diameter is suggested. Otherwise if the distance should be smaller, equation 3.3.1 should be used to calculate the bond stresses.
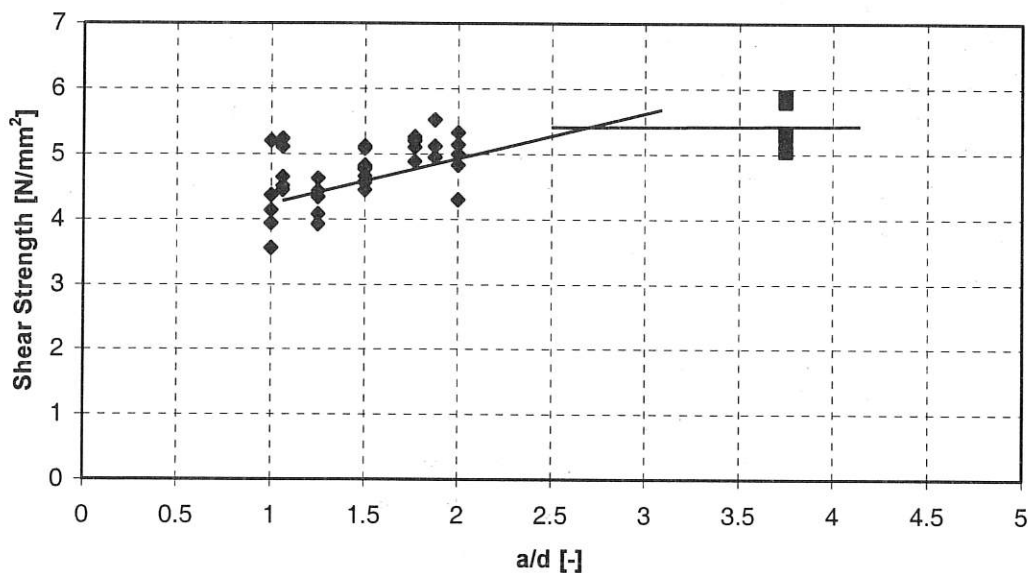
Figure 3.3.4 Mean shear strength versus distance a *to rod diameter* d.

3.3.2 Rods glued-in perpendicular to the grain and loaded axially

The materials were the same as mentioned in paragraph 3.3.1. An overview of the test program is given in Table 3.3.3. The glued-in length was either 160 mm or 320 mm. The edge distance of the rod was chosen to be 60 mm to avoid any influence on the load-carrying capacity.

Table 3.3.3 Test program.

	H [mm]	B [mm]	L [mm]	glued-in length [mm]
Giq-1	320	120	3200	320
Giq-2	400	120	4000	320
Giq-3	480	120	4800	320
Giq-4	560	120	5600	320
Giq-5	240	120	2400	160
Giq-6	280	120	2800	160
Giq-7	320	120	3200	160
Giq-8	500	120	5000	160

37

Test Results

The failure mode was pulling-out the rod combined with wood splitting for the test series with a glued-in length that was the same as the height of the beam. With increasing beam depth, the observed failure mode changed from pulling out the rod towards tension perpendicular to the grain failure of the beam. The corresponding crack always occurs at the end of the rod. The pull-out strength of the rods which are glued-in perpendicular to the grain and glued-in the same as the height of the beam are similar to those results achieved by the tests with rods glued-in parallel to the grain. The failure was reaching the tensile strength perpendicular to the grain.

Figure 3.3.5 shows the test results for the glued-in lengths of 320 mm and 160 mm. It is obvious that the load-carrying capacity decreases with increasing height of the beam or a descending ratio of the glued-in length l_0 to the height of the beam H.

Theoretical Investigations

The test results with tension failure perpendicular to the grain were evaluated on the basis of the work of Ehlbeck et al. 1989 who investigated connections loaded perpendicular to the grain. The load-carrying capacity of the specimens which failed due to pulling out the rod can be described by using the design rules for glued-in rods given in the draft of the German Timber Design Code DIN 1052. The ultimate load for a rod glued-in perpendicular to the grain may be calculated as

$$F_{90} = \frac{13 A_{ef}^{0.8} f_{t,90}}{\eta k_r} \qquad (3.3.2)$$

where

$$\eta = 1 - 3\left(\frac{l_0}{H}\right)^2 + 2\left(\frac{l_0}{H}\right)^3$$

l_0: glued-in length

H: Height of the beam

$$k_r = \frac{1}{n}\sum_{i=1}^{n}\left(\frac{h_1}{h_i}\right)^2 = \frac{H - l_0}{H}$$

$$A_{ef} = l_{r,ef} \cdot t_{ef}$$

$$l_{r,ef} = \sqrt{l_r^2 + (cH)^2}$$

$$l_r = d$$

$$c = \frac{4}{3}\sqrt{\frac{l_0}{H}\left(1 - \frac{l_0}{H}\right)^3}$$

$$t_{ef} = \min\begin{cases} b \\ 6 \cdot d \end{cases} \quad \text{(draft DIN 1052)}$$

b: Width of the beam

d: Outer diameter of the rod

Figure 3.3.5 shows a comparison between the failure loads reached in the tests and the calculated failure loads. The horizontal lines describe the pull-out capacity of both glued-in lengths used in the tests according to the proposal of DIN 1052:

$$R_{ax} = l_0 \pi d f_{k1} \qquad (3.3.3)$$

where f_{k1} = bond strength.

38

Görlacher's model (in Ehlbeck et al. 1989) assumes a tensile stress distribution perpendicular to the grain at both sides of the connection reaching a maximum at the end of the glued-in rod and decreasing with increasing distance from the rod. Since an undisturbed distribution is only possible in one direction, the calculated load carrying capacities are divided by 2, although a certain amount of stresses is also transferred between rod and end grain surface. These stresses are disregarded in the following. Characteristic values of the material properties according to the draft DIN 1052 were used when evaluating the load-carrying capacities.

For $\alpha = \dfrac{l_0}{H}$ approaching 1 the calculated load-carrying capacity reaches infinite values. In this case α is the ratio of the glued-in length to the height of the beam. In the case of a notched beam $\alpha = 1$ would represent a beam without a notch. Therefore it is obvious that the model used gives infinite values. In reality the ultimate load is limited by rod pulling-out. The horizontal lines describe the pull-out strengths of rods glued-in perpendicular to the grain according to the draft of the German national standard DIN 1052. Considering the fact that the calculated results are based on characteristic material properties, Görlacher's equations describe the behaviour quite well.
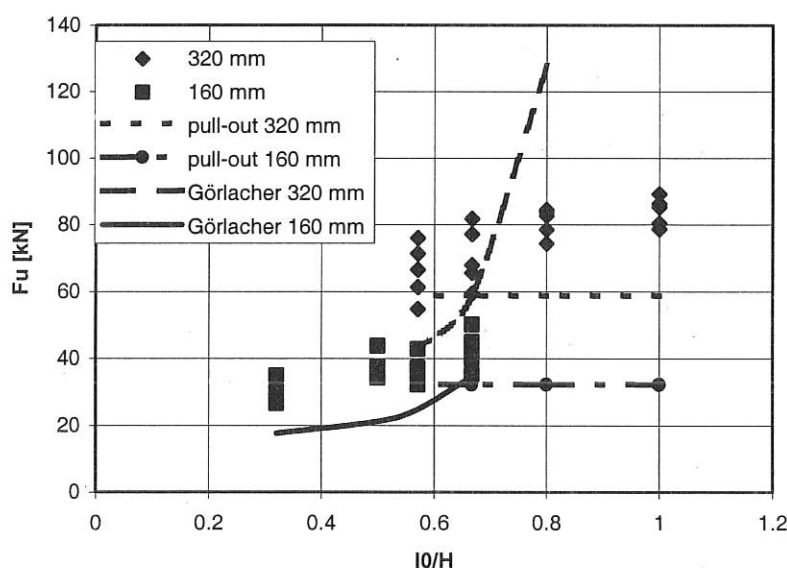
Figure 3.3.5 Test results compared to equations according to Ehlbeck et al. 1989.

In the draft DIN 1052 simplified equations based on the theory of Görlacher are given. The difference between the original and the simplified equations in DIN 1052 is not significant. Further information on these design rules are given in the next paragraph.

3.3.3 Rods glued-in parallel to the grain and loaded laterally
The materials were almost the same as mentioned in paragraph 3.3.1. An overview of the test program is given in Table 3.3.4. The edge distances of the rods varied. The glued-in length was 320 mm. The adhesive used for all tests was PRF. The test specimens had either one or two glued-in rods. Additionally some tests with rods corresponding to strength class 4.6 were performed to investigate the influence of the steel quality on the load-carrying capacity. One test series was performed with a larger beam width.

Table 3.3.4 Test program.

Test series	Glu-lam	Strength class of the rod	H [mm]	B [mm]	L [mm]	Edge distance a_2 [mm]	Edge distance a_3 [mm]	Spacing a_1 [mm]	No of rods	No of tests
Gil4.6	Gl24h	4.6	220	100	2380	110	110	-	1	5
Gil8.8-1	Gl24h	8.8	220	100	2380	110	110	-	1	5
Gil8.8-2	Gl32h	8.8	300	100	3500	50	250	-	1	5
Gil8.8-3	Gl32h	8.8	300	100	3500	100	200	-	1	5
Gil8.8-4	Gl32h	8.8	300	100	3500	150	150	-	1	5
Gil8.8-5	Gl32h	8.8	300	100	3500	200	100	-	1	5
Gil8.8-6	Gl32h	8.8	300	150	3500	50	250	-	1	5
GilII-1	Gl32h	8.8	400	100	4500	50	270	80	2	5
GilII-2	Gl32h	8.8	400	100	4500	100	220	80	2	5
GilII-3	Gl32h	8.8	400	100	4500	150	170	80	2	5
GilII-4	Gl32h	8.8	400	100	4500	200	120	80	2	5

Test Results

The failure was in most cases first a simultaneous embedding failure of the timber and bending failure of the rod and subsequently almost all specimens failed due to tension failure pependicular to the grain. Especially in the rods of strength class 4.6 two plastic hinges were formed, one in the timber and the other at the supporting steel plate. With decreasing edge distance, a_3, larger embedding displacements were observed. Nevertheless also these specimens failed at last due to tension failure perpendicular to the grain.

Figures 3.3.7 and 3.3.8 show the test results with one or two rods, respectively. The maximum load is the force at the support of the threaded rods. In the tests with two glued in rods the maximum load is the force on both rods. The type of adhesive for all tests was PRF.
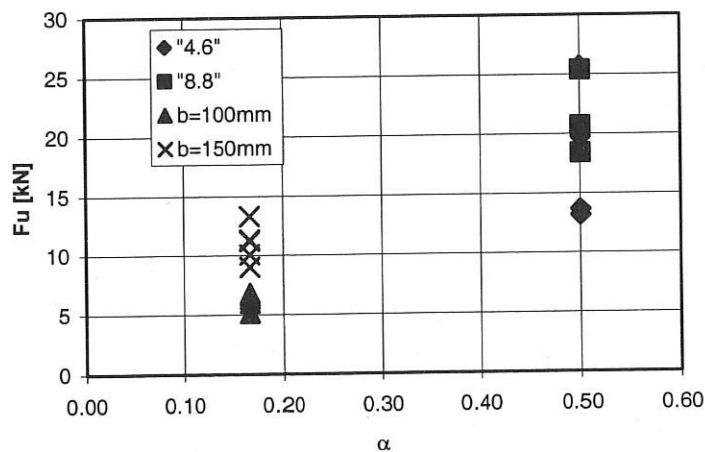
Figure 3.3.6 Comparison of different test results.

Parallel tests were performed to study the influence of the rod steel grade on the load-carrying capacity. Threaded rods of strength class 4.6 and 8.8 were used. With decreasing edge distance, a_3, the load-carrying capacity rises and the failure mode is increasingly determined by the embedding strength of the timber and the bending capacity of the rod. Nevertheless at the end of the test almost all specimens failed due to tensile failure perpendicular to the grain.

For larger edge distances a_3 the tensile strength perpendicular to the grain was reached earlier and with smaller embedding deformations.

Figure 3.3.6 presents a comparison of different test results with one glued-in rod. For a small ratio α the beam width was varied. The load-carrying capacities of the wider specimens are higher. A reason for this is that the fracture area of these specimens is larger. Therefore more fracture energy is necessary to split the timber and larger ultimate loads result.

The comparison of different steel qualities does not show significantly different failure loads for strength classes 4.6 and 8.8. The mean value of the tests with rods 4.6 were slightly lower than those with a steel grade 8.8. An explanation could be that the most frequent failure mechanism was reaching the tensile strength perpendicular to the grain. Consequently, the embedding strength of the timber was not the governing parameter. Hence, the steel quality has hardly any influence for the described failure mechanism. However, for smaller values a_3 the rod steel grade will increasingly influence the load-carrying capacity, since embedding strength and bending capacity then mainly determine the failure mode.

Theoretical Investigations

Similar to the preceding paragraph concerning the rods glued-in perpendicular to the grain the equations based on the work of Görlacher were used to calculate the load-carrying capacity for failures caused by splitting of the timber. The simplified equations from the draft DIN 1052 were used. To describe the behaviour of the threaded rods in the case of smaller edge distances a_3 the Johansen theory was used.

First the design rules given in the draft DIN 1052 are presented. The load-carrying capacity is reduced by 50%, because similiar to the tests with rods glued-in perpendicular to the grain no tensile stresses are carried outside of the timber. The parameter a_r giving the width of the connection is assumed as the distance of the plastic hinge from the end grain surface.

The load-carrying capacity of a rod glued-in parallel to the grain is given as

$$R_{90} = 0.5 \cdot k_s \cdot k_r \cdot \left(6.5 + \frac{18a^2}{H^2} \right) \left(t_{ef} H \right)^{0.8} \qquad (3.3.4)$$

where

$$k_s = \max \begin{cases} 1 \\ 0.7 + \dfrac{1.4a_r}{H} \end{cases}$$

$$k_r = \frac{n}{\displaystyle\sum_{i=1}^{n} \left(\dfrac{h_1}{h_i} \right)^2}$$

$a = H - a_3$ in mm

a_r = Distance from the end grain to the plastic hinge of the rod according to the theory of Johansen

H = Height of the beam

$$t_{ef} = \min \begin{cases} B \\ 6d \end{cases}$$

B = Width of the beam

d = Outer diameter of the rod

n = Number of rods

h_i = Distance of the rod i from the lower edge.

41

Based on the theory of which Johansen equations were derived a gap between the end grain and the support was taken into account. Only the failure mechanism with two plastic hinges was regarded because of the failure mode observed in the tests, caused by the clamped support of the rods. The distance of the plastic hinge to the end grain is:

$$b_1 = -t + \sqrt{t^2 + 4\frac{M_y}{f_{h,1}d}} \qquad (3.3.5)$$

The load-carrying capacity results as:

$$R = f_{h,1}db_1 \qquad (3.3.6)$$

where $\quad M_y = 0.26 \cdot f_u \cdot d_m^{2.7} \qquad$ (according to the draft DIN 1052)

f_u =Tensile strength of the steel

d_m = Mean of the outer diameter and the core diameter of the rod

$f_{h,1}$ = Timber embedding strength according to the draft DIN 1052

t = Distance from the end grain to the support.

With characteristic values for the embedding strength and the fastener yield moment, respectively, b_1 according to equation (3.3.6) results as $b_1 = 137$ mm. Here, the embedding strength for rods arranged parallel and loaded perpendicular to the grain is assumed as 10 % of the embedding strength of rods arranged perpendicular and loaded parallel to the grain. Because of the adhesive between rod and surrounding timber and the subsequent friction between fastener and wood, the embedding strength is then increased by 25%. The corresponding load-carrying capacity was multiplied by two because of the tensile forces in the inclined part of the fastener, not taken into account in the Johansen theory. DIN 1052 suggests this increase in load-carrying capacity to be 25% of the axial load-carrying capacity for screws but not more than 100 % of the load-carrying capacity according to Johansen. For glued-in rods the limit of the 100 % increase always applies.

Figure 3.3.7 and 3.3.8 show the test results with one or two rods, respectively, compared with the calculations based on characteristic values. The suggested equations fit the test results quite well. Only for very small ratios α the calculated results are not conservative. However, Görlacher's model is limited to ratios $\alpha > 0,2$. Considering this limit, only one test result yields a value below the calculated curve. Therefore the minimum of the results according to equations 3.3.4 and 3.3.6 is proposed as the characteristic load-carrying capacity of rods glued-in parallel to the grain and loaded laterally, but limited to $\alpha > 0,2$.
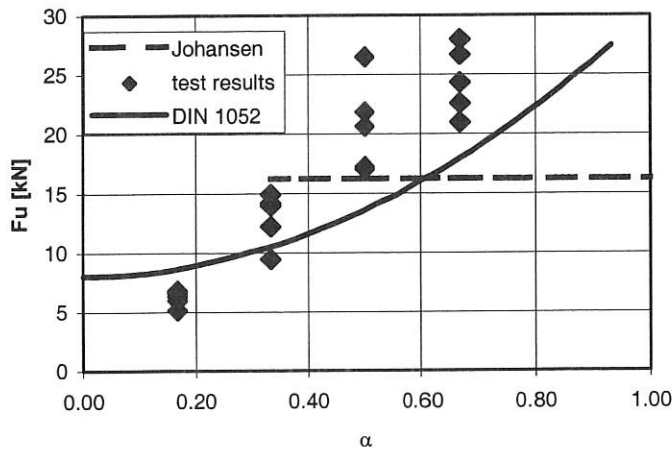
Figure 3.3.7 Test results with one rod compared with calculation models.

42
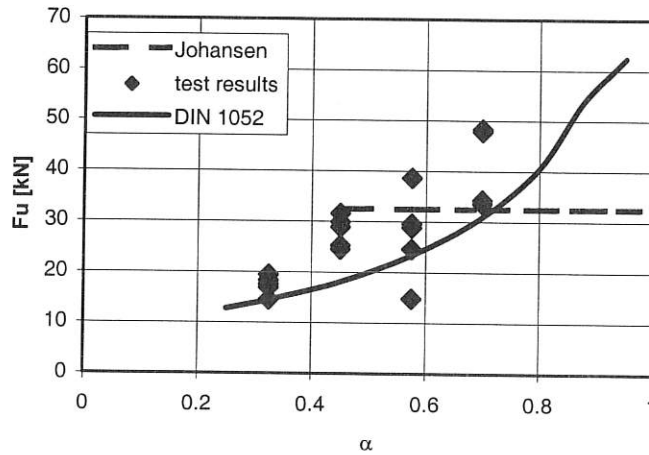
Figure 3.3.8 Test results with two rods compared with calculation models.

3.3.4 Conclusion

The objective of the third working package of GIROD was to study and to quantify the effect of the spacing between rods and the distance to the timber edges on the axial and lateral load-carrying capacity. Furthermore theoretical investigations were carried out to describe the behaviour of glued-in rods depending on spacings and distances of rods.

In addition to this it was possible to propose design equations for rods glued-in parallel and perpendicular to the grain and loaded laterally and axially. Minimum distances to the timber edge and spacings for rods are also suggested. Details of the work carried out within this WP can be found in the Technical report (Blass and Laskewitz 2001).

3.4 WP 4 – Effect of moisture conditions

3.4.1 Objectives
The objective of work package 4 (WP 4) was to investigate to what extent the axial resistance of glued-in rods, determined in ramp loading, is affected by various constant and variable climate conditions acting on specimens for significantly different time spans. The effects of moisture, time and internal stresses were investigated without superimposed mechanical (long-term) loads during the different climate exposure times. The latter issue was covered in work package 5.

3.4.2 Work content
The work plan of the experimental work of WP 4 is stated in Table 3.4.1. The experimental work, consisting of 20 different test series, was shared by the three project partners
- LUND University, Division of Structural Mechanics, Sweden, (ULUND),
- Trada Technology, High Wycombe, United Kingdom, (TTL), and
- Otto-Graf-Institute, University of Stuttgart, Germany, following (FMPA).

The 20 test series, all with axial tension loading of the rods, comprised
- four nominally different climates,
- four different climate exposure times,
- five different specimen geometries and sizes, respectively including two different angles between rod and grain and
- three different adhesive types.

All test series, except one, were performed with metrically threaded steel rods. In one test series fiber reinforced plastic (FRP) rods were used. The four investigated climate/moisture conditions comprised, on the one side, three considerably different constant artificial climates and, on the other side, naturally varying climates (sheltered outdoor conditions) at three European locations. The artificial constant climates were
- 20° C/65 % RH (reference climate conditions),
- 20° C/85 % RH (very humid climate) and
- 20° C/40 % RH (very dry climate).

The tests with the naturally varying outdoor climates were performed at the geographic locations of Southern Sweden (Asa), South-East of England (High Wycombe), and Southern Germany (Stuttgart).

Four different exposure times to the respective climates were investigated, being nominally: 3, 6, 15 and 21 months. In detail, the different conditioning configurations, comprising the climate and the exposure times, were (performing institutes in parentheses):
- 6 months at const. 20° C/65 % RH (FMPA),
- 15 months at const. 20° C/40 % RH (TTL),
- 15 months at const. 20° C/85 % RH (FMPA),
- 6 months at sheltered outdoor climate (ULUND, TTL),
- 15 months at sheltered outdoor climate (ULUND, TTL, FMPA),
- 21 months at sheltered outdoor climate (ULUND, TTL, FMPA).

Additionally two conditioning configurations tested in WP 5 and WP 1.3 were incorporated

in the comparative evaluation
3 months at const. 20° C/85 % RH (FMPA),
6 months at 20° C/65 % RH (FMPA).

The investigated specimen configurations A to E (see Table 3.4.1), differentiated by d_a = nominal rod diameter, ℓ_a = anchorage length $(\lambda = \ell_a/d_a$ = rod slenderness ratio), and α = angle between rod and grain, were

A:	$d_a = 8$ mm,	$\ell = 160$ mm,	$\lambda = 20$,	$\alpha = 0°$,
B:	$d_a = 16$ mm,	$\ell = 160$ mm,	$\lambda = 10$,	$\alpha = 0°$,
C:	$d_a = 16$ mm,	$\ell = 320$ mm,	$\lambda = 20$,	$\alpha = 0°$,
D:	$d_a = 16$ mm,	$\ell = 160$ mm,	$\lambda = 10$,	$\alpha = 90°$,
E:	$d_a = 16$ mm,	$\ell = 320$ mm,	$\lambda = 20$,	$\alpha = 90°$.

The vast majority of the test series in WP 4 with threaded steel rods were performed with a special softening type phenolic resorcinol adhesive, here termed PRFs (17 test series out of 19 series). Two test series with threaded steel rods were performed with an epoxy and a polyurethane adhesive, respectively.

Table 3.4.1 Workplan of experimental work package WP 4

test series	institute	climate conditions	climate duration	test time (season of the year)	rod diameter	anchorage length	slender-ness	angle load to grain	specimen configura-tion [1]	adhesive type	No.of specimens
-	-	-	[months]	-	$d_a=d_{nom}$ [mm]	l_a [mm]	λ [-]	α [degree]	-	-	–
4.1/s	FMPA	65 % RH	6	-	16	160	10	0	B	PRFs	7
4.2/s	TTL	65 % RH	6	-	16	320	20	90	E	PRFs	7
4.3/s	FMPA	65 % RH	6	-	16	320	20	0	C	PRFs	7
4.4/s	FMPA	85 %	15	-	16	160	10	0	B	PRFs	5
4.5/s	FMPA	85 %	15	-	16	320	20	90	E	PRFs	5
4.6/s	FMPA	85 %	15	-	16	320	20	0	C	PRFs	5
4.7/s	TTL	40 %	15	-	16	160	10	0	B	PRFs	5
4.8/s	TTL	40 %	15	-	16	320	20	90	E	PRFs	5
4.9/s	TTL	40 %	15	-	16	320	20	0	C	PRFs	5
4.10/s	TTL	sh. - out	15 [2]	winter	8	160	20	0	A	PRFs	10
4.11/s	ULUND	sh. - out	15	winter	16	160	10	90	D	PRFs	7
4.12/s	FMPA	sh. - out	15	winter	16	160	10	0	B	PRFs	10
4.13/s	TTL	sh. - out	21 [3]	summer	8	160	20	0	A	PRFs	10
4.14/s	ULUND	sh. - out	21	summer	16	160	10	90	D	PRFs	6
4.15/s	FMPA	sh. - out	21	summer	16	160	10	0	B	PRFs	10
4.16/s	ULUND	sh. - out	6	winter	16	160	10	0	B	PRFs	7
4.17/s	ULUND	sh. - out	6	winter	16	160	10	0	B	PUR	7
4.18/s	ULUND	sh. - out	6	winter	16	160	10	0	B	EP	7
4.19/s [4]	TTL	sh. - out	18	winter	16	160	10	0	B	EP	7
4.20/s	ULUND	sh. - out	6	winter	16	160	10	90	D	PRFs	7

[1] comprises rod diameter, anchorage length and angle between load and grain
[2] actually 18 months
[3] actually 22 months
[4] FRP rod; all other test series steel rods with metric thread

45

3.4.3 Determination of moisture content evolution of specimens at sheltered outdoor conditions

The moisture content of the specimens at sheltered outdoor conditions and especially the moisture history is of significant importance for interpretation of the obtained bond shear strength results. The moisture content of the specimens at test time was generally determined by oven-drying method after testing. The evolution of the (mean) moisture content was measured differently by the co-operating institutes: A direct measurement was performed by ULUND through weighing of reference specimens every second week. At institutes TTL and FMPA the climate data (temperature and relative humidity) were recorded. The moisture content evolution of the specimens was then calculated from the climate data as 2 to 3 weeks floating means of the theoretical equilibrium moisture content smoothed by a least square fitted higher order approximation function. The agreement between the computed moisture contents and the measured moistures at test time was good.

3.4.4 Comparative evaluation of the different test series

It should be stated that the load displacement (slip) curves, the failures and the fracture appearances were not affected by the different climate conditionings and fully resembled the results of the ramp load reference tests at 20°C/65%RH. Table 3.4.2, contains a comprehensive compilation of the bond shear strength results of all tests. Note, that bond shear strength is throughout related to hole diameter d_h The specified 5% fractile (characteristic) values are related to lognormal fits of the test results. All statements refer to metrically threaded steel rods and a nominal glue line thickness in the range of about 0,5 mm. It should be stated that the results obtained for the employed specific phenolic resorcinol adhesive and probably for the polyurethane adhesive, may not be fully generalized for these adhesive classes.

Effect of constant very wet and very dry climates on three different specimen configurations B, C and E (PRFs adhesive)

A compilation of the results is given in Table 3.4.3. In case of the constant wet climate of 85% relative humidity, leading to a mean moisture content of about 18%, the strength reductions vs. the results at reference climate conditions 20°C/65%RH were very similar on the mean and characteristic strength level. Specimen configurations B and E, although differing significantly with respect to anchorage length and angle between rod and grain, showed closely matching strength results. On the average a strength reduction to 80% of the reference climate conditions was obtained. Specimen configuration C revealed a less severe strength reduction to about 90% of the reference values. However, the number of specimens and test series allows no conclusion whether this difference is systematic or arbitrary. In a rough summary of all test series (ΣBCE) at wet climate the following can be stated: A constant wet climate (85%RH, MC=18%) acting on mechanically unloaded specimens for a period of about 15 months, delivers a strength reduction to about 85% of the ramp load reference values. Complementary tests performed in the frame of WP 5 indicate comparable results in case of a climate exposure time of only a few (3 to 6) months.

In case of the constant dry climate of 40%RH, leading to a mean moisture content of about 8%, the following effects on bond shear strength were obtained. For specimen configuration B no strength reduction vs. the reference values at 20°C/65%RH occured. In case of configuration E, consistent on the mean and characteristic strength level, a reduction to about 92% of the reference conditions was obtained. Configuration B showed on the mean strength level a moderate decrease to 95% of the reference values; the increased strength reduction at the 5% fractile level has to be seen in view of the high scatter of that test series. In a rough

46

summary of all test series (ΣBCE) at dry climate the following can be stated: A constant dry climate (40%RH, MC=8%) acting on mechanically unloaded specimens for a period of about 15 months delivers in average a very moderate strength reduction to about 97% of the ramp load reference values.

Table 3.4.2 Compilation of test results of all test series of WP 4

test series	institute	climate	climate duration	moisture content	adhesive	angle grain to rod	specimen configuration	No. of specimen	bond shear strength $f_{v,(k)}$ [1]		
-	-	' .	[months]	MC [%]	-	α [degree]	-	-	mean [N/mm²]	C.O.V. [%]	characteristic [N/mm²]
4.1/s	FMPA	const. 65% RH	6	11	PRFs	0	B	7	6,47	5,1	5,93
4.2/s	TTL					90	E	7	6,05	4,9	5,58
4.3/s	FMPA					0	C	7	5,95	5,0	5,47
4.4/s	FMPA	const. 85% RH	15	18	PRFs	0	B	7	5,24	3,9	4,92
4.5/s	FMPA					90	E	7	4,81	5,3	4,40
4.6/s	FMPA					0	C	7	5,60	7,3	4,93
4.7/s	TTL	const. 40% RH	15	7.6	PRFs	0	B	7	6,66	7,6	5,87
4.8/s	TTL					90	E	7	5,57	4,2	5,19
4.9/s	TTL					0	C	7	5,70	15,5	4,38
4.10/s	TTL	sh. - out	18 (winter)	14.6	PRFs	0	A	7	6,26	7,4	5,51
4.11/s	ULUND		15 (winter)	17,5		90	D	7	6,86	6,1	6,19
4.12/s	FMPA			15,5		0	B	10	6,57	8,1	5,72
4.13/s	TTL	sh. - out	22 (summer)	10.3	PRFs	0	A	7	6,54	7,3	5,81
4.14/s	ULUND		21 (summer)	14		90	D	6	6,25	5,2	5,73
4.15/s	FMPA			14		0	B	10	5,94	11,0	4,87
4.16/s	ULUND	sh. - out	6 [3] (winter)	18,3	PRFs	0	B	7	6,39	4,1	5,97
4.17/s	ULUND			18,3	PUR	0	B	7	6,47	12,4	5,25
4.18/s	ULUND			18,3	EP	0	B	7	7,55	9,4	6,40
4.19/s [2]	TTL			14.6	EP	0	B	7	4,58	8,7	4,09
4.20/s	ULUND			18,3	PRFs	90	D	7	6,38	4,8	5,88

[1] related to hole diameter $d_h = d_{nom} + 1$ mm; $f_v = F_u / (d_h \pi l_a)$

[2] FRP rod; all other test series steel rods with metric thread

[3] test series 4.19/s was tested after 18 months conditioning

Table 3.4.3 Compilation of test results on the effect of constant very wet and constant very dry climate, respectively, on three different specimen configurations bonded with phenolic resorcinol adhesive. Given are the bond shear strength ratios of the results at the different climate conditions vs. the ramp load reference results at 20°C/65%RH, both, on the mean and the characteristic level.

specimen configuration	Bond shear at strength ratios			
	constant wet climate (85% RH)		constant dry climate (40% RH)	
	mean strength level	characteristic strength level	mean strength level	characteristic strength level
B	81 %	83 %	103 %	99 %
C	94 %	90 %	95 %	80 %
E	80 %	79 %	92 %	93 %
Σ BCE	85 %	84 %	97 %	91 %

Effect of two different sheltered outdoor conditioning configurations at three European countries (PRFs adhesive)

Table 3.4.4 reveals major results of the test campaigns performed at TTL, ULUND and FMPA with sheltered outdoor conditions and test times in winter (15 months storage) and in summer (21 months storage), respectively. The moisture content of the specimens tested in winter varied between the samples in the different countries/climates from 14.6% to 17.5%. In case of the specimens tested in summer, the moisture contents varied between the samples in the different countries from 10.3% to 14%. The differences in mean moisture content between winter and summer tested specimens at the three different European locations were in the range of 2 to 4%. Irrespective of the different specimen configurations the following major result can be stated:

Despite the reduced moisture content in summer, the strengths of the specimens tested in summer were partly statistically significant lower as compared to the strengths of the specimens tested in the winter period. The strength values in summer, rather equally on the mean and characteristic level, conformed to about 0,92 of the strength values in the wet winter period.

It is assumed that the consistent result trend depends primarily on the different moisture history of the specimens tested in winter and summer, respectively, and the related internal stresses. Hereby it is assumed, backed by other results in the project, that the pure time difference of a few months between the specimen sets tested in winter and in summer has no influence.

Table 3.4.4 Ratios of bond shear strengths related to 21 months conditioning (testing in summer) vs. results obtained at 15 month conditioning (testing in winter) for 3 different specimen configurations (A, B and D) both, on the mean and characteristic strength level. Also given are the mean moisture contents

moisture contents strength ratios	specimen configuration and test site/institute			
	A	B	D	Σ BCE
	TTL South-East England	FMPA Southern Germany	ULUND Southern Sweden	Central Europe
mean moisture content MC 21 months [1] 15 months [2] mean moisture content difference ΔMC	10,3% 14,6% 4,2%	14% 15,5% 1,7%	14% 17,5% 3,5%	summer $\approx$ 12,7% winter $\approx$ 15,8% ΔMC $\approx$ 3,1%
$f_{v, mean, 21 months}/ f_{v, mean, 15 month}$	0,96	0,90	0,91	0,92
$f_{v, 05, 21 months}/ f_{v, 05, 15 month}$	0,95	0,85	0,93	0,91

[1] 22 month in case of config. A

[2] 18 months in case of config. A; 16 months in case of config. D

Effect of two humid conditionings on specimen configuration B bonded with three different adhesives

Following the effect of a 6 months storage at sheltered outdoor climate conditions with test time in winter (MC = 18,3 %) is compared with the bond capacities obtained after storage in a constant humid climate of 85 % RH for 3 months (MC = 18,1 %) and with the strength values at reference conditions of 65 % RH. Table 3.4.5, contains a compilation of the mean and

characteristic bond shear strength values obtained in the respective test series for the three different adhesives. Also given are the strength ratios of the mean and characteristic values at 3 and 6 months climate storage respectively related to the ramp load results. The following major results can be stated:

Table 3.4.5 Compilation of mean and characteristic bond shear strength values obtained in two humid conditionings (3 months storage in 85% and 6 months sheltered outdoor storage with test time in winter) and at reference conditions (20°C/65% RH). Also given are the strength ratios of the results at both humid conditionings vs. the results at reference conditions.

strength level	type of adhesive	bond shear strength			strength ratios	
		conditioning configurations				
		ramp 65%	3 months 85%	6 months winter	3 months 85% vs. ramp 65%	6 months (winter) vs. ramp 65%
		N/mm^2				
$f_{v,mean}$	PRF	6,47	5,52	6,39	0,85	0,99
	PUR	7,99	6,80	6,47	0,85	0,81
	EP	6,71	6,92	7,55	1,03	1,13
$f_{v,0,5}$	PRF	5,93	4,99	5,97	0,84	1,01
	PUR	6,77	5,76	5,26	0,85	0,78
	EP	4,93	5,58	6,40	1,13	1,30

For PUR, in case of the storage in constant humid climate of 85 % RH, bond strengths decreased to 0,85 of the reference values at 65%RH, equally on the mean and characteristic strength level. Bond strengths of the sheltered outdoor test series decreased rather equal on the mean and characteristic level to about 0,79 relative to reference bond strengths. Disregarding minor differences in moisture contents, it is interesting to note that the strength decrease at sheltered outdoor climate was more expressed as compared to constant humidity conditions. This result trend was not obtained in case of the related PRFs test series although the strength decrease of the PRFs at constant 85 % RH conditions was equal to that of the PUR bonds. For PRFs the strengths of the sheltered outdoor climate tests were equal to those at reference conditions.

The reason for the different behaviours of the PUR and PRFs adhesives in the 6 months test series is not obvious. On the other hand, it is highly probable that the difference is not accidental. A possible explanation could be that the bond lines of the specifically employed PUR adhesive age faster; however this could only be verified with additional tests with longer conditioning times.

For the epoxy significant differences as compared to the PUR and PRFs bonds exist. Contrary to the PUR and PRFs adhesives, the storage at constant 85 % RH did not forward an expressed strength decrease but instead an increase vs. the reference values at 65 % RH of 3% and 13 % at the mean and characteristic level, respectively. This strength increase was even more pronounced in the test series with 6 months storage and test in winter; here the mean and characteristic strengths surpassed the reference values by 13% and 19 %, respectively.

The reason for the strength increases of the epoxy after conditioning in constant or variable humid environment is at least twofold. First, the epoxy adhesive is moisture insensitive, at least for the regarded moisture content ranges, what was verified in specific adhesive tests acc. to EN 302-1, too. This, however, would exclusively forward an insensitivity vs. increased

moisture content, but not strength increases. The latter are assumed to result partly from a less steep stress gradient along bond length due to reduced timber stiffness at higher moisture content and from post curing effects.

3.4.5 Conclusions

The results of the experimental study revealed that the moisture content at test time and the moisture history and hereby the conditioning time affect the bond strength of mechanically unloaded specimens with glued-in steel rods. The effects are qualitatively and quantitatively different for different adhesive types. The influences of moisture and time (in terms of moisture history) are in the same order of magnitude for different specimen configurations comprising rod dimensions and angle between rod and grain. The investigated climates comprised the whole spectrum of moisture scenarios realistically perceivable for service class 1 and 2 conditions.

During the different climate histories internal stresses may occur due to several reasons, being cross-sectional anisotropy of shrinkage/swelling coefficients, strain mismatch between hygroscopic wood and non-hygroscopic steel and uneven moisture distributions in the cross-section. The internal stresses may act favourable or unfavourable on load capacities hereby compensating partly or completely pure moisture and time effect features of the bond line layer. The experienced moisture/time effects very roughly lead to changes of ± 15% of the short-term ramp load bond strength at reference conditions 20°C/65% RH. The obtained results and trends were in general consistent on the mean and characteristic strength level. Concerning the different adhesive types, the following can be stated:

The employed specific phenolic resorcinol adhesive (PRFs) and the polyurethane adhesive are obviously strongly susceptible to an increased moisture content. Compared to reference climate conditions (20 °C/65 % RH) the bond shear strengths decrease by maximally 20 % after several months of exposure to constant/variable humid climate. However, comparable strength decreases can also occur after sheltered outdoor storage of about 2 years and testing at a rather moderate mean moisture content of about 13 % in summer. This result is most probably bound to internal stress effects due to uneven cross-sectional moisture distributions. The climate history and the related moisture evolution plays an important role. This is obvious from results of tests performed at winter and summer where consistently the effect of pure moisture was fully compensated by a moisture history leading to unfavourable internal stresses. Vice versa there are also results suggesting, otherwise unexplicable, a strength increasing effect of internal stresses.

The epoxy adhesive reveals a strength increase of maximally about 20 % at higher moisture content and tends to increased strength with longer conditioning times. These results are assumingly bound to the combined effects of moisture insensitivity of the adhesive, strength increasing post curing of the adhesive, and to stiffness reduction and increased stress relaxation of the timber at higher moisture content. Details from this WP can be found in Aicher 2001d.

3.5 WP 5 – Duration of load test on full-sized glued-in rod specimens
3.5.1 Objectives
The objective of work package 5 (WP 5) was to investigate the time and climate (moisture and temperature) dependent strength degradation, i.e. duration of load (DOL) effect of a constant load of a certain nominal ramp load strength level acting on full-sized glued-in rod specimens made of glulam. The results shall serve for a prediction of the creep-rupture in different climate scenarios comprising naturally variable climates at sheltered outdoor conditions, constant very wet climate and cyclically changing very warm and dry climate conditions. The content of the extensive experimental campaign was shared by three partners, ULUND, TLL and FMPA. Detailed descriptions of the performed work and of the results are given in the technical reports (Bainbridge and Mettem 2001c, Aicher 2001c and Aicher 2002).

3.5.2. Work program
The workplan of WP 5 is stated in Table 3.5.1; the workplan conforms with some minor revisions, agreed upon by all WP 5 partners, to Table 10 of the Technical Annex of the research contract. All stated tests were performed and several complementary investigations (see below) were done in order to enable a better interpretation of the results. The experiments comprised three completely different experimental campaigns with respect to climate conditions, being

- DOL tests at sheltered outdoor climate. The tests were conducted by TTL in the South-East of England and by ULUND in Southern Sweden; a condensed description of the climate conditions is given below.
- DOL tests in an artificial very humid constant climate of 85% RH at 20°C (FMPA).
- DOL tests in an artificial cyclically (sinsoidally) varying very warm and dry climate within the limits of 25°C to 55°C and a relative humidity of 45% to 12% (FMPA).

The climate conditions in the TTL tests were such: relative humidity RH (daily averages) varied roughly from 55 to 85 % and in average was about 70%; the average temperature throughout the test period was about 15°C. In the ULUND tests, the relative humidity varied from 65 to 95% with an average value of 79%; the average temperature was 9°C.

Within six test series groups, 5.1 to 5.6, comprising several sub-groups, in total 30 different DOL test series were performed. The majority of the tests (26 series) was conducted with axially tension loaded rods glued-in parallel to grain; four test series were performed with rods glued-in perpendicular to grain. Almost all tests, except one test series with FRP rods, were done with metrically threaded steel rods. Two different configurations concerning rod diameter d_a and length ℓ_a resp. rod slenderness ($\lambda = \ell_a / d_a$) were investigated: 18 test series were performed with rod dimensions of $d_a = 16$ mm and $\ell_a = 160$ mm (so, $\lambda = 10$) and 12 test series were done with $d_a = 8$ mm, $\ell_a = 160$ mm (so, $\lambda = 20$).

Most of the six test series groups 5.1 to 5.6 comprised a comparative evaluation of the effect of three different adhesive types being a special softening type phenolic resorcinol adhesive (PRFs), an epoxy adhesive (EP) and a polyurethane adhesive (PUR).

51

Table 3.5.1 Workplan for workpackage WP5; conforms to revised table 10 of Technical Annex of the research contract.

Institute	Test series group	Test series sub group	Climate in ramp load	Climate in DOL	material combination*	rod Ø (mm)	anchorage length (mm)	slenderness λ	angle load to grain	adhesive type	ramp load tests [1]	DOL tests [1] 0.8 Fu	DOL tests [1] 0.7 Fu
ULUND	5.1	5.1a	20°/65 %	outdoor	ST/W_{ref}	16	160	10	0	PRF	5.1a/r (7)	5.1a/0.8 (5)	5.1a/0.7 (5)
ULUND		5.1b	20°/65 %	outdoor	ST/W_{ref}	16	160	10	0	PUR	5.1b/r (7)	5.1b/0.8 (5)	5.1b/0.7 (5)
ULUND		5.1c	20°/65 %	outdoor	ST/W_{ref}	16	160	10	0	EP	5.1c/r (7)	5.1c/0.8 (5)	5.1c/0.7 (5)
TTL	5.2	5.2	20°/65 %	outdoor	FRP/W_{ref}	16	160	10	0	EP	5.2/r (7)	5.2/0.8 (5)	5.2/0.7 (5)
ULUND	5.3	5.3a	20°/65 %	outdoor	ST/W_{ref}	16	160	10	90	PRF	5.3a/r (7)	5.3a/0.8 (5)	5.3a/0.7 (5)
ULUND		5.3b	20°/65 %	outdoor	ST/W_{ref}	16	160	10	90	PUR	5.3b/r (7)	5.3b/0.8 (5)	5.3b/0.7 (5)
ULUND	5.4	5.4a	20°/65 %	outdoor	ST/W_{ref}	8	160	20	0	PRF	5.4a/r (7)	5.4a/0.8 (5)	5.4a/0.7 (5)
TTL		5.4b	20°/65 %	outdoor	ST/W_{ref}	8	160	20	0	PUR	5.4b/r (7)	5.4b/0.8 (5)	5.4b/0.7 (5)
TTL		5.4c	20°/65 %	outdoor	ST/W_{ref}	8	160	20	0	EP	5.4c/r	5.4c/0.8 (5)	5.4c/0.7 (5)
FMPA	5.5	5.5a	20°/65 %	20°/85 %	ST/W_{ref}	16	160	10	0	PRF	5.5a/r 85 (7)	5.5a/0.8 (5)	5.5a/0.7 (5)
FMPA		5.5b	20°/65 %	20°/85 %	ST/W_{ref}	16	160	10	0	PUR	5.5b/r 85 (7)	5.5b/0.8 (5)	5.5b/0.7 (5)
FMPA		5.5c	20°/65 %	20°/85 %	ST/W_{ref}	16	160	10	0	EP	5.5c/r 85 (7)	5.5c/0.8 (5)	5.5c/0.7 (5)
FMPA	5.6	5.6a	20°/65 %	50°C	ST/W_{ref}	8	160	20	0	PRF	5.6a/r 50 (7)	5.6a/0.8 (5)	5.6a/0.7 (5)
FMPA		5.6b	20°/65 %	50°C	ST/W_{ref}	8	160	20	0	PUR	5.6b/r 50 (7)	5.6b/0.8 (5)	5.6b/0.7 (5)
FMPA		5.6c	20°/65 %	50°C	ST/W_{ref}	8	160	20	0	EP	5.6c/r 50 (7)	5.6c/0.8 (5)	5.6c/0.7 (5)

[1] number in parenthesis is number of specimens

* ST = steel, FRO = glassfiber, W_{ref} = C 35, W_{bw} = C 24

The specimen built-up conformed closely to the configurations investigated in WP 1. The specimens with axially tension loaded rods glued-in parallel to grain consisted of two opposite rods acting in one load line. In order to enforce failure at the distinct test rod where partially slip measurements were performed, both rods had different dimensions whereby the support rod had a 1,8 times higher bond area. The specimens with axially tension loaded rods bonded-in perpendicular to grain were beam-like with the test rod glued-in at mid-span parallel to beam depth; the loading conformed to 3-point bending. At all test institutes the specimens were loaded in specially designed resp. adapted test rigs. The rigs used at TTL and FMPA were based on a lever principle, the rigs at ULUND incorporated a load amplification system with wheels and ropes. The time to failure was throughout captured with electrical counters. Slip-time curves were measured in all test series groups 5.5 and 5.6 in order to obtain deeper insight into the damage evolution. The climate was monitored at all test sites.

The applied loads conformed as planed in most test series to nominal load (or stress) levels of 0,8 and 0,7 of the mean ramp load capacity of the specific specimen configuration at a constant reference climate. In all tests conducted at sheltered outdoor climate and at high constant relative humidity (85%RH), the reference climate was 20°C/65%RH. In the tests at cyclic very warm and dry climate, the load levels (0,7 and 0,8) were related to ramp load results at a reference climate of 50°C. The ramp load reference values (15 test series) were throughout determined with 7 specimens each, then fitted with a lognormal distribution. About half of the ramp load test series (those at 20°/65% RH) were conducted as part of WP 1, part WP 1.3. For each nominal stress level of the DOL tests 5 equal specimens were used in most test series. The respective third failing specimen (No. 50%) was considered to represent the median time to failure $t_{F, mean}$ at the respective nominal stress level of the specific DOL series.

3.5.3 Moisture and temperature modification factors

The time and climate dependent strength degradation $k_{DOL} = k_{mod}$ (following equivalently termed k_{mod}) as related to ramp load reference conditions at 20°C/65% RH may be separated into the "pure" effects bound to time, moisture and temperature, i.e. $k_{DOL} = k_{time} \cdot k_{mc} \cdot k_T$. Factors k_{mc} and k_T represent the ratios of mean or characteristic ramp load bond strengths, here at constant 85% RH and at constant 50°C conditions, respectively, vs. strengths at reference conditions 20°C/65%RH. The moisture content of the ramp load and DOL specimens tested at 85%RH was 18,1% in average. Table 3.5.2a, contains a compilation of here obtained modification factors.

It can be stated that the bonds with the specific PRFs and PUR adhesives exhibited distinct climate induced short-term strength reductions. In the moist climate PRFs and PUR strengths equally decreased by 15%. In the warm climate the mean strength reduction for PRFs was 23% and 13% for PUR. Contrary, slightly (4%) resp. considerably (16%) increased mean and characteristic short-term strengths of the epoxy bonded connections were recorded under the influence of both climates, probably due to post-curing (temperature) resp. stress redistribution (moisture) processes. The imposed climate treatments seeming reduce the strength scatter.

Table 3.5.2a Compilation of moisture and temperature modification factors obtained in ramp loading

modification factors for	PRFs mean	charact.	PUR mean	charact.	EP mean	charact.
moisture k_{mc}	0,85	0,84	0,85	0,85	1,03	1,13
temperature k_T	0,77	0,66	0,87	0,91	1,05	1,18

Table 3.5.2b Nominal DOL or target stress levels related to reference conditions of 65%RH and 85%RH, respectively

nominal DOL stress levels	PRFs 'low'	'high'	PUR 'low'	'high'	EP 'low'	'high'
$SL_{nom,65\%RH}$	0,7	0,8	0,7	0,8	0,7	0,8
$SL_{nom,85\%RH}$	0,82	0,94	0,82	0,94	0,68	0,76

Table 3.5.2c Nominal DOL stress levels related to reference conditions of 20°C and 50°C, respectively

nominal DOL stress levels	PRFs 'low'	'high'	PUR 'low'	'high'	EP 'low'	'high'
$SL_{nom,50°C}$	0,7	0,8	0,7	0,8	0,7	0,8
$SL_{nom, 20°C}$	0,54	0,62	0,61	0,70	0,74	0,84

3.5.4 DOL results – comprehensive compilation

Table 3.5.3 contains a condensed compilation of the most important results of all DOL test series 5.1a to 5.6c. Given are the experimental median times to failure $t_{F,mean}$ for both investigated nominal load levels SL_{nom} = 0,7 and 0,8. For test series 5.4a the $t_{F, mean}$ values are derived from a linear regression through data points at several different nominal load levels. In case of test series 5.4b and 5.4c with more than 2 nominal stress levels, estimates for the median times to failure at one of both load levels (0,7 resp. 0,8) are given. Further, for test series 5.2 dealing with the DOL effect of glued-in FRP rods, no substantial DOL conclusions are possible as almost all specimens failed premature due to loading eccentricities (Bainbridge and Mettem 2001c). Additionally, Table 3.5.3 specifies for all test series except for 5.4b and 5.4c and for the tests at elevated temperatures (5.6b and 5.6c), the coefficients of linear DOL trend lines i.e. stress level vs. time to failure curves, as a basis of k_{DOL} or k_{mod} and k_{time} values.

Figures 3.5.1 to 3.5.3 give graphical representations of the test/analysis results in terms of stress level (SL) vs. time to failure (t_F) curves and data points. Figure 3.5.1 shows the results at constant humid climate, Figure 3.5.2 contains the results at sheltered outdoor climate and Figure 3.5.3 visualizes the results at varying elevated temperature. For most test series where empiric median times to failure exist, exclusively the median values and their linear interpolation is given. For those test series where the DOL trend lines are based on regressions through individual or multiple nominal stress levels or in case of time-independent results (5.6b and c) the individual data points are given, too. For a comparative assessment of the results, all graphs show the Madison DOL trend line, too. Following the results are discussed in detail.

Table 3.5.3 Compilation of test results of all DOL test series 5.1a to 5.6c in different climate environments. Given are the median times to failure at two load levels and the coefficients of linear DOL trend lines.

angle rod to grain (degree)	glued rod length (mm)	adhesive	test series	institute	rod diameter (mm)	climate at DOL test	median times to failure at nominal load/stress levels (related to 20°C/65% RH [1]) $t_{F,mean}$ SL = 0,8 (h)	median times to failure SL = 0,7 (h)	coefficient of linear DOL trend line SL(t) = a - b lg t [h] a	coefficient b
0	160	PRFs	5.1a	ULUND	16	sh. outdoor	6,58	157,15	0,589	0,073
			5.5a	FMPA	16	20°85%	0	2,48	0,714	0,049
			5.4a	TTL	8	sh. outdoor	0,58 [2]	27,12 [2]	0,786	0,060
		PUR	5.1b	ULUND	16	sh. outdoor	1,60	55,58	0,813	0,065
			5.5b	FMPA	16	20°85%	0	1,15	0,690	0,032
			5.4b	TTL	8	sh. outdoor	-	≈ 144 [3]	- [4]	- [4]
		EP	5.1c	ULUND	16	sh. outdoor	42,7	2136,0	0,896	0,059
			5.5c	FMPA	16	20°85%	83,2	3120,0	0,922	0,064
			5.4c	TTL	8	sh. outdoor	≈ 96 [5]	-	- [4]	- [4]
90	160	PRFs	5.3a	ULUND	16	sh. outdoor	64,97	457,30	1,014	0,118
		PUR	5.3b	ULUND	16	sh. outdoor	1,26	435,45	0,809	0,041
0	160	EP	5.2	TTL	16 [6]	sh. outdoor	-	-	- [5]	- [5]
0	160	PRFs	5.6a	FMPA	8	cyclic	(0,62) [7] 56,9	(0,54) [7] 3858	0,688	0,042
		PUR	5.6b	FMPA	8	temperature	(0,70) [7] 23,0	(0,61) [7] 4,5	-	-
		EP	5.6c	FMPA	8	25°C – 55°C	(0,84) [7] 31,5	(0,74) [7] 50,3	-	-

[1] except for test series 5.6a – c; there the nominal stress levels 0,7 and 0,8 are related to ramp tests after conditioning at 50°C,
[2] acc. to specified DOL trend line, [3] derived for average nominal stress level of 0,72 ± 3 (Aicher 2002), [4] no trend line evaluation possible,
[5] rough estimate based on 3 specimens with nominal stress levels of 0,78...0,80...0,83 (Aicher 2002), [6] FRP rod, [7] stress levels related to 20°C/65% RH
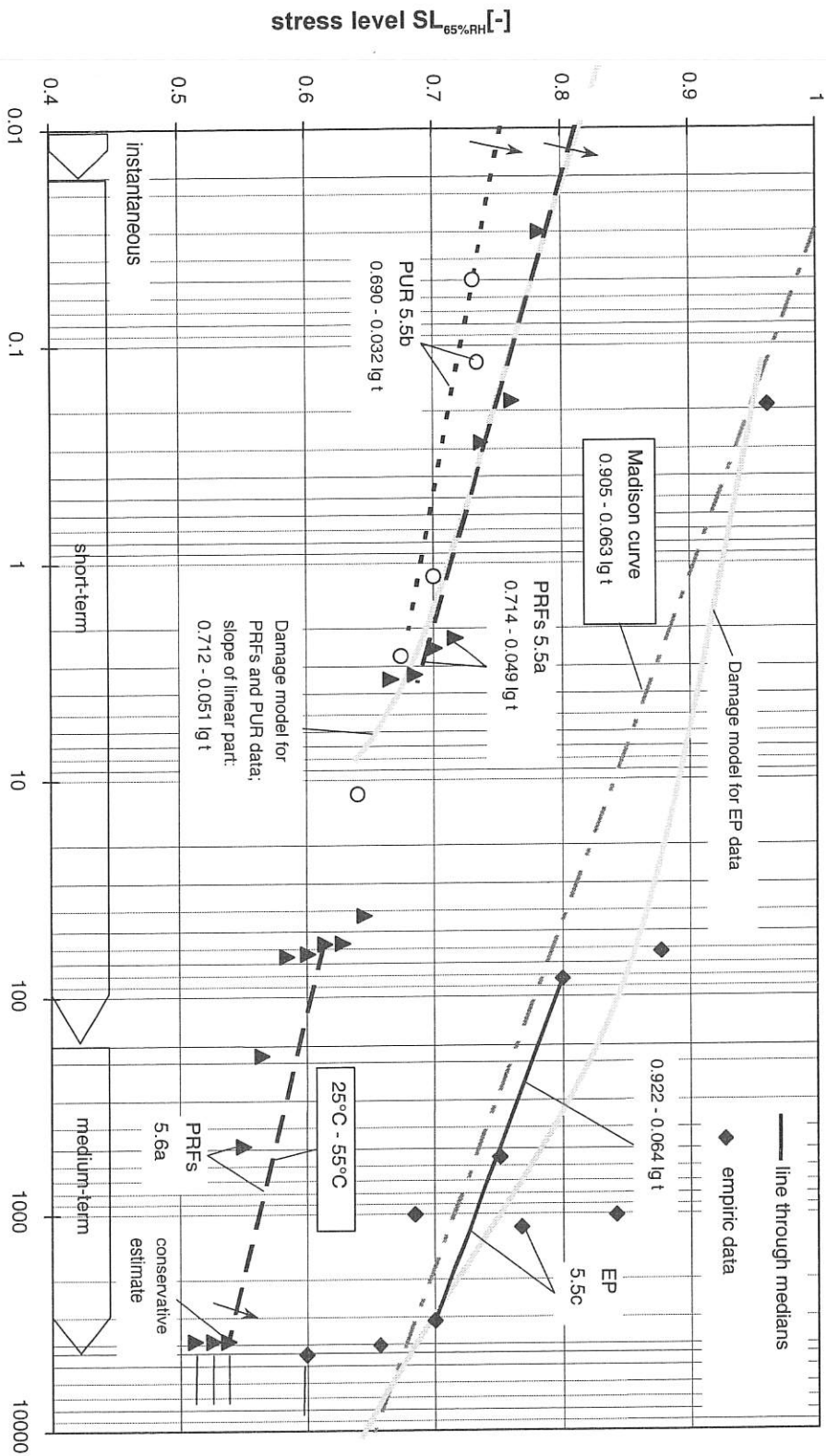
stress level SL$_{65\%RH}$ [-]

time to failure t$_f$ [h]

instantaneous

short-term

medium-term

instantaneous

conservative estimate

PUR 5.5b
0.690 - 0.032 lg t

Madison curve
0.905 - 0.063 lg t

PRFs 5.5a
0.714 - 0.049 lg t

Damage model for
PRFs and PUR data;
slope of linear part:
0.712 - 0.051 lg t

Damage model for EP data

0.922 - 0.064 lg t

25°C - 55°C

PRFs
5.6a

EP
5.5c

—— line through medians
◆ empiric data

Figure 3.5.1 Stress level vs. time to failure diagram of the DOL results at constant humid (85%RH) climate and for PRFs bonds at cyclic warm climate. Given are the individual failure stress levels, linear DOL approximation lines through median times to failure (EP) and through all data in case of PRFs and PUR, respectively. Theoretical DOL lines based on damage modelling are given, too.
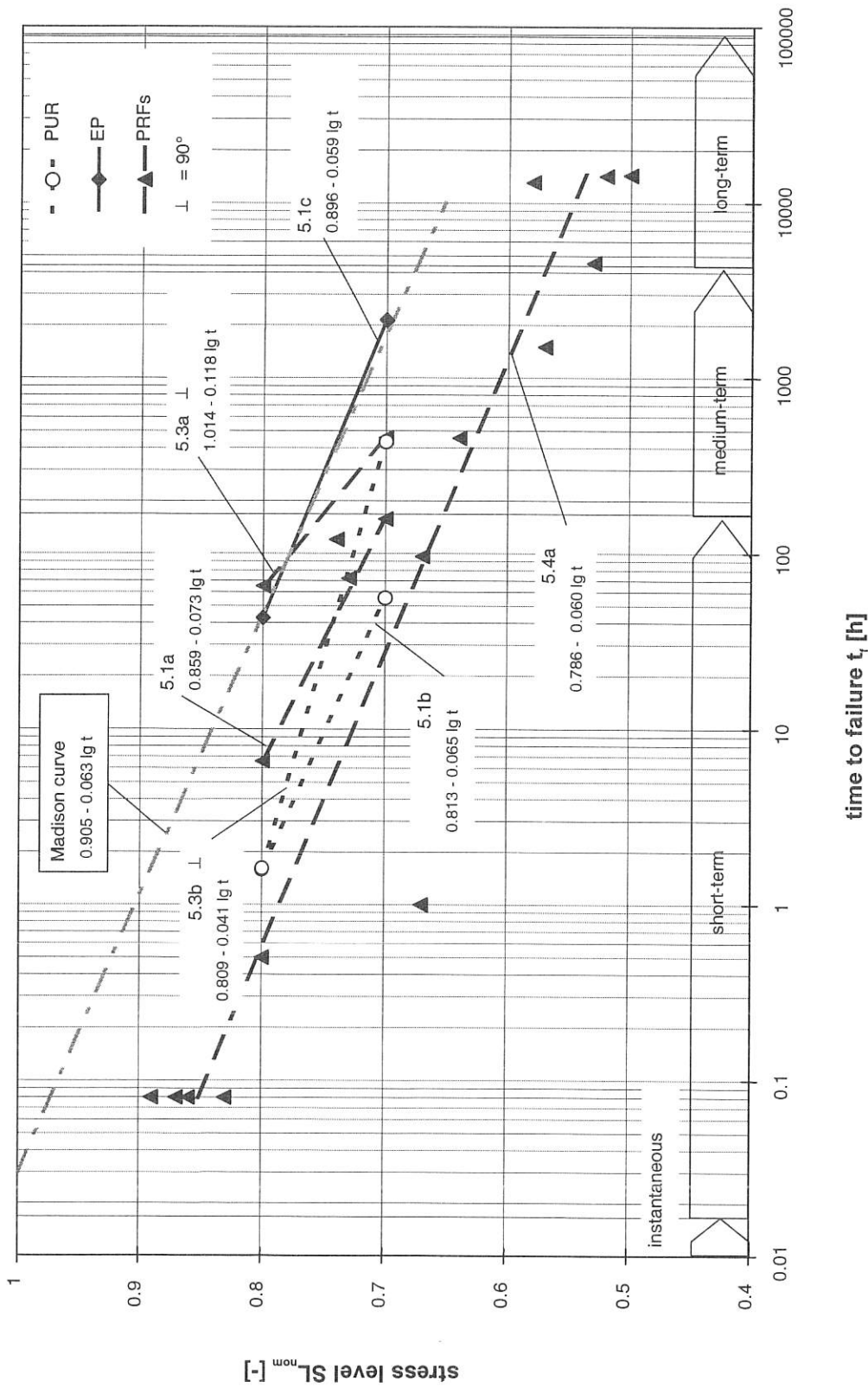
56

Figure 3.5.2 Stress level vs. time to failure diagram of the DOL results at sheltered outdoor conditions. All DOL trend lines except for test series 5.4a represent lines through the median times to failure. The line for 5.4a represents a linear regression through all results at different (> 2) nominal load levels.
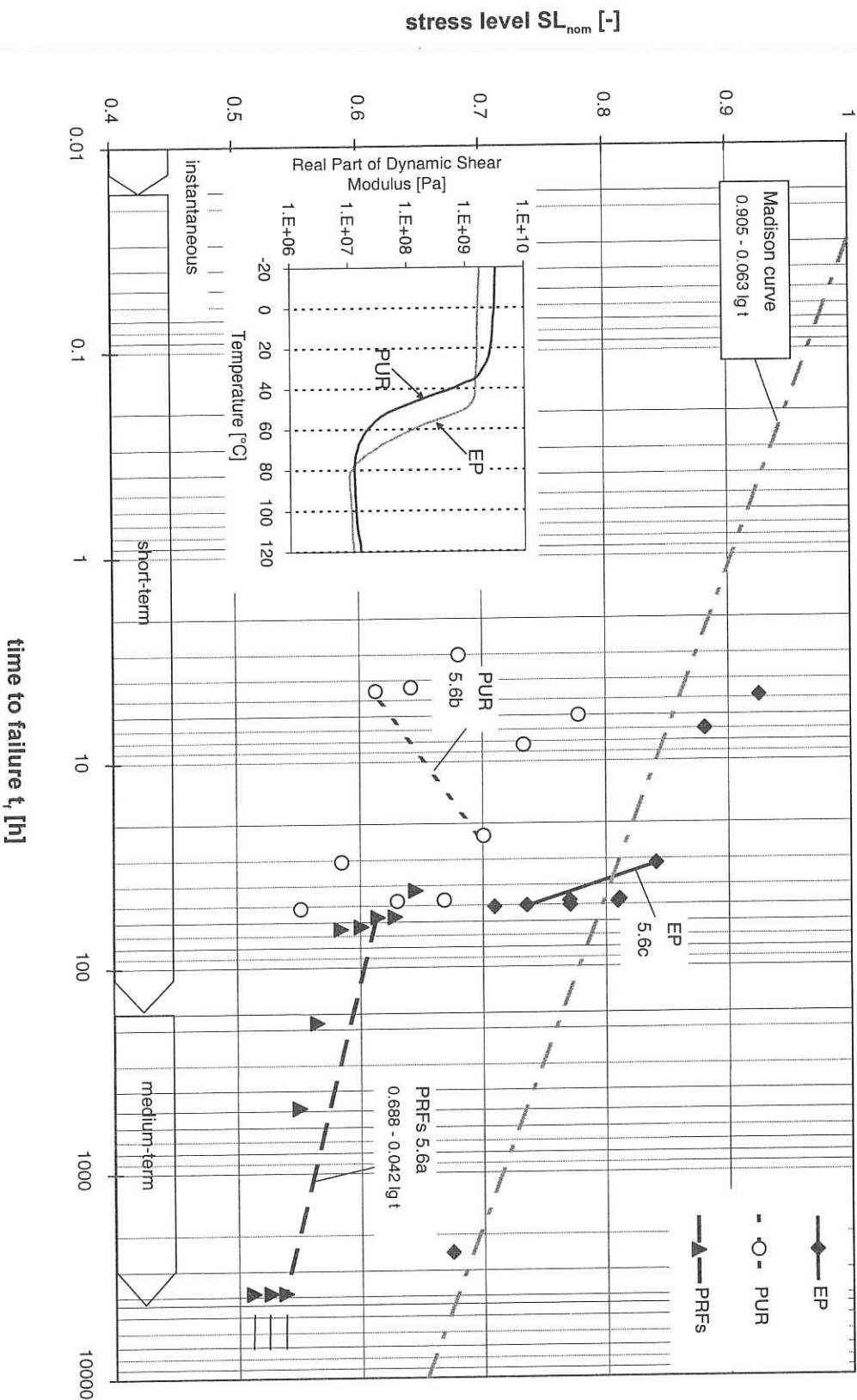
Figure 3.5.3 Graphical representation of the DOL test results at varying warm temperatures between 25 to 55°C. Given are the individual stress level – time to failure data points and the lines through the median times to failure. For EP and PUR the lines do not represent a DOL trend line (see text) ! Also given are shear modulus vs. temperature results of thermo-mechanical tests acc. to ASTM D 4065 for the EP and PUR adhesive.

Table 3.5.4 Compilation of duration of load modification factors $k_{DOL} = k_{mod}$ and k_{time} of load times (1week respl 6 months) for short and medium term duration for all (except 2) DOL test series, based on the linear trend lines given in Table3.5. 3. For test series 5.6b and 5.6c, i.e. EP and PUR bonds subjected to warm temperatures of $25 - 55°C$ no sensitive values can be given.

adhesive or wood	test series of reference	climate °C / %RH	k_{mc} (k_T)	short term duration of load (1 week) $k_{DOL}(1week) = SL(168h)$	short term $k_{time} = k_{DOL} / k_{mc/T}$	medium term duration of load $k_{DOL}(6months) = SL(4380h)$	medium term $k_{time} = k_{DOL} / k_{mc/T}$
wood	EC5	service class 1 & 2	--	0,9	0,9	0,8	0,8
	Madison curve	20/65	--	0,76	0,76	0,67	0,67
Epoxy	5.5c	20/85	1,03	0,78	0,76	0,69	0,67
	5.1c	sh.-out	--	0,76	0,76	0,68	0,67
	all	service class 1 & 2	--	0,76	0,76	0,67	0,67
PRFs	5.5a	20/85	0,85	0,60	0,71	0,54	0,64
	5.1a	sh.-out	--	0,70	0,7	0,59	0,59
	5.3a	sh.-out	--	0,75	0,75 (} 0,70)	0,58 (} 0,58)	0,58 (} 0,58)
	5.4a	sh.-out	--	0,65	0,65	0,57	0,57
	all	service class 1 & 2	--	0,71	0,71	0,60	0,60
	5.6a	25°C-55°C	0,77	0,59	0,77	0,54	0,70
PUR	5.5b	20/85	0,85	0,60[1]	0,71[1]	0,54[1]	0,64[1]
	5.1b	sh.-out	--	0,67	0,67	0,58	0,58
	5.3b	sh.-out	--	0,72	0,72 (} 0,70)	0,66 (} 0,58)	0,66 (} 0,62)
	all	service class 1 & 2	--	0,70	0,70	0,63	0,63

1) acc. to slope of damage analysis curve

59

3.5.5 DOL results at constant humid (85% RH) conditions
General

The DOL specimens were conditioned about 4 months to weight equilibrium in the humid test climate before loading. The nominal DOL or target stress levels SL_{nom} were set to 0,7 and 0,8 of the ramp load results at 20°C/65%RH, equally for all adhesive types, i.e. $SL_{nom,\,65\%RH} = 0,7$ and 0,8. The corresponding nominal stress levels at 85%RH DOL conditions, $SL_{nom,\,85\%RH} = SL_{nom,\,65\%RH}\,(1/k_{mc})$, are specified in Table 3.5.2b. For the PRFs and PUR adhesive the nominal stress levels at the humid test conditions, $SL_{nom,\,85\%RH}$, are considerably higher compared to $SL_{nom,\,65\%RH}$, whereas for the epoxy adhesive the $SL_{nom,\,85\%RH}$ are slightly lower. It is obvious that for PRFs and PUR the 'high' stress level, $SL_{nom,\,85\%RH} = 0,94$ results in some overlapping of the ramp load strength distribution and the long-term stress level.

Results for PRFs and PUR bonds

At the 'high' stress level, in case of both adhesives, 3 of the 5 specimens failed premature during the rather long ramp loading time (0,5 h), so forwarding a median time to failure of zero. At the 'low' stress level only one PUR specimen failed premature. However, the survival times were very short for both adhesive types, stretching from a few minutes to maximally 11 hours. The median times to failure (t_F of the respective 3rd failing specimen) at $SL_{nom,65\%RH} = 0,7$, were 2,5 h and 1,2 h for the PRFs and PUR bonds, respectively, so not more than about 2 to 5 times longer than the duration of the ramp loading. In order to construct a DOL line, despite the lacking median t_F at the 'high' stress level, the individual stress levels of the specimens were determined with a ranking procedure. Hereby it was assumed that the DOL test batch has the same lognormally distributed ramp load strength distribution as obtained in the reference testing. The individual short term strength of each DOL specimen, and hence its individual stress level, was then assessed acc. to its cumulative DOL failure frequency. The individual SL – t_F data points were then fitted with a linear regression. An obvious inaccuracy however results from the very short survival times at the DOL load level. The damage accumulation beyond a certain stress threshold value SL_{thresh} – during the long duration of the ramp loading – results in a reduction of the recorded t_F times at the DOL level. In order to assess the pre-damage effect in ramp loading the PRFs and PUR test results were analyzed with the Canadian (Foschi) damage model, enabling the inclusion of the premature ramp load failures, too. The analysis delivered for both adhesives a rather similar set of model parameters (Aicher and Dill-Langer 2001). The theoretical damage curve, equal for the PRFs and PUR bonds is given in Figure 3.5.1 too. Especially for the PUR adhesive a considerable but plausible shift of the DOL curve towards a steeper inclination can be seen.

Results for EP bonds

A completely different DOL feature as compared to the PRFs and PUR bonds was obtained, only outwardly related to the fact that the nominal stress levels $SL_{nom,85\%RH}$ were considerably lower (compare Table 3.5.2b).

The median times to failure for the EP specimens at the 'high' and 'low' stress levels were 83 h and 3120 h, respectively. One specimen with the lowest individual stress level of SL = 0,6 (acc. to ranking method) survived the test end at 4450 h. The high residual ramp load capacity of the survivor fully confirmed the calculated individual stress level. The slope of the DOL trend line through the median times to failure (-0,064) almost coincides with the slope of the linear Madison curve (-0,063); a rather similar good agreement exists for the constant values of the straight lines. As for the PRFs and PUR bonds also the epoxy data were analyzed by damage modelling, giving a completely different set of parameters hardly affected by ramp

load damage accumulation (no shift of empiric failure data points). The resulting damage model curve is given in Figure 3.5.1, too.

3.5.6 DOL results at sheltered outdoor conditions
General

Contrary to the tests at constant moist climate the tests at sheltered outdoor conditions were performed with 3 different specimen configurations (FRP bonds not counted); the rod length conformed always to 160 mm. The experiments comprised two rod diameters (d_a = 8 and 16 mm) and two angles (0° and 90°) between rod and grain (i.e. rod parallel resp. perpendicular to grain). Further, the tests were performed in different sheltered outdoor climates at two different places (South East of England and Southern Sweden). As lined out in detail following, the majority of the test series show a rather high degree of agreement (see Figure 3.5.2) and further, the results in general are very plausible when related to the tests at constant moist climate. The different climate and moisture evolutions in the specimens at the two test locations are discussed in (Bainbridge and Mettem 2001c, Aicher 2002). In a rough average the mean moisture contents (MC) of the specimens at the English test site varied in the range of about 11 to 14% (average MC ≈ 13%) whereas for the Swedish specimens a moisture range of about 13 to 18.5% (average MC ≈ 15.5%) was obtained.

Results for PRFs bonds

The discussion relates to test series 5.1a and 5.4a, both with rods parallel to grain, and test series 5.3a with rods perpendicular to grain. In case of test series 5.1a and 5.3a the median times to failure at both nominal stress levels represent empiric data points and the DOL trend lines are lines through the medians. In case of test series 5.4a the specified median times to failure at $SL_{nom,65\%RH}$ = 0,8 and 0,7 are based on a linear regression through 15 data points with considerably different nominal load levels. The latter test series comprised 5 specimens more than the other DOL test series due to an agreed shift of tests from WP 4. Compared to the tests at constant humid climate no premature failures at ramp loading to the 'high' stress level $SL_{nom,65\%RH}$ = 0,8 occurred, but the survival times, varying noticeable between the different test series, were very/rather short. In view of the anticipated scatter, the results are very consistent especially when regarding lower stress levels and longer times to failure.

For the 'high' stress level $SL_{nom,65\%RH}$ = 0,8 the median times to failure revealed the largest spread between the 3 test series (5.4a, 5.1a and 5.3a) differing by two logarithmic decades in the range of 0,5 h....<u>6.6 h</u>....65 h; the average median time to failure at the 'high' stress level was 24 h. For the 'low' nominal stress level $SL_{nom,65\%RH}$ = 0,7 the differences reduced to one logarithmic decade, i.e. 24 h...<u>157 h</u>..457 h, giving an average median time to failure of 213 h.

The assessments of the times to failure by the derived linear DOL trend lines for times of 1 week (168 h) and 6 months (4380 h), marking the EC5 time spans for short and medium term duration of load, give the following results (Table 3.5.4). For 1 week, the k_{DOL} values for the 3 test series are 0,70, 0,75 and 0,65, so in average 0,70. The latter value has to be compared to k_{DOL} = 0,60, derived in a rough estimate from the linear test approximation of the data at constant humid conditions. The fact that k_{DOL} at constant 85%RH is about 14% less compared to the test at variable climate is clearly related to the strong impact of the 'static' moisture modification factor k_{mc} = 0,85. If we compare k_{DOL} of the variable climate tests to the predominantly time dependent degradation factor k_{time} = k_{DOL}/k_{mc} = 0,71 of the tests at constant high humidity, then perfect agreement is obtained.

For 6 months duration of load the k_{DOL} values for the 3 test series, being 0,59, 0,58 and 0,57

with an average value of 0,58, differ only marginally. Comparing the mean $k_{DOL} = 0,58$ value of the variable climate environment to $k_{DOL} = 0,54$ and $k_{time} = 0,64$ of the constant high humidity tests, it can be noticed that $k_{DOL,var.climate} = 0,58$ is smaller compared to $k_{time,const.climate} = 0,64$ and rather close to $k_{DOL,const.climate} = 0,54$. This suggests, disregarding the very small statistical basis of the conclusions, that in variable climate acting over a longer period of accumulated load the pure time dependent strength degradation is aggravated by (mechano-sorptive) eigenstresses.

Regarding the effect of an angle between rod and grain on the DOL effect (investigated with same rod dimensions (test series 5.1a and 5.3a)), it has to be stated that the empiric median times to failure at the 'low' stress level 0,7 are in the same order of magnitude, i.e. 160 h and 460 h for the rods glued-in parallel and perpendicular to grain, respectively. The k_{DOL} extrapolations of the DOL trend lines to 6 months differ only marginally for both rod/grain angle configurations. Regarding the effect of rod diameter the tests do not prove a significant influence. In case of the bonds with 8 mm rod diameter this is empirically well supported especially for longer times to failure (data for more than 1 year). For times spans of 6 to about 12 months the extrapolated DOL trend lines for the bonds with 16 mm rods merge with experimental / regression data for the 8 mm rods.

Results for PUR bonds
The discussion relates to test series 5.1b and 5.4b, both with rods parallel to grain, and test series 5.3b with rods perpendicular to grain. In case of test series 5.1b and 5.3b the median times to failure at both nominal stress levels represent empiric data points and the DOL trend lines are lines through the medians. For test series 5.4b an empiric $t_{F,mean}$ time for the 'low' stress level can be deduced from the tests, being too tentative for the 'high' stress level, due to statistical reasons (Aicher 2002). Compared to test series 5.5b at constant humid climate with 3 premature failures during loading to the 'high' stress level $SL_{nom,65\%RH} = 0,8$, in all 3 PUR test series at variable climate only one specimen failed (test series 5.1b).

For the 'high' stress level, similarly to PRFs bonds at variable climate, the median times to failure (test series 5.1b and 5.3b) are very short, being 1,3h and 1,6 h, giving an average $t_{F,mean}$ of 1,4 h. For the 'low' nominal stress level $SL_{nom,65\%RH} = 0,7$ the median times to failure of test series 5.1b, 5.4b and 5.3b were 56 h...144 h...435 h, giving an average median time to failure of 212 h. (Note: the latter value does not change significantly when test series 5.4b with a specific test data evaluation (Bainbridge and Mettem 2001c, Aicher 2002) is excluded, then: $t_{F,mean} = 246$ h).

The assessments of the times to failure by the derived DOL trend lines (test series 5.1b and 5.3b) for times of 1 week and 6 months forward the following results. For 1 week the k_{DOL} values are 0,67 and 0,72, so in average 0,70. The average $t_{F,mean,1week}$ conforms exactly to the result obtained for the PRFs bonds at variable climate. For 6 months duration of load the k_{DOL} values are 0,58 and 0,66 with an average value of 0,62, again being rather close to the results obtained for PRFs bonds. Comparing the specified average k_{DOL} values for both time spans (1 week, 6 months) to the k_{DOL} results at constant humid climate conditions it is deemed sensible to base the comparison on the linear part of the damage model curve for PUR bonds, being almost similar to the linear regression based DOL trend line for PRFs bonds. Using this assumption, similar conclusions for k_{DOL} at variable climate vs. k_{DOL} and k_{time} at constant humid climate as in case of PRFs bonds are obtained. Regarding the effects of an angle between rod and grain and of rod diameter on the DOL effect, similar as for PRFs, no significant influences of both parameters can be stated in the frame of the rather limited

statistical basis of the conclusions.

Results for EP bonds

The discussion relates in first instance to test series 5.1c and 5.4c both with rods parallel to grain. The test results revealed that test series 5.5c dealing with DOL tests in constant humid climate could be incorporated in this evaluation, too. In case of test series 5.1c (and 5.5c) the median times to failure at both nominal load levels represent empiric data points and the DOL trend lines are lines through the medians. For test series 5.4c an empiric $t_{F,mean}$ time for the 'high' stress level can be deduced from the tests, being too tentative for the 'low' stress level due to statistical reasons (Bainbridge and Mettem 2001c, Aicher 2002).

At the 'high' stress level the median times of failure (test series 5.1c and 5.4c) were well comparable, i.e. 43 h and 96 h, giving an average $t_{F,mean}$ of 69 h. These results differ only very little from the median time to failure obtained at constant humid climate, where 83 h were obtained. The average $t_{F,mean}$ of the 3 test series regarded then becomes 74 h. At the 'low' stress level, test series 5.1c forwarded a median time to failure of 2136 h which in case of logarithmic scaling of life time, sensible for DOL data representations, is not very different from

$t_{F,mean} = 3120$ h of test series 5.5c at constant humid conditions (there also a slightly lower stress level of $SL_{nom,65\%RH} = 0,68$ due to $k_{mc} = 1,03$ existed). The linear DOL regression trend line obtained for test series 5.1c conforms very closely to the DOL approximation line for test series 5.5c. For a duration of load time of 1 week the trend line for test series 5.1c gives a k_{DOL} value of 0,76; compared hereto the DOL trend line for test series 5.5c forwards $k_{DOL} = 0,78$ and

$k_{time} = k_{DOL} / k_{mc} = 0,76$. Regarding 6 months duration of load, k_{DOL} for test series 5.1c is 0,67; for test series 5.5c (constant humid climate) the fully conforming quantities $k_{DOL} = 0,69$ and

$k_{time} = 0,67$ were obtained.

The test results do not prove assumptions on significant influences of the rod diameters on the DOL effect of epoxied rods, being in line with the results for PRFs and PUR bonds.

3.5.7 DOL results at very warm and dry climate

General

Due to the even more pronounced effect of the elevated temperature on the ramp load results of PRFs ($k_T = 0,77$), as in case of constant high humidity, the nominal stress levels of 0,7 and 0,8 were set with respect to ramp load results at 50°C ($SL_{nom, 50°C} = 0,7$ and 0,8); the resulting stress levels related to 20°C conditions, $SL_{nom, 20°C} = SL_{nom, 50°C} \cdot k_T$, are shown in Table 3.5.2c. The DOL loads were applied to the specimens within 2 minutes at a temperature of 20°C. Then the temperature variations/rises started. Due to technical reasons, the regular sinusoidal temperature cycling started 60 h after the first temperature increase.

Results for PRFs bonds

All specimens subjected to the 'high' stress level, $SL_{nom, 50°C} = 0,8$, failed within a rather narrow time range of 67 to 90 hours ($t_{F,mean} = 82$ h). No obvious relationship of the failures with the hight of the elevated temperatures could be stated: four specimens failed at temperatures of about 35°C. At the 'low' stress level, $SL_{nom, 50°C} = 0,7$, two specimens failed after about 200 resp. 500 hours and the remaining 3 specimens survived until the experiments were ended after 3860 h (Figure 3.5.3). The slip time curves of the survivors showed a rather constant creep rate after the initial primary creep; the residual strength of the survivors

63

determined in ramp loading at 20°C conditions were higher than the mean value in the ramp load tests at 50°C. Thus, any damage accumulation seems to have been ruled out by some hardening process.

The results indicate that the DOL behaviour reflects in first instance a time dependent degradation; the pure temperature effect is comprised in the rather servere modification factor for temperature $k_T = 0,77$. The results enable a rather conservative approximation of a stress level vs. time to failure line through $t_{F,mean} = 82$ h at $SL_{nom, 20°C} = 0,62$ and $t_F \approx 3860$ h of the surviving 3rd specimen at $SL_{nom, 20°C} = 0,54$: $SL_{20°C} = k_{DOL} = 0,69 - 0,042$ lgt [h]. Conversion to 50°C conditions delivers $SL_{50°C} = k_{time} = k_{DOL}/k_T$.

Results for PUR and EP bonds
Equally for both adhesives, PUR and EP, and completely different to the PRFs bonds the experiments revealed that the stress level has apparently no influence on the times to failure. In case of PUR, $t_{F,mean} = 4,5$ h at the 'low' stress level (failure times counted since first rise of temperature), was less compared to $t_F = 7,3$ h at the 'high' stress level. In fact, the bond failures are predominantly related to the temperature (in presence of the applied stress levels). The ambient temperature did not exceed 40°C in case of the 1st four failed specimens at $Sl_{nom, 50°C} = 0,7$; the bond line temperature acc. to measurements lags by about 5°C. Thermo-mechanical testing of the pure adhesive (see below) confirmed that the critical temperature of the specific PUR adhesive is in the specified range.

Qualitatively similar, the EP bonded specimens failed almost independent of stress level within very short time differences in the first temperature cycle reaching 55°C (critical temperature range: 50 to 55°C). The results for the PUR and EP specimens do not enable the derivation of a k_{DOL} or k_{time} relationship. Thus the lines through the median failures at the 'high' and 'low' stress levels of both adhesives given in Figure 3.5.3 just illustrate the location of the median t_F times.

The extreme temperature susceptibility of the specific PUR and EP adhesive bonds, not anticipated to that extent[1], was verified in several additional tests. These investigations comprised i.a. thermo-mechanical testing (relaxation spectrometry acc. to ASTM D 4065) and differential scanning calorimetry DSC acc. to DIN 53765-A-20. The thermo-mechanical tests (frequency 1 Hz) with pure adhesive specimens revealed for both adhesives extreme decreases of the dynamic shear modulus in the range of the glass transition temperature T_g (see inserted graph in Figure 3.5.3).

For PUR the glassy region ends already at about 25°C with a subsequent catastrophic decrease of the shear modulus between 30°C and 45°C. For EP, the glassy region ends at about 45°C with an expressed decrease between 45°C and 60°C. The latter is confirmed by the DSC results forwarding a glass transition temperature of 52°C in the first heating of the EP; in the subsequent second heating, due to effects of post-curing a far higher T_g value of 74°C was obtained.

---

[1] Based on the experience obtained from the temperature modification factor testing and in case of the EP from tests acc. to EN 301, the obviously extreme effect of post-curing at no or very low applied bond stresses was not anticipated.

3.5.8 Conclusions

The results of the performed DOL tests may be summarized in a comprehensive manner as following:

- The most important influence on the DOL effect is the adhesive type or class.
- The influence of the angle between rod and grain direction as well as of the rod dimensions (diameter and length) was not significant, irrespective of the specific adhesive.
- The DOL investigations on 3 different types of adhesives (an epoxy (EP), a 2component polyurethane (PUR) and a special softening type phenolic resorcinol (PRFs)) in different climates revealed that different adhesive classes, differentiated by different moisture susceptability moisture (modification factor k_{mc}) and temperature susceptability (temperature modification factor k_T and glas transition temperature T_g), show different life times under sustained loads.
- The investigated PRFs and PUR adhesive types showed rather similar behaviour concerning the DOL behaviour as related to moisture aspects and following are termed „moisture susceptible adhesives", denoted by a significant ramp load moisture modification factor (here: $k_{mc} = 0.85$).
- The investigated epoxy, as probably most epoxies, revealed almost indifference vs. moisture in short- and long-term loading, so can be termed a „moisture insusceptible adhesive".
- Despite of the completely different behaviour of the PUR and EP vs. moisture, and despite of very different short-term temperature modification factors k_T, both adhesive types revealed very low glass transition temperature ranges; both adhesive types are termed „low T_g adhesives". Note: „high" and „low" short-term temperature modification factors may be associated with comparably „low" T_g values, i.e. k_T and T_g values in general show very little or no correlation.
- Regarding the DOL behaviour of moisture susceptable (PRFs, PUR) and moisture insusceptable (EP) adhesives in different humid climate environments (without temperatures beyond about 30°C) the following quantitative results compiled in summary 1 were obtained:

Summary 1. Comprehensive compilation of all DOL test results at sheltered outdoor and constant humid (85% RH) climate with temperature below about 30°C. For comparison also the relevant numbers acc. to the Madison curve and Eurocode 5 are given.

adhesive (group) or wood	climate	DOL modification factor $k_{DOL} = k_{mod}$		median times to failure $t_{f, mean}$ in [h] at nominal stress levels (related to 20°C / 65% RH) of	
		short term 1 week (= 168 h)	medium term 6 months (= 4380 h)	SL = 0,8	SL = 0,7
PRFs + PUR	sheltered outdoor	0,7	0,6	13	213
	const. 85% RH	0,6	0,54	–	1,9
EP	sheltered outdoor + const. 85% RH	0,77	0,68	74	2628
solid wood (Madison curve)	≈ service class 1	0,76	0,67	46	1795
solid wood / glulam (Eurocode 5)	service class 1 & 2	0,9	0,8	≈ 4380	–

For the combined PRFs + PUR adhesive group it is not advisable to combine the results (in terms of $k_{DOL} = k_{mod}$ factors) at sheltered outdoor and constant 85% RH conditions, as the constant humid condition delivers for this group of moisture susceptible adhesives a distinctly set-off lower bound regarding the DOL behaviour. (Note: Rigorously taken, the climate with constant 85% RH acting over several weeks is in the frame of (severe) service class 2 climate conditions). For the PRFs + PUR adhesive group the $k_{DOL,1week}$ factors at const. 85% RH and at sheltered outdoor climate are 0,6 and 0,7 and for $k_{DOL,6months}$ values of 0,54 and 0,6 are obtained. For the epoxy adhesive (group) the results at sheltered outdoor and at constant 85% RH can be well combined. The DOL modification factors for the regarded time spans of accumulated load are $k_{DOL,1week} = 0,77$ and $k_{DOL,6months} = 0,68$.

Comparing the obtained k_{DOL} values (which are in line with the also given fully empiric median times to failure at the nominal stress levels of 0,7 and 0,8) with the values for solid wood acc. to the Madison curve and for solid wood / glulam acc. to Eurocode 5 the following can be stated: In case of epoxy a perfect agreement between the DOL results for the glued steel rod-timber bonds and the Madison curve predictions exists. This result is in line with the general failure feature of the EP bonds where the failure is predominantly a rather 'pure' wood failure in the adhesive / wood interface or at some distance from the interface (block pull-out). The group of moisture susceptible adhesives shows a more severe DOL effect as compared to the Madison curve. Roughly the k_{DOL} values of PRFs and PUR are 10%

66

(sheltered outdoor) and 20% (const.
85% RH), lower as compared to the Madison curve results.

Comparing the obtained DOL results with the k_{mod} values specified in Eurocode 5 for solid wood and glulam equally for service class 1 and 2 conditions, considerable discrepancies have to be stated. For EP the k_{DOL} values are 15% lower (equally for both regarded time spans) whereas for the PRFs and PUR adhesive group the k_{DOL} values are 24% and 33% lower (equally for both regarded time spans) in case of sheltered outdoor climate and constant 85% RH conditions, respectively.

Regarding the DOL behaviour of the temperature susceptable/low T_g adhesives the following results were obtained: In this context it is necessary to recall that the applied DOL loading/temperature regime (sequence of load application and temperature rise) is of eminent importance for the life time of the bonds. The crucial loading/temperature regime is that applied in the GIROD DOL tests where first the loads were applied at normal temperature of about 20°C and subsequent rises and variations of the temperature were started. With such a loading regime the considerable potential of post-curing of several "low T_g adhesives" is not/very little activated. The observed "DOL" failures of the "low T_g adhesives", PUR and EP, do not represent a time dependent bond degradation but a mere temperature induced bond failure. The tests revealed the vital importance of a sufficiently accurate determination of the glass transition temperature range of the employed adhesives by thermo-mechanical/ DSC tests. In view of the present classification of adhesives (type I and II) acc. to EN 301 the minimum T_g requirement for an adhesive employed for glued-in rods should aim at a safe use of the adhesive up to temperatures of 50°C. Depending on the width of the glass transition range of the specific adhesive this can lead to minimum T_g requirements in the range of about 55°C to 60°C. For several applications and/or locations (countries) higher T_g requirements up to about 70°C to 80°C may be necessary.

Regarding the design of glued-in rods acc. to Eurocode 5 and related thereto the approval / certification of appropriate adhesives, primarily the following two alternatives A and B regarding a safe inclusion of the duration of load effect are possible.

Alternative A: Appropriate testing (see below) of the DOL behaviour of the respective adhesive based on sufficient ramp load / temperature testing for determination of the modification factors k_{mc}, k_T and of the glass transition temperature T_g. Use of the adhesive specific bond properties (short-term bond strength **and** k_{mod} values) on the basis of a building certificate (eventually ETA) in the analysis.

Alternative B: Basis of alternative B is the assumption that no additional k_{mod} values beyond those specified today in EC 5 for solid wood and glulam should be introduced in the design analysis for sake of simplicity. In this case, obviously the difference between the effective k_{mod} values of the specific adhesive (group) and the settled / prescribed k_{mod} values in EC 5 have to be accounted for in a fictive reduction of the short-term bond shear strength of the specific adhesive. So roughly, the ramp load bond strength of moisture insusceptible adhesives, such as EP, excelled be k_{mc} values of about 1, should be reduced by about 15%. In case of moisture susceptible adhesives, such as PRFs and PUR, excelled by k_{mc} values of about 0,85, the ramp load bond strength should be reduced by about 30%. An additional reduction of the short-term bond strength values in case of low temperature modification values k_T can be necessary.

3.6 WP 6 - Effect of fatigue

Structural members are by their definition required adequately to resist the effects of actions applied to them throughout their design life. Structural components are subjected to two forms of action, variable (Q) and permanent (G). Permanent actions produce instantaneous effects and also have a further influence over time due to the effects of creep. Variable actions normally result in the repeated development of stresses below the ultimate strength of the material. Whilst they therefore induce instantaneous reversible effects, their repeated application can induce failure at even low stress levels due to fatigue.

The term fatigue is applied to a range of time and load related effects. In the context of this WP, fatigue relates to 'dynamic fatigue' or the influence of cyclic variations in load over time. The influence of constant load over time, sometimes referred to as 'static fatigue' is considered under WP 5 as duration of load effects. This repeated stress might occur as a result of rotation, bending or vibrations. Even though the stress is below the ultimate strength, failure may be experienced after a large number of applications of the stress, which when considering the long design life for structures can relate to relatively low frequency load events.

The research work package WP 6 of the GIROD project is summarised in Part A of the project proposal description as *"a minor investigation of the sensitivity to low frequency fatigue ... carried out on full sized glued-in rod specimens."*

The fatigue study under WP 6 has considered the results from earlier work related to the topic and has resulted in the development of a technical report on the subject, thus providing information for consideration under programme item WP 8, the drafting of design rules for Eurocode 5. In the future, glued-in rods will be common in timber bridges, where fatigue may be a significant issue. The objective is to give an indication of whether or not the fatigue behaviour of glued-in rods may limit their use in certain applications, for instance in bridges.

3.6.1 Methodology and experimental methods

The methods and findings from the experimental study are reported and discussed in the interim project progress reports TTL PR1, TTL PR3, TTL PR5, TTL PR7 and TTL PR9 (Bainbridge and Mettem 1999-2001)

Partner 4 has conducted all the work, comprising desk based studies, experimental testing and analysis of results. The key tasks carried out under WP 6 are identified in Table 3.6.1.

Table 3.6.1 WP 6 Project plan.

Task	Description
1	Define Experimental Methods
2	Produce WP Progress Report
3	Perform Tests
4	Produce WP Progress Report
5	Conclude WP 6
6	Present Results in Final WP Report

In line with the project schedule, WP 6 activities have involved participation in project meetings and completion of project tasks 1 to 6.

– Project tasks 1 & 2 were reported in report TTL PR1 (Bainbridge and Mettem 1999a)

- Project tasks 3 & 4 are recorded in report TTL PR3 and TTL PR5 (Bainbridge and Mettem 1999b, 2000a)
- Project task 5 was reported in report TTL PR7 (Bainbridge and Mettem 2000b)
- Project task 6 is detailed in progress report TTL PR9 (Bainbridge and Mettem 2001a)

There have been no principal deviations from the work plan, with revisions being confined to the development of the test proposals outlined in the first progress report (Bainbridge and Mettem 1999a) in the light of practical test experiences. Bonded-in steel rod specimens were exposed to low frequency (approximately 1 Hz) cyclic tension fatigue (R=0.1) at fixed stress rates. Three types of adhesive have been considered in this fatigue study – an Epoxy (EP), a PUR and a filled PRF. The number of cycles to failure and mode of failure have been examined for two geometries of test specimen, as described in Table 3.6.2. Further details of the experimental investigations are available in project progress reports and published references, see Bainbridge et al. 1999 and Bainbridge et al. 2000.

Table 3.6.2 Fatigue test specimens

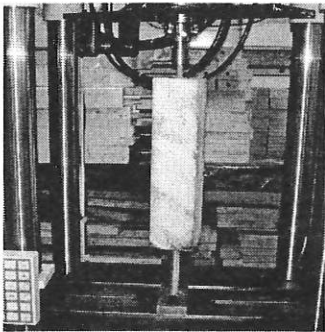| Test Series	6.1	6.2
Component Laminate Strength Class	C35	C35
Moisture Content (%)	12% ±1%	12% ±1%
Glued-in Length to Rod Diameter Ratio, λ	10	20
Bar Diameter	16mm	8mm
Bar Grade	8.8	10.9
Anchorage Length (mm)	160	160

Figure 3.6.1 Test configuration.

3.6.2 Results

Four distinct failure modes were observed through the tests - rod failure, failure in the adhesive (causing breakdown of the material in the bond-line itself), failure in the wood substrate and failure at the interface between timber and adhesive. The majority of the fatigue failure modes are relatively consistent with static test observations. From the results, it is apparent that fatigue does have the potential to cause damage in bonded-in rods, and that there is sufficient variation in failure modes to confirm that failure may be due to damage in any of the component materials (steel rod, adhesive or timber substrate) or breakdown of the timber to adhesive bond interface. The incidence of these modes is compiled in Table 3.6.3.

Table 3.6.3 Recorded fatigue failure modes.

Test Rod Type	Adhesive	Failure Modes Recorded			
		Timber	Steel Rod	Adhesive	Adhesive/Timber Interface
16mm mild steel	PRF			√	
	PUR	√	√		√
	Epoxy	√	√		
8mm HT Steel	PRF			√	
	PUR	√	√		√
	Epoxy	√	√		

69

The data obtained from the tests at R=0.1 (i.e. maximum tensile load = 10 x minimum tensile load) is presented in the form of cycles to failure versus load in Figures 3.6.2-3.6.4. It must be noted that observations and projected fatigue lives presented herein must be taken in the context of extrapolations based upon a limited data set, lacking confirmatory data at high numbers of load cycle ($>10^6$).
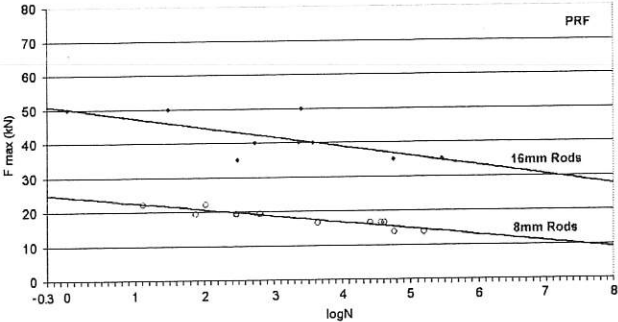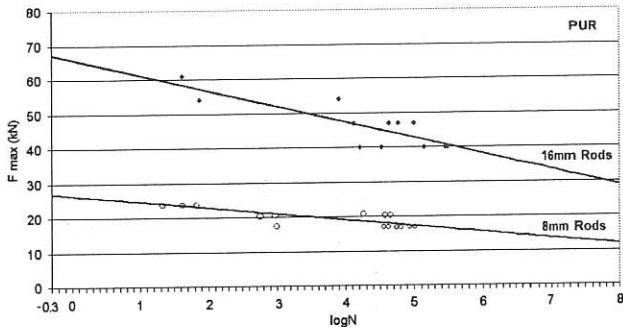

Figure 3.6.2 Results for PRF Bonded Specimens

Figure 3.6.3 Results for PUR Bonded Specimens
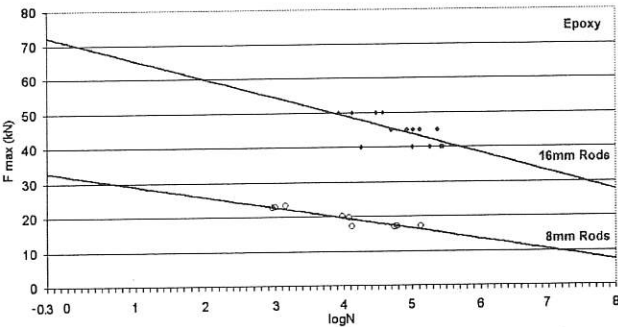
Figure 3.6.4 Results for Epoxy Bonded Specimens

Fatigue Failure Modes

Timber Failure: Figure 3.6.5 presents the combined data set from all tests where fatigue failure occurred in the timber. The extrapolated strength at 10^7 cycles as compared to the first half cycle strength in tension (logN = -0.3) represents a 55% reduction. This is of the order that would be expected from tests performed on clear unidirectional laminated timber, based upon evidence illustrated in Figure 3.6.6.
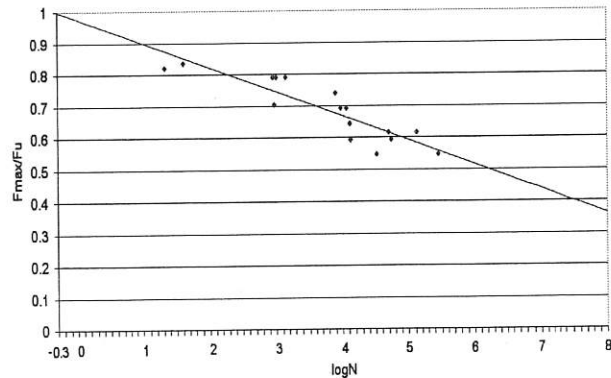

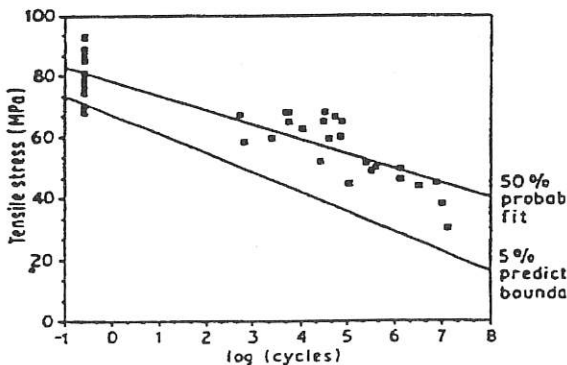*Figure 3.6.5 Fatigue Performance Associated with Timber Failure Modes*

Figure 3.6.6 σ-logN Data for Khaya at R=0.1 (Bonfield et al 1994).

Steel Failure: There is clearly a potential risk of fatigue failure in the bonded-in rod used to form the connection. Recorded failures in the mild steel (Grade 8.8) rods were observed at a lower number of cycles (or alternatively in a lower stress range) than the basic material data would suggest. The explanation for this can be attributed to the threaded surface on the rod acting as a series of stress raising notches. This has a recognised impact upon fatigue damage development, the feature often being much more important than the steel composition when

70

determining fatigue resistance (Hingwe 1982). The higher-grade steels have a higher fatigue resistance in terms of the average stress causing failure in the data set obtained between 10^5 and 10^4 cycles, but it is of note that a greater number of samples suffered rod failure with the higher-grade steel. In addition to the thread effect, contributory factors defining the rod mode of failure include brittleness in the rods coupled with minor flaws and eccentricities in the test specimens resulting in combined bending and tension stress development. This may explain in part, the increased incidence of failure in the more slender and more brittle high-grade rods.

Bond Line (Cohesive) Failure: Failures within the bond-line were only encountered with the filled PRF adhesive. The adhesive is brittle and prone to shrinkage as it cures. This sets up stresses within the unloaded bond which can result in a damaged bond line, leading to failure in fatigue when subjected to cyclic load. It is of note that the sample set with 8mm rods (λ=20) is more consistent with the linear approximation of anticipated behaviour than the 16mm test set (λ=10). This indicates an influence of sample geometry upon fatigue behaviour, in addition to the basic fatigue resistance of the material acting as the critical component in the system.

Bond Line/Timber Interface (Adhesive) Failure: Failures at the timber/adhesive interface were observed only in the PUR bonded samples. This is due to CO_2 bubble formation at the bond ("foaming" of the bond-line), causing a reduction in the effective cohesion area. This is the result of reaction of the adhesive components with moisture in the timber.

3.6.3 Design code fatigue verification

The basis for fatigue verification in Eurocode 5: Part 2 (DD ENV 1995-2) is through application of a fatigue coefficient, k_{fat} (as summarised in Figure 3.6.7) and an appropriate fatigue safety factor $\gamma_{M,fat}$. This form of assessment in relation to number of cycles to failure provides a common link between test data and design basis.

The factor k_{fat} is then employed in the following equation:

$$f_{fat,d} = \frac{k_{fat} f_k}{\gamma_{M,fat}}$$ (3.6.1)

where:
f_k= characteristic strength for static load
k_{fat}= fatigue coefficient obtained graphically (Figure 3.6.7)
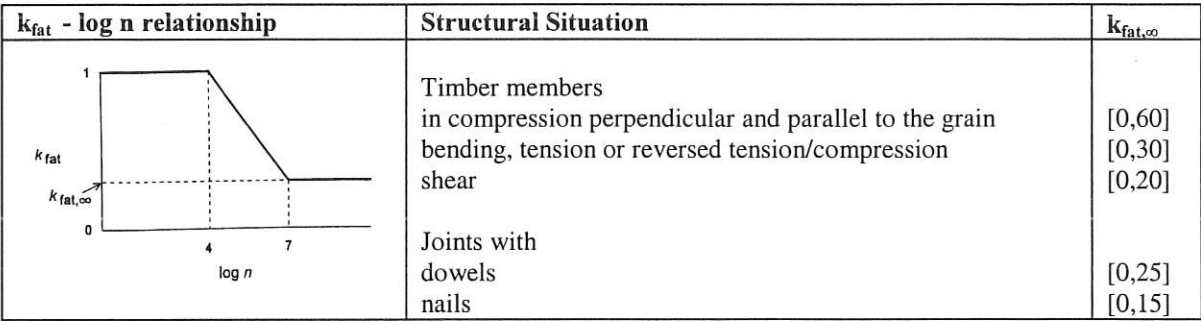$\gamma_{M,fat}$= material safety factor for fatigue (from EC1-Part1)

k_{fat} - log n relationship	Structural Situation	$k_{fat,\infty}$
	Timber members in compression perpendicular and parallel to the grain bending, tension or reversed tension/compression shear	[0,60] [0,30] [0,20]
	Joints with dowels nails	[0,25] [0,15]

Figure 3.6.7 Relationship between k_{fat}, log n and values of $k_{fat,\infty}$ as presented in EC5: Part2

The derivation of an appropriate $\gamma_{M,fat}$ factor depends on the structure and its status with

regard to damage tolerance. For structures that can be verified as damage tolerant, this safety factor can be taken as 1.00 (DD ENV 1991-1). Other cases require further consideration as to derivation of an appropriate factor. Taking the case of a damage tolerant structure, this means that the end design result is determined as the product of a characteristic design value and the fatigue coefficient.

3.6.4 Evaluation of experimental evidence

It must be borne in mind that the tests performed relate to a variable tension cycle (R=0.1), employed for test practicality but which might not prove to be the most severe. For example, tests on timber have shown reversed loading (R=-1) to be the most severe, as illustrated in Figure 3.6.8.

Whilst it is not possible to construct curves from the data set of this limited study to derive characteristic values appropriate to definition of absolute values for k_{fat}, it is possible to benchmark observations against those proposed for general structural timber applications. It is apparent from test observations that there is a deviation from suggested behaviour in the graph used to derive k_{fat}. The experimentally observed s-logN relationship is linear from 0.5 to 107 cycles, whereas the k_{fat}-logN curve indicates no effect up to 104 cycles. From the data plots, the ratio of strengths at the key numbers of cycles can be summarised and compared as in Figure 3.6.9. Considering the results in relation to the specimen types, independent from the failure mode, there is a consistent trend in the ordering of fatigue effect upon the test specimens. The separation of the series 6.1 and 6.2 counterparts also indicates that there is not only a clear influence of adhesive type, but also of specimen geometry. It is essential to note that these curves do not reflect the actual comparative performance of specimens, merely the degree to which fatigue effects a sample type.
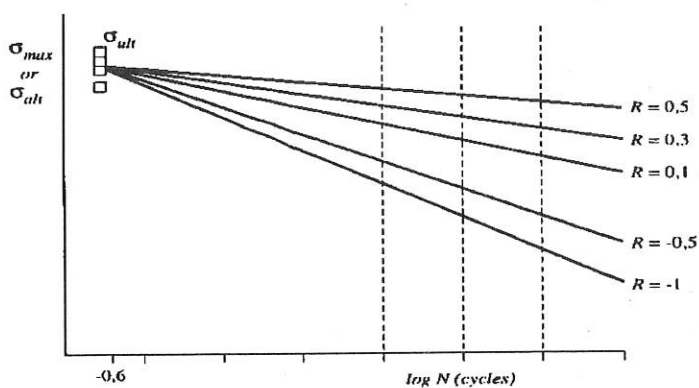

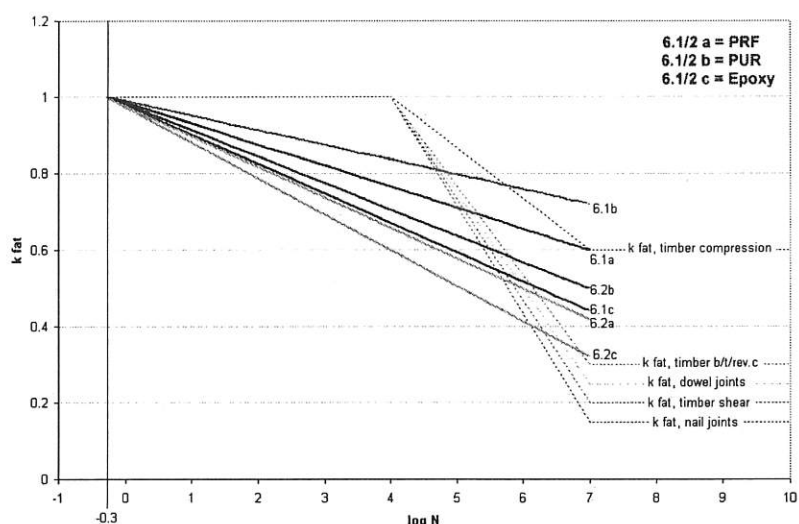*Figure 3.6.8 Timber fatigue performance over a range of R ratios (Ansell 1995).*

Figure 3.6.9 Fatigue factors and logN relationship as defined in EC5: Part2 and translated directly from test observations

Hence the potential conclusion that could be drawn from this curve set that PUR is best, PRF second best and Epoxy least effective in fatigue resistance is not true. For example, consider the peak load data drawn from the test sets in Table 3.6.4. It is clear that at the half cycle point Epoxy has superior resistance, as is the case at 10^4 cycles. However the gradient of the projected log-linear relationships means that at the 10^7 cycle point, the difference is massively reduced, resulting in a reversal of order in the case of the 8mm test rods.

Table 3.6.4 Selected fatigue resistance data from linear extrapolations of performance.

Sample		F@ 1/2 cycle (kN)	F@ 10^4 cycle (kN)	F@ 10^7 cycle (kN)
	PRF	51	38	30
16mm rods	PUR	67	47	33
	EP	72	50	33
	PRF	25	17	12
8mm rods	PUR	27	19	13
	EP	32	20	10

It should also be noted that these performances are based upon approximated extrapolations from a limited test set and that there is no experimental data to validate the low-stress/high-cycle number performance. For example, it could be that at such low stress levels, fatigue limits might emerge in some cases, whereby fatigue failure does not manifest.

The data can also be similarly compared with the test curves on the basis of the critical failure modes, as shown in Figure 3.6.10. From these plots it is clear that in the specimens tested, the fatigue performance relationship for all modes appear to be very close.

It is important to note that in the graphs, the curves do not directly represent the performance (i.e. capacity of the specimen), but the degree to which the specimen is affected by cyclic loading. Since the curves in EC5:Part 2 are also intended as a mechanism to relate 'static' load resistance to fatigue, there are a number of issues that require consideration in potential application of these curves in design.
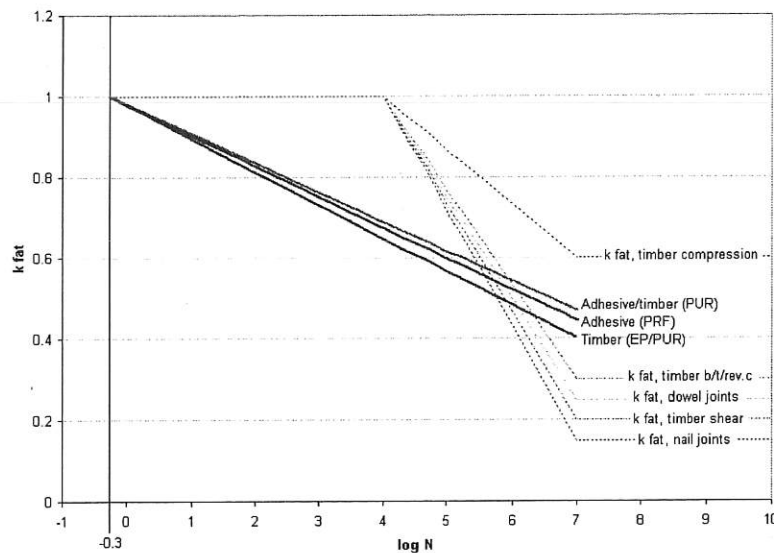
73

Figure 3.6.10 Fatigue Factor - logN Relationship as Defined in EC5: Part2 and Translated Directly from Test Observations of Failure Modes

3.6.5 Discussion

The study reported herein draws upon only a limited number of experimental observations, but it has highlighted a number of key issues for further consideration and future address. Observations and projected fatigue lives presented herein must be taken in the context of extrapolations based upon a limited data set, lacking confirmatory data at high numbers of load cycle. There is a massive scope for work that has not been covered by this investigation.

With this in mind, however, there are some key fatigue performance aspects that are demonstrated by these results:

- The majority of fatigue failure modes were common to those observed in static test counterparts to the fatigue test specimens. Significant incidents of alternative failure modes were however also recorded, especially failures in the steel rods.
- It is apparent that different adhesive types behave in fundamentally different ways with respect to the fatigue performance and the eventual mode of failure at the fatigue ultimate limit state.
- The geometry of the test specimens is at least as important under the conditions of this test as the adhesive type, but the general order of performance across the adhesive types was found to be consistent between specimen sets.

Qualification of the variability in performance and the impact of variations in their fabrication upon refined prediction of fatigue failure mode is not possible from a test set of this size. It is not therefore possible to confirm whether the projected trends truly represent a reasonable mean performance or to directly link the values to characteristic properties that will be used in design.

The impact of varying cyclic load regimes (differing R ratio and frequency) and alternative geometric configurations would also be necessary to fully develop appreciation of the fatigue performance. With this in mind, it might be necessary to refine the definition of fatigue factors with respect to the different influences (e.g. $k_{fat,n}$, $k_{fat,f}$, $k_{fat,R}$). Development of a fatigue safety factor specific to bonded-in rod connections might also be worthy of consideration.

3.6.6 Development of design recommendations

As a result of this study, provisional design recommendations have been drafted, as described in the following text. It should be noted that the limited study has not facilitated full resolution of many areas concerning the fatigue performance. Thus much of the numerical content of this (in particular k_{fat} factors) draws upon previously developed design guidance for timber structures under fatigue loads, specific numerical factors for GIRODS not yet being available.

1. Fatigue effect should be considered in relation to the relevant Ultimate and Serviceability Limits States.

2. The effect of likely combinations of compression and tension should be considered

3. Compression components of load cycling should be considered separately from tensile components for effects deriving from rod slenderness and bearing at the end of the rod.

4. A simplified verification should be related to:

the stress range, $\qquad \Delta\sigma = \sigma_{k,max} - \sigma_{k,min} \qquad (1)$

the fatigue ratio, $\qquad R = \sigma_{k,max} / \sigma_{k,min} \qquad (2)$

the fatigue frequency, $\qquad f = 1 / T \qquad (3)$

where
$\sigma_{k,max}$ is the characteristic maximum stress from the fatigue action
$\sigma_{k,min}$ is the characteristic minimum stress from the fatigue action
T is the period of action cycle (s)

Note: Tensile actions taken as +ve , compression actions -ve

5. The stress should be determined by an elastic analysis under the specified action.

6. The fatigue performance should be checked with respect to the critical component or material in each possible failure mode

7. A fatigue verification is not required if :

$$|\sigma_{k,t}|_{max} \le 0.1 \, f_{d,t} \qquad (4)$$

and $\qquad |\sigma_{k,c}|_{max} \le 0.1 \, f_{d,c} \qquad (5)$

8. For a periodic loading with n cycles, it should be verified that

$$\sigma_{t,max} \le f_{fat,d} \qquad (6)$$

and $\qquad \sigma_{c,max} \le f_{fat,d} \qquad (7)$

where $f_{fat,d}$ is the design fatigue strength

9. The design fatigue strength should be calculated at the R ratio and frequency appropriate to the fluctuating action as

$$f_{fat,d} = \frac{k_{fat} \, f_k}{\gamma_{M,fat}} \qquad (8)$$

75

where f_k is the characteristic strength for static load and k_{fat} is given in figure 1

10. The value of $k_{fat,\infty}$ relating to the failure mode under consideration should be taken from table 1.

11. The fatigue partial factor $\gamma_{M,fat}$ should be related to the appropriate limit state as described in table 2.

12. For damage intolerant structural systems, provisional factors can be identified for adhesive bonded connections from Table 3
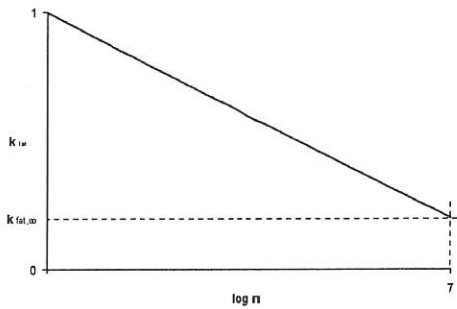

Figure 1: Relationship between k_{fat} and the number of cycles n.

Table 1   Values of $k_{fat,\infty}$

Failure Mode	$k_{fat,\infty}$
Failure in host members, due to	
– compression action cycles	0.60
– tensile action cycles	0.30
– reversed tension/compression action cycles	0.30
Failure in localised timber pull-out of 'plug' around bar	0.20
Failure in adhesive - failure through bond line or at interphase	0.20
Failure in rods steel rods laterally loaded	0.25
steel rods axially loaded	0.15

Table 2. Limit States Basis for consideration of fatigue partial factor

Status of Structure	Limit State	$\gamma_{M,fat}$
Damage Tolerant	SLS	1.00
Damage Intolerant	ULS	assessment required on basis of uncertainties in fatigue actions, fatigue effects, fatigue resistance and possibility of decrease in resistance due to time dependant phenomena

Degree of Inspection	$\gamma_{M, fat}$	
	Fail-safe joints	Non fail-safe joints
Periodic inspection, good access	1.5	2.0
Periodic inspection, poor access	2.0	2.5
No inspection/maintenance	2.5	3.0

Table 3 Provisional fatigue partial factors for ULS calculations

13. For periodic loading of a complex nature, the fatigue performance should be verified with respect to the component cyclic actions, such that:

$$\sum \frac{n_i}{N_i} \leq 1 \qquad (9)$$

where

n_i is the number of component action cycles of stress range during the required design life

N_i is the number of component action cycles of stress to cause failure

3.6.7 Recommendations for further study in bonded-in rod connections

Whilst the study reported herein draws upon only a limited number of experimental observations, it has highlighted a number of key issues for further consideration and future address. There is a massive scope of work that has not been covered by this investigation.

The observations drawn are made upon a small sample group. The variability displayed in the sample group and the impact of variations in their fabrication upon refined prediction of fatigue failure mode is not possible from a test set of this size. It is not therefore possible to confirm whether the projected trends truly represent a reasonable mean performance or to directly link the values to characteristic properties, which will be used in design

The impact of varying cyclic load regimes (differing R and frequency) and alternative geometric configurations would also be necessary to fully develop appreciation of the fatigue performance. With this in mind, it might be necessary to refine the definition of fatigue factors with respect to the different influences (e.g. $k_{fat,n}$, $k_{fat,f}$, $k_{fat,R}$). Development of a fatigue safety factor specific to bonded-in rod connections might also be worthy of consideration.

3.6.8 Conclusions

WP 6 has demonstrated that fatigue performance is a significant factor in the performance of bonded-in rods and recommendations are made as to how further work, beyond the scope of GIROD, could improve understanding and design treatment of the fatigue behaviour of these types of connection. In relation to the stated objectives of the study, the experimental study has indicated that the fatigue behaviour of glued-in rods may limit their use in certain applications.

Observations and projected fatigue lives presented herein must be taken in the context of extrapolations based upon a limited data set, lacking confirmatory data at high numbers of load cycle. There are however some key conclusions that can be drawn from this limited experimental study:

- The majority of fatigue failure modes were common to those observed in static test counterparts to the fatigue test specimens. Significant incidents of alternative failure

modes were however also recorded, especially failures in the steel rods.

- It is apparent that different adhesive types behave in fundamentally different ways with respect to the fatigue performance and the eventual mode of failure at the fatigue ultimate limit state.
- Both the geometry of the test specimens and the adhesive type are important under the conditions of this test, but the general order of performance across the adhesive types was found to be consistent between specimen sets.
- The scope for further work to enhance the knowledge and design methods employed is very large.

A full description of failure mode-related fatigue performance basis of design would require further experimentation. To determine the full relationship with geometry and to verify the influence of R ratio and frequency upon the application of design methods based upon the observations drawn from the test set would be key to development of such development.

3.7 WP 7 – Test methods for production control

The objective of the work within this WP was to develop test methods which enable reliable and simple testing of glued-in rods for timber structures during production. The method should be capable of revealing serious production errors, e.g. insufficient adhesive application, insufficient hardening, and other gluing errors. Two alternative test methods have been studied: a destructive method, and a proof-loading method. Further details of the work carried out within this WP can be found in Johansson 2000.

3.7.1 Experiments
Preparation of specimens
The specimens were made of Norway spruce (*Picea abies*) glulam. The cross section consisted of three laminations, visually graded to LT30 (INSTA 142), which corresponds to the C35 strength class (EN 338) as far as the tension parallel to grain properties are concerned. All rods (threaded M16, galvanised of quality 8.8) were bonded in centrally, parallel to the grain, into the glulam blocks. Three test series were carried out, destructive tests (series 1), proof-loading (series 2) and one test series with specimens containing errors (series 3). An overview of the test series is given in Table 3.7.2.
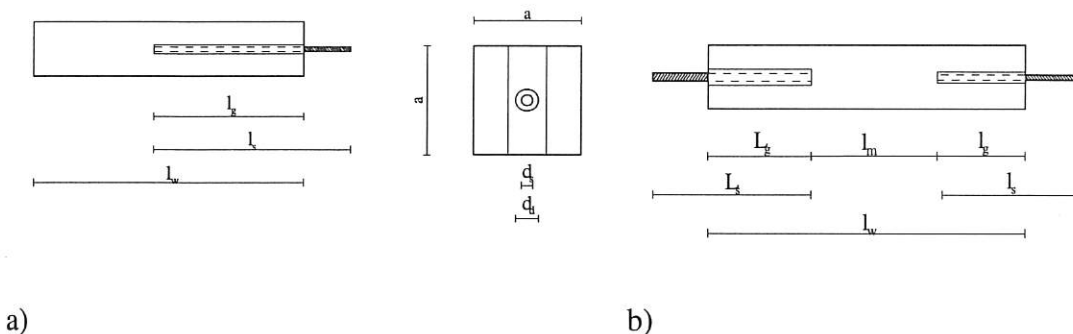

Figure 3.7.1 Design of test specimens a) Type A, b) Type B.

Table 3.7.1 Dimensions of test specimens

	$\lambda=10$	$\lambda=20$
Type A		
d_s [mm]	16	16
d_d [mm]	17/18/20	17/18/20
a [mm]	115	115
l_w [mm]	288	576
l_s [mm]	260	420
l_g [mm]	160	320
Type B		
d_s [mm]	16	16
D_s [mm]	24	24
d_d [mm]	17	17
D_d [mm]	25	25
a [mm]	115	115
l_w [mm]	576	1152

	$\lambda=10$	$\lambda=20$
l_s [mm]	280	440
L_s [mm]	310	500
l_g [mm]	160	320
L_g [mm]	190	380
l_m [mm]	226	452

Table 3.7.2 Overview of the test series.

Loading mode	Test series 1				Test Series 2			Test series 3		
	λ	Adh.	t	Steel plate shape	λ	Adh.	PLL	λ	Adh.	Error type
test type A	10 20	EP PRF PUR	0,5 1,0 2,0	circle						
test type A	10 20	EP	0,5	square						
test type B	10 20	EP PRF PUR	0,5							
test type A					10 20	EP PRF PUR	50 65 80 90			
test type A								10 20	EP PRF PUR	1 2 3 4 5 6 7

legend:	1 too little adhesive
	2 burnt wood
λ rod slenderness	3 incorrect component mixture
t glue line thickness	4 rod temperature -10°C
Adh. Adhesive	5 hole diameter too large
PLL proof-load level	6 oily rod
	7 control (no error)

As can be seen in Table 3.7.1, two different glued-in lengths were studied, $l_g=160$ mm and $l_g=320$ mm. This resulted in two slenderness ratios $\lambda=10$ and $\lambda=20$ ($\lambda=l_g/d_s$). Three glue line thicknesses were studied, 0.5 mm, 1 mm and 2 mm and three different adhesives were used. These were a two-component epoxy (EP), a two-component phenol-resorcinol (PRF) and a two-component polyurethane (PUR). The adhesives were mixed and handled according to the manufacturers recommendations and they were injected into the bottom of the drilled holes.

Thereafter, the rods were inserted by hand under continuous pressure and rotation. The rods were centred visually in the hole. The specimens were stored in a climate room (20°C and 65% relative humidity) during at least two weeks before they were tested. Closer details on the test specimens are given by Hausmann and Reil (1999).

Test set-up

The tests were carried out as one-sided pull-compression tests and as two-sided pull-pull tests. The one-sided tests are described in Figure 3.7.2. This test-method is newly developed. The two-sided tests are regarded as more or less "standard" and the details of the test set up can be found in Hausmann and Reil (1999). The one-sided test set-up was chosen with regard to the test set-up practicality. The pull-out load was determined with a load cell and the pull-out displacement of the rod in relation to the wood surface was measured by two transducers. In order to make this test set-up as compact and stable as possible, the load cell was screwed to the hydraulic cylinder with the help of two steel plates, see Figure 3.7.2. On the top of the hydraulic jack, a thin steel plate was fixed in order to get a plane surface against which the pull-out displacement was measured. This test apparatus was put onto a stand to facilitate handling. Both transducers were assembled with a small metal sheet for simplified handling. As the jutting-out part of the glued-in rod was only 100 mm, an elongation was necessary to fix the rod to the hollow hydraulic jack. A higher steel quality was chosen for this extension (quality 10.9). The elongation was screwed on the top of the rod and put through the hollow hydraulic jack. Further description of this test set-up can be found in (Hausmann and Reil 1999).
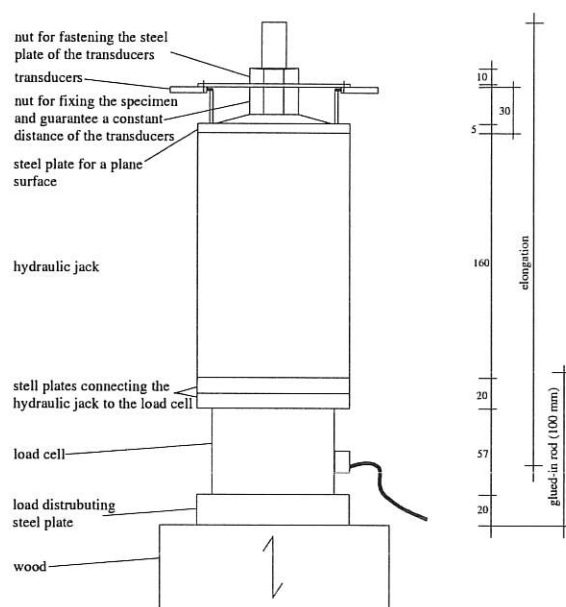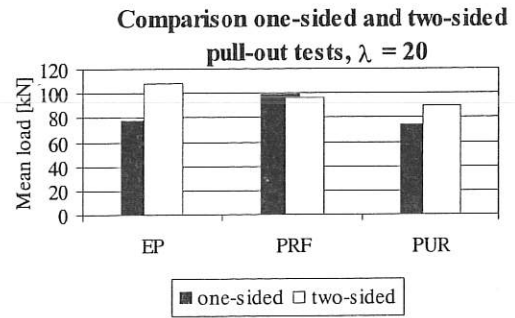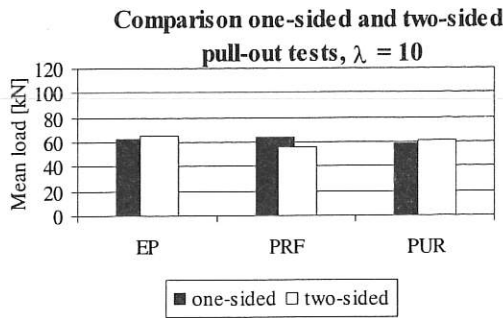

Figure 3.7.2 Details of the one-sided test set-up.

a)   b)

Figure 3.7.3 Comparison between pull-out loads obtained from one-sided and two-sided pull-out tests. The showed pull-out loads are mean values of ten specimens.
a) Specimens with slenderness, λ=10, b) Specimens with slenderness, λ=20.

Two-sided pull-out tests were, as mentioned, performed to verify the newly developed test-method described above. These tests were performed with a glue line thickness of 0.5 mm, all three adhesives were tested as well as the both slenderness ratios. The pull-out loads shown in Figure 3.7.3 are mean values of ten specimens. The two-sided pull-out test specimens bonded with EP and PUR produced higher pull-out loads than the specimens tested one-sided. For EP and PUR specimens with λ=20 the difference in pull-out loads between the two test methods was considerable. The two-sided tests gave higher loads.

3.7.2 Experimental results
Destructive tests
For all destructive tests, the failure occurred within three to five minutes. All failures were sudden. Figure 3.7.4 shows examples of load-slip curves for three specimens bonded with different adhesives. The shape of these three curves was rather similar but among all the test results there are also load-slip curves with steeper slopes. Steeper load-slip curves were found mainly for specimens bonded with EP and PUR. The non-linear beginning of the load-slip curve was possibly caused by irregularities between the wood surface and the adhesive.
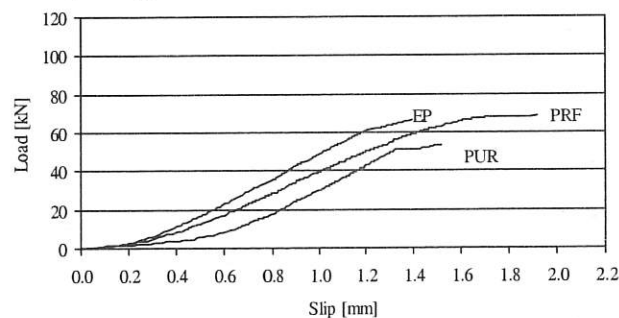

Figure 3.7.4. Load-slip curves for three specimens bonded with different adhesives (slenderness λ=10).

To analyse the failure modes precisely the failed specimens were opened and the failure was examined and quantified in percentage of wood failure. The specimens bonded with PRF displayed a uniform type of failure which can be classified as cohesive. There was poor adhesion to the steel. The EP-bonded specimens mostly displayed solid wood failures. Also the PUR-bonded specimens displayed a high percentage of wood failures but also cohesive failures occurred due to bubbles in the adhesive. Different failure modes are illustrated by Kemmsies (1999).

Three different thicknesses of the glue lines, 0.5 mm, 1 mm and 2 mm, were investigated. For specimens bonded with EP and PUR an increased glue line thickness leads to increased pull-out strengths. For specimens bonded with PRF the pull-out strength decreased with increasing glue line thickness. The decrease was drastic. The decreased pull-out strength of PRF-bonded specimens is partly caused by shrinkage of the PRF adhesive.

Proof-loading

Four different proof-load levels (PLL) were tested to try to find the maximum load that does not cause structural damage of the bond line. The levels selected were: 50%, 65%, 80% and 90% of the maximum pull-out loads obtained from the destructive tests. Both slenderness ratios were tested and a glue line thickness of 0.5 mm was used for all cases. Seven test pieces in each group were loaded up to the determined proof-load level (loaded during 30 seconds), then the load was held for 15 seconds. Thereafter, the specimens were unloaded and reloaded until failure within five minutes. Below (Figure 3.7.5), the mean values of the pull-out loads for each of the tested group of seven specimens are shown together with the mean value of the maximum loads for the group of ten specimens tested destructively.

Table 3.7.3 shows the mean pull-out loads and the coefficients of variation (CV) for the destructive tests and for the groups of proof-loaded specimens. For the EP-bonded specimens, the coefficients of variation were largest for the largest slenderness ratio. For the PRF-bonded specimens it was the other way around; the groups of specimens with the smallest slenderness ratio displayed the largest coefficients of variation.

For the specimens bonded with EP, it is remarkable that the specimens loaded to the proof-load levels 80% and 90%, on the average, reached higher pull-out loads than the specimens only tested destructively. The effect was most pronounced for the specimens with the longest glued-in length (λ=20). The pull-out loads were approximately 20% higher for the proof-loaded specimens. Additional tests with EP-bonded specimens loaded to the proof-load levels 80% and 90% were performed. These new tests confirmed the original effect. The reason for this behaviour is still unknown. One speculation can be that proof-loading to high load levels leads to redistribution of stresses along the glue line. Such a redistribution seems to be advantageous for the pull-out strength of EP-bonded rods.
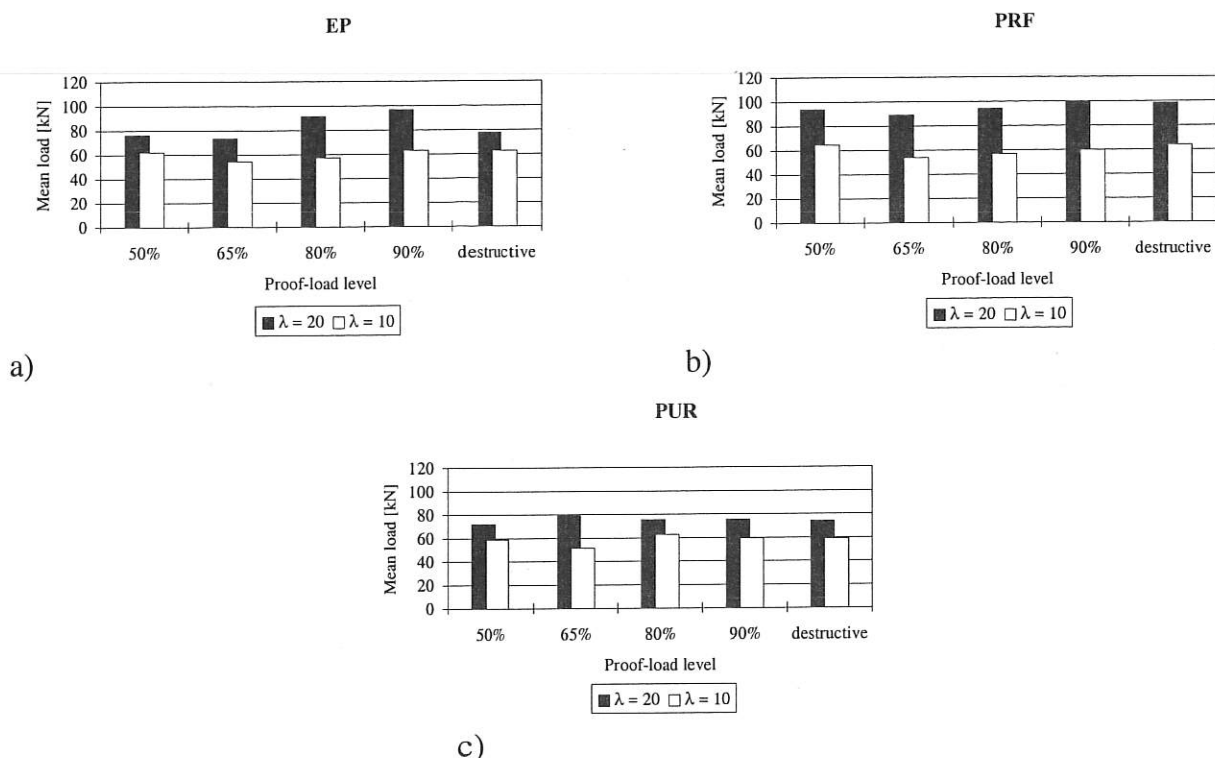
EP

PRF

PUR

c)

Figure 3.7.5 Mean values of the pull-out loads for the groups of specimens tested at different proof-load levels and for the group of specimens tested destructively.
a) Specimens bonded with epoxy, b) Specimens bonded with phenol-resorcinol, c) Specimens bonded with polyurethane.

For PUR-bonded specimens, with $\lambda=20$, there seemed to be no pronounced effect on the pull-out loads of the proof-loading. For all specimens proof-loaded at the 65% level there was a decrease in pull-out loads (except for PUR with $\lambda=20$). For PRF and for EP ($\lambda=10$) this decrease was statistically significant compared to the destructive tests. This decrease in mean pull-out load, after proof-loading to 65%, is not yet explained.

Table 3.7.3 Mean values and coefficients of variation (CV) of the pull-out loads for the destructive tests (dest) and the proof-loaded specimens (PLL50 = proof-load level of 50%,...)

	EP, $\lambda=10$					EP, $\lambda=20$				
	dest.	PLL50	PLL65	PLL80	PLL90	dest.	PLL50	PLL65	PLL80	PLL90
Mean [kN]	62.6	62.2	54.3	57.3	63.2	77.4	76.3	73.3	91.2	96.6
CV [%]	4.7	9.1	15.6	14.2	15.2	14.7	19.5	16.0	19.9	19.8
	PRF, $\lambda=10$					PRF, $\lambda=20$				
Mean [kN]	63.8	64.6	53.8	56.6	59.9	98.4	93.9	88.8	94.0	99.6
CV [%]	7.3	13.1	14.5	10.5	11.7	6.4	7.9	7.4	6.8	6.3
	PUR, $\lambda=10$					PUR, $\lambda=20$				
Mean [kN]	59.0	58.9	51.4	63.5	59.4	74.1	71.8	78.9	75.4	75.5
CV [%]	16.8	20.5	9.1	9.3	11.8	13.2	11.0	8.8	13.9	16.5

Based on the test results shown above the objective was to determine a proof-load level suitable for production control of glued-in rods. In addition to the results shown above, the

84

density and the moisture content of the wood surrounding the glued-in rod was registered. A total amount of 196 specimens were proof-loaded to the different load levels. Of these specimens, 21 failed before reaching the proof-load level, and approximately ten specimens failed during the re-loading very near the actual proof-load. None of the specimens failed before reaching the 50% proof-load level and only one specimen failed before reaching the 65% load-level. The amount of failures were equally distributed between the three types of adhesive. Not surprisingly, 16 of the specimens that failed before reaching the proof-load level were loaded at the 90% level. The average middle lamella density for all tested specimens in the study was 419 kg/m³ (density at 12% moisture content). For some specimens the wood surrounding the glued-in rod was relatively low, around 370 kg/m³. However, also specimens with high density, around 450 kg/m³, in the middle lamella failed. Furthermore, as will be shown below, the correlation between density and pull-out load was poor in present study and therefore it is not possible to draw any conclusions based on the value of the density.

However, for the continuation of the present study it was decided to use 80% as a suitable proof-load level.

Error-detection

To ensure that the proof-loading method can detect possible defects of the bonded connection, specimens with six different defects were prepared. The premeditated defects were:
1. Too little adhesive
2. Burnt wood surface in the drilling hole
3. Incorrect mixing proportions of the adhesive components
4. Rod temperature at -10°C
5. Too large drilling diameter
6. Oily rod

In addition, a control series (with no defects) was tested at the same occasion. Each group of specimens consisted of seven specimens and a total amount of 308 specimens was tested. The hardening time for all specimens tested in this test series was seven days.

The results of the proof-loading to 80% of the defect specimens are shown in Figures 3.7.6-3.7.8. The number of errors detected are marked black. It can be seen that the number of detected errors varies with type of adhesive, slenderness ratio and type of error. In the case of too little adhesive the amount of adhesive was reduced by a factor two. This defect resulted in decreased mean pull-out loads of between 20% and 39% compared to the control test series. All PRF-bonded specimens and a majority of the EP- and PUR-bonded specimens, with this defect, failed before reaching the 80% proof-load level.

Burnt wood affected the PRF-bonded specimens most seriously. The pull-out loads were decreased by, on the average, 10% to 24%.

The incorrect mixing of the adhesives was detected in all cases. The amount of hardener was strongly reduced ($\geq 40\%$). It is possible that this incorrect mixing was too coarse to act as a indicator for determining whether 80% is a suitable proof-load level. Incorrect mixing of the adhesives components lead to a reduction of the pull-out loads by 31%-55% for PRF- and PUR-bonded specimens. The EP adhesive did not harden and therefore these specimens were not possible to test.

The frozen rod and the oily rod only had a small influence on the pull-out loads for the bonded connections and, consequently, this error was only detected in a few cases.

Producing the hole diameter too large gives the same results as increasing the glue line thickness, i.e. increased pull-out strength for the EP- and the PUR-bonded specimens (by 5% to 29%) and decreased pull-out strength for the PRF-bonded specimens (by 27%-45%).

EP, λ = 10

EP, λ = 20
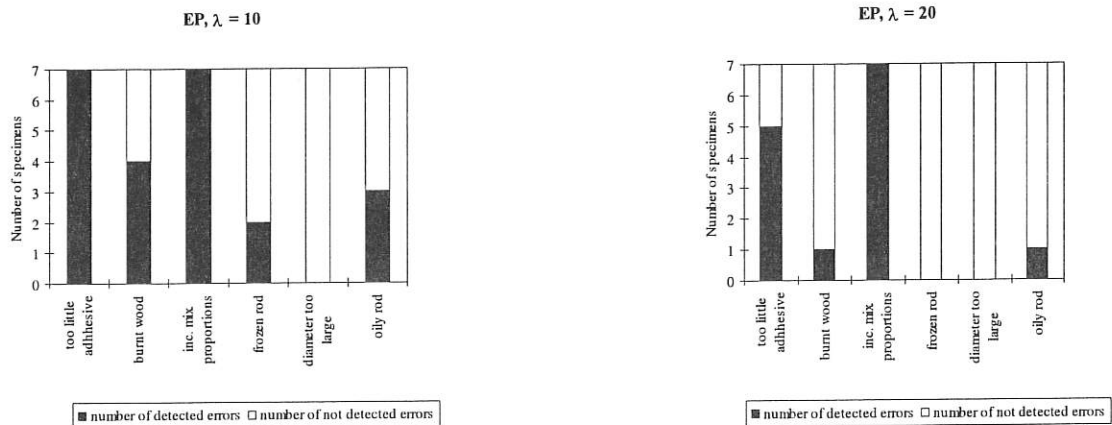
Figure 3.7.6 Number of specimens, bonded with EP, with defects found by proof-loading to 80%.

PRF, λ = 10

PRF, λ = 20
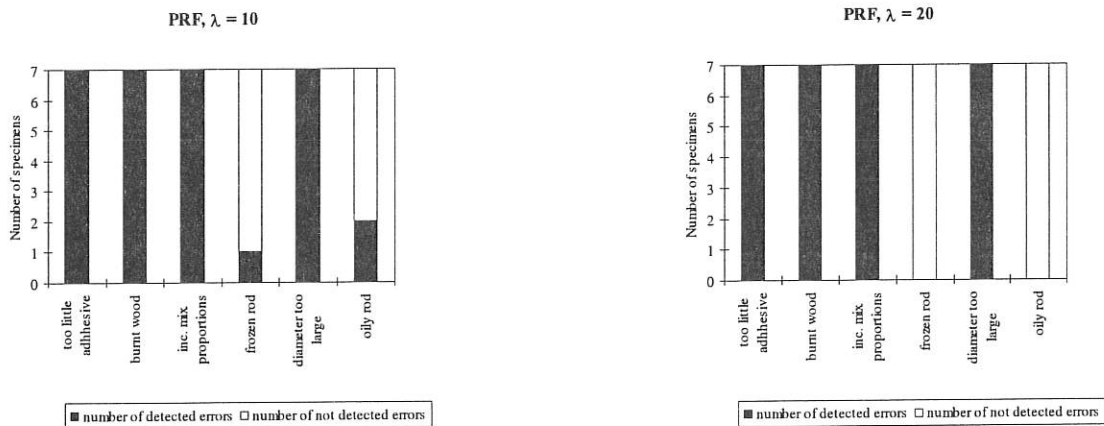
Figure 3.7.7 Number of specimens, bonded with PRF, with defects found by proof-loading to 80%.

PUR, λ = 10

PUR, λ = 20

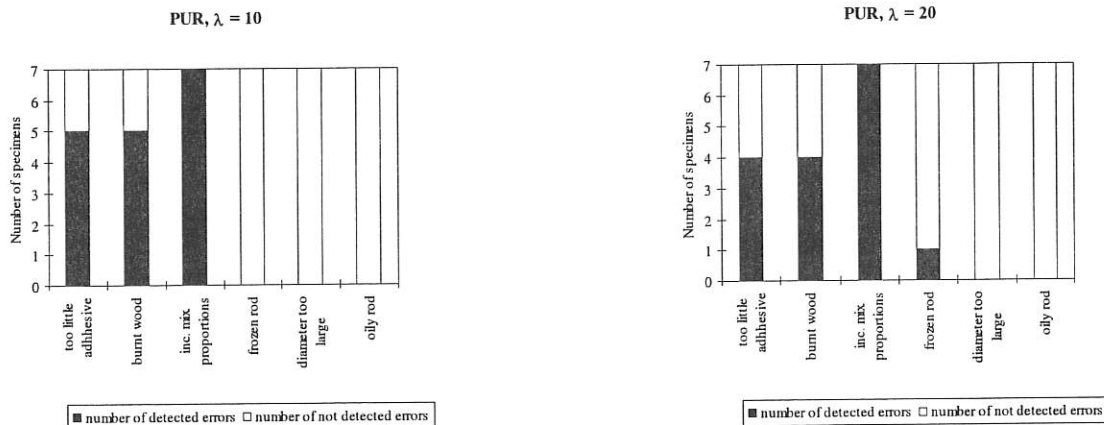*Figure 3.7.8 Number of specimens, bonded with PUR, with defects found by proof-loading to 80%.*

3.7.3 Influence of density on the pull-out strength

The correlation between the density of the wood surrounding the glued-in rod and the pull-out strength was examined for the different groups of tested specimens. In some cases there was no correlation at all between density and pull-out strength, see as example Figure 3.7.9a. Relationships showing decreased pull-out loads for increased density are not rare within the studied material. However, for a few groups of specimens the correlation between density and pull-out strength was stronger, see for example Figure 3.7.9b. This strong correlation was caused by one low density value. In general, no relationship was found between wood density and pull-out strength of the glued-in rod.

a)   b)

Figure 3.7.9 Density of the wood surrounding the glued-in rod versus pull-out strength of the rod. a) Specimens bonded with EP, λ=10 and a glue line thickness of 2 mm.
b) Specimens bonded with PRF, λ=10 and a glue line thickness of 0.5 mm.

3.7.4 Conclusions

A newly developed test method, suitable for production control by proof-loading, was used for testing glued-in rod connections. The method is a one-sided pull-out test. Specimens bonded with epoxy, phenol-resorcinol and polyurethane were examined. Four different proof-load levels, 50%, 65%, 80% and 90% of pull-out loads obtained from destructive tests, were tested to try to find the maximum load that does not cause structural damage of the bond line. Specimens bonded with epoxy, on the average, reached higher pull-out loads after proof-loading until 80% and 90% than the specimens tested destructively. None of the tested groups of specimens displayed a decrease in pull-out strength after proof-loading to such high levels as 80% and 90%. The groups of specimens proof-loaded to 65% displayed a decreased pull-out strength. The reason for this behaviour was not explained in the present study. Error detection was possible for coarse errors by proof-loading up to the 80% level. The induced errors in the present study were sometimes extreme errors.

Generally, no relationship between density of the wood surrounding the glued-in rod and pull-out strength was found. This fact needs to be further investigated.

It was found out that the EP and the PUR are nearly of the same stiffness. They follow similar load-slip curves. Compared to EP and PUR, PRF reached lower loads at the same slip. Consequently, the PRF has a lower stiffness. The test type comparison resulted in: The adhesives, except the PRF, reached higher mean pull-out load values with the two-sided pull-out test method than with the one-sided pull-compression test type. Due to the non-uniform stress distribution along the glued-in length a twice as high slenderness did not generate twice as high pull-out load values. This fact was verified by the tests.

The variation of the glue line thickness led to increasing pull-out loads for larger glue line thicknesses in case of EP and PUR, whereas for the PRF, the load-bearing capacity decreased. As the destructive testing is done on specially produced test specimens, representative for a certain batch, the tests do not determine the reliability of the actual connection.

3.8 WP 8 - Draft design rules for Eurocode 5

The research work package WP 8 of the GIROD project is summarised in Part A of the project proposal description as follows: *"Based on the calculation model in WP 1, and considering results from WP 3, WP 4, WP 5 and WP 6, proposals for inclusion in Eurocode 5 will be elaborated."*

The objectives of this work package are closely linked with the other work packages as described in Table 3.8.1.

Table 3.8.1 Status of WP 8 within The GIROD Project

Links	WP 1, WP 3, WP 4, WP 5 and WP 6.
Output	A technical report on WP 8

To elaborate a proposal for design rules based on the calculation model from WP 1, taking into account the information gained under WP 3, WP 4, WP 5 and WP 6.

3.8.1 Methodology

Based on early project meetings and the calculation model in WP 1, an initial draft of the proposed Code rules was created, leaving blanks and indications where theoretical equation results were expected, and markers for information anticipated in later stages of the project. Eurocode formatting, protocols and terminology were used. An alpha-numerical indexing system was set up for progressive "Code Draft" versions, with all of the related information being stored electronically and backed up.

As stages of the project progressed, and as meetings took place, this maintained draft was updated, along with the accompanying recording documentation. Hence, and considering results from WP 3, WP 4, WP 5 and WP 6, final project proposals for inclusion in Eurocode 5 have been reached.

Partner 4 has conducted the work in co-operation with the other partners. The key tasks identified in the project plan and carried out under WP 8 are identified in Table 3.8.2. In line with the project schedule, WP 8 activities to date have involved participation in project meetings, completion of project tasks 1-4 and preparation of project progress reports TTLPR2 (Bainbridge and Mettem 1999c), TTLPR4 (Bainbridge and Mettem 1999d), TTLPR6 (Bainbridge and Mettem 2000c), TTLPR8 (Bainbridge and Mettem 2000d) and TTLPR10 (Bainbridge and Mettem 2001b). As the project progressed, it was necessary to expand these tasks to include more revisions of the draft design rules in the latter stages of the project, as described in the following text.

Table 3.8.2 WP 8 Project Plan.

Task	Description	Comment
1	Produce Initial Draft	Initial draft and development schedule included in TTPR2
2	Protocol For Circulation of Drafts	
3	1st Revision Of Draft	Included in TTPR4
4	2nd Revision Of Draft	Included in TTPR6
5	3rd Revision Of Draft	Included in TTPR8

Based on early project meetings and the calculation model in WP 1, an initial draft of the proposed Code rules was created, leaving blanks and indications where theoretical equation

results are expected, and markers for information anticipated in later stages of the project. Eurocode formatting, protocols and terminology have been used. An alpha-numerical indexing system has been set up for progressive "Code Draft" versions, with all of the related information being stored electronically and backed up.

As stages the project progressed, and as meetings took place, this maintained draft has been updated, along with the accompanying recording documentation. Hence, and considering results from WP 3, WP 4, WP 5 and WP 6, final project proposals, developed in the spirit of Eurocode 5 have been developed. The revisions of this draft and the location of its printed copy in the project deliverables is summarised in Table 3.8.3.

Table 3.8.3 Schedule of draft design code recommendation updates through GIROD.

Version	Date	Comment	Delivery
01	November 1998	Initial draft (17 Pages)	Annex C of TTLPR2
02	June 1999	Revised draft (24 Pages)	Annex A of TTLPR4
03	January 2000	2nd Revision (26 Pages)	Annex A of TTLPR6
04	October 2000	3rd Revision (22 Pages - reduced font)	Annex A of TTLPR8
05	February 2001	Revision following Month 32 Progress Reports from other WPs	Annex A of TTLPR10
06	April 2001	Revision following Project meeting, March 2001	As part of final project output package

In addition, it was identified at the 4th Project meeting that whilst the drafted document is an important output from this work, it is too lengthy to be considered for direct adaptation into the body of EC5. Therefore a shorter set of principles and application rules have been developed from the full set of design recommendations. The initial draft of these was included in project report TTLPR10, and discussed at the project meeting held in March 2001. Following discussions at this meeting, these have been revised to their current revised state. These revised concise set of rules is also included as part of the final project output package.

3.8.2 Results

The development of the design rules through WP 8 has been coupled with the development and progress of the other GIROD WPs, which have provided results and findings that have been included in the draft design rules. The inter-relation of WPs with WP 8 is illustrated in Figure 3.8.1.

An initial set of draft design rules was produced, as contained in Annex C of the first progress report (Bainbridge and Mettem 1999c). The format of the draft is compatible with that of the existing Eurocode 5: Part 1.1.

The draft drew principally from Annex A of Eurocode 5: Part 2 (DD ENV 1995-2), but the scope has been expanded to include sections relevant to the anticipated outputs of the other GIROD work programme items. Other pertinent existing codified information from EC5 has also been identified and cross-references have been incorporated in the draft.

Other existing design code clauses have also been identified with relevance to particular items under the scope of GIROD investigations, including EC5: Part 2: Annex B (DD ENV 1995-2)

(Fatigue – WP 6), Sections of EC5: Part 1.1 (DD ENV 1995-1-1) concerning adhesives (all WPs), EC1: Part1 (DD ENV 1991-1) (general basis for design) and the EUROCOMP Design Guide (Clarke J. L. 1996) (structural FRP composites as alternatives to steel rods).

The format of the initial draft, revised following the project meeting held in October 1998, was as presented in Table 3.8.4.
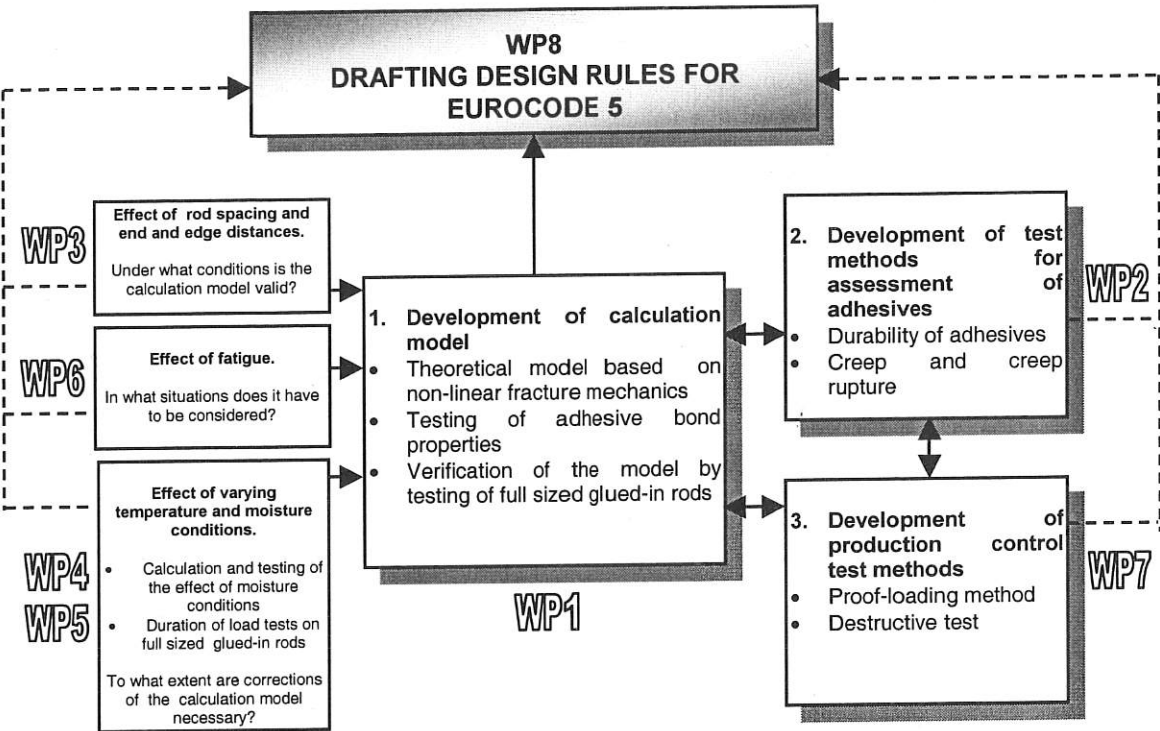

Figure 3.8.1 Development of WP 8 From Other WP Results.

Table 3.8.4 Format for initial draft design rules

Ref.	Item	Note
1.	INTRODUCTION	
1.1 **1.2**	SCOPE DEFINITIONS	• As draft develops, these may find suitable placement within the draft clause set , or in the main body of EC5
N.	GLUED IN RODS	
N.1	GENERAL	• A series of general principles has been drafted
N.2	MATERIALS	• Rod Materials • Adhesives • Material Combinations
N.3	MOISTURE EFFECTS	
N.4	DURATION OF LOAD EFFECTS	
N.5	FATIGUE	• (based upon existing EC5: Part2 Annex B)
N.6	AXIALLY LOADED RODS	• General • Ultimate Limit State (individual rod and groups) • Serviceability Limit States
N.7	LATERALLY LOADED RODS	• General • Ultimate Limit State (individual rod and groups) • Serviceability Limit States
N.8	COMBINED LATERALLY AND AXIALLY LOADED RODS	• Not Part of GIROD but implications of findings on this may require later consideration
N.9	TESTING	• Test Methods For Adhesives • Prototype Testing
N.10	EXECUTION	
N.11	PRODUCTION CONTROL	• Destructive Test Methods • Non-Destructive Test Methods

The draft has been revised in the light of findings and observations made in the GIROD programme, and in associated studies funded through UK national projects in which the authors are involved. Previous revisions have been included in WP 8 progress reports. This has been subject to further revision into its current form, 'GIROD:WP 8:V06 (2001)'. The scope of this revised and expanded document is illustrated in Figure 3.8.2.
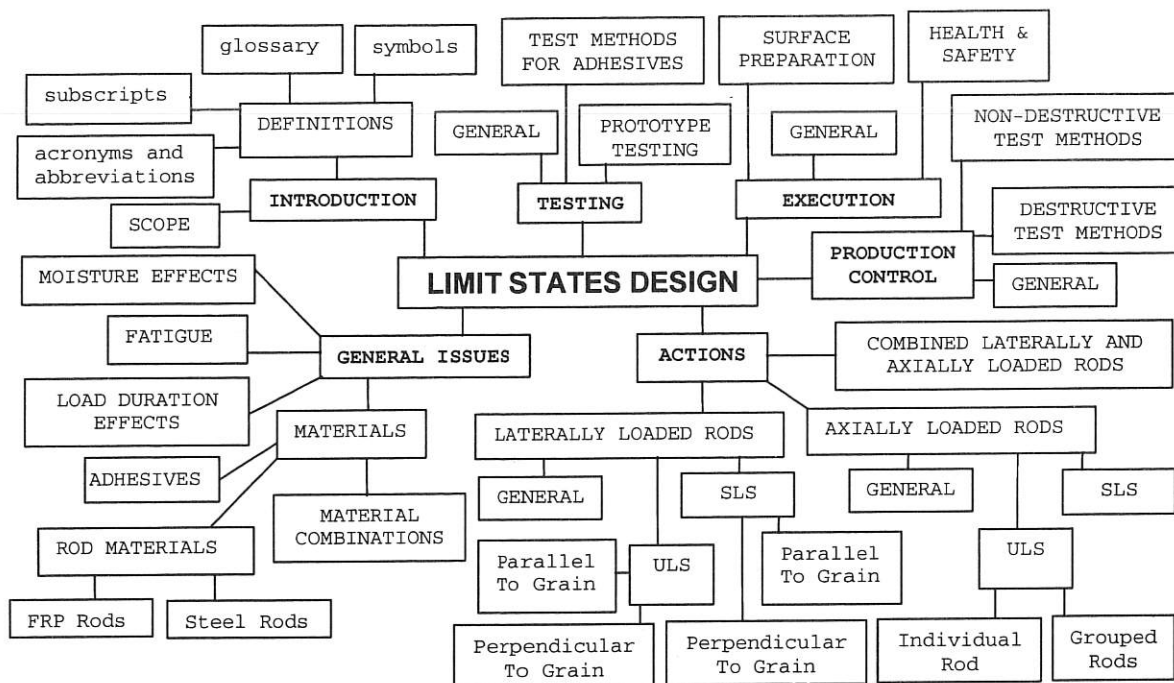
91

Figure 3.8.2 Overview of the design methodology structure developed through GIROD

At the 4th Project meeting, the draft design methodology was discussed and it was identified that although the methodology developed through the activities of WP 8 had lead to a useful summary document, containing almost all GIROD results. It is, however, only contracted that this WP should lead to a series of design rules in a form suitable to be considered for incorporation in Eurocode 5. In response to this, a concise set of expressions and application rules have been extracted.

3.8.3 Conclusions

WP 8 has led to the development of a guidance document style set of design rules drawn from the GIROD project and a condensed set of concise design rules more suited to consideration for incorporation in the body of EC5.

These have met the objective of elaborating a proposal for design rules based on the calculation model from WP 1, taking into account the information gained under WP 3, WP 4, WP 5 and WP 6.

3.9 WP 9 – Project coordination

Carl-Johan Johansson at SP has been the project coordinator. He has been assisted by Martin Kemmsies, SP from the start of the project to July 1999 and by Charlotte Bengtsson, SP from December 1999 to the end of the project.

Meetings have been held at the following dates and locations:

February 5-6, 1998 (kick-off meeting)	Stuttgart, Germany
October 22-23, 1998	Karlsruhe, Germany
July 1-2, 1999	High Wycombe, UK
June 27-28, 2000	Lund, Sweden
March 21-22, 2001	Borås, Sweden
May 21, 2001	Stuttgart, Germany

4. Technology implementation plan

The project results are aimed at being implemented in the standardization work of the following CEN committees:

CEN/TC250/SC5 – Eurocode 5. Design of Timber Structures

The final project report and detailed results from WP 1, WP 3, WP 4, WP 5 and WP 8 will be used by this committee to draft design rules for glued-in rod connections. This work has already started. The GIROD project coordinator has exchanged information with CEN/TC250/SC5 during the early spring of 2002, which is presently drafting rules for design of timber bridges. The final report of the GIROD project will be sent to the convenor of CEN/TC250/SC5.

CEN/TC193/SC1 – Wood adhesives

The final project report and the detailed results from WP 2 will be used by this committee to draft test standards for adhesives to be used in connection with glued-in rods. This work has already started in CEN/TC193/SC1 and a working group – *WG6 Adhesive for glued-in rods* - has been formed to deal with the matter. Two meetings have been held in the working group. The final report of the GIROD project will be sent to the convenor of CEN/TC193/SC1/WG6.

CEN/TC124 – Timber Structures

The final report and the detailed results from WP 7 will be used by this committee to draft a product/production standard on glued-in rods The final report of the GIROD project will be sent to the convenor of CEN/TC124.

5. Conclusions

5.1 General

The objective of the project has been to provide the information necessary to prepare European standards for glued-in rods. The steps involved in reaching this objective have been:

1. Theoretical and experimental work leading to a calculation model for axially loaded glued-in rods based on the adhesive bond properties as well as the wood and rod material properties. This must take into account the effect of varying climatic and loading conditions as well as fatigue. This step will give information required by CEN/TC250/SC5 in the preparation of Eurocode 5 - Design of Timber Structures.
2. Development of test methods for the evaluation of adhesives for glued-in rods with respect to strength, durability, creep and creep rupture behaviour under different climatic conditions. This will support the work of CEN/TC193/SC1.
3. Derivation of test methods for the production control of structural glued-in rod connections. This will support the work of CEN/TC124.

5.2 Step 1 – Design rules

As far as step 1 is concerned the following conclusions can be drawn:

5.2.1 Calculation model

A calculation model based on a combination of Volkersen theory and fracture mechanics gives good prediction of the pullout strength for adhesives that bond to the rod such as PUR and EP. The pullout strength is controlled by two material property parameters that can be easily determined in full-scale pull-compression tests. The information provided should be sufficient to draft design rules by CEN/TC250/SC5.

The parameters in a design formula can be derived in many different ways. One option is to use results from full-scale pull-compression tests on glued-in rods for each adhesive type. Another option is to use the EP and PUR test data from the GIROD project and base the design expression on that.
Comment: The latter option was chosen when design rules were proposed to CEN/TC250/SC5 in early 2002.

5.2.2 Effect of distance between rods and between rods and timber edgee on the axial strength

The effect of rod spacing and edge distances has been clearly demonstrated and proposals to be used in design have been made.

5.2.3 Effect of moisture conditions

The results of the experimental study revealed that the moisture content at test time and the moisture history and hereby the conditioning time affect the bond strength of mechanically unloaded specimens with glued-in steel rods. The effects are qualitatively and quantitatively different for different adhesive types. The influences of moisture and time (in terms of moisture history) are in the same order of magnitude for different specimen configurations comprising rod dimensions and angle between rod and grain. The investigated climates comprised the whole spectrum of moisture scenarios realistically perceivable for service class 1 and 2 conditions.

The effect of moisture will have to be considered in CEN/TC250/SC5 by introduction of correction factors or in CEN/TC193/SC1 by requirements on the adhesives.

5.2.4 Duration of load (DOL) effects

This issue appears to be the most difficult one to handle in preparation of design rules for glued-in rods. The results of the performed DOL tests may be summarized in a comprehensive manner as following:

- The most important influence on the DOL effect is the adhesive type or class.
- The influence of the angle between rod and grain direction as well as of the rod dimensions (diameter and length) was not significant, irrespective of the specific adhesive.
- The DOL investigations on 3 different types of adhesives (an epoxy (EP), a 2component polyurethane (PUR) and a special softening type phenolic resorcinol (PRFs)) in different climates revealed that different adhesive classes, differentiated by different moisture susceptibility (modification factor k_{mc}) and temperature susceptibility (temperature modification factor k_T and glas transition temperature T_g), show different life times under sustained loads.
- The investigated PRFs and PUR adhesive types showed rather similar behaviour concerning the DOL behaviour as related to moisture aspects and following are termed „moisture susceptible adhesives", denoted by a significant ramp load moisture modification factor (here: $k_{mc} = 0.85$).
- The investigated epoxy, as probably most epoxies, revealed almost indifference vs. moisture in short- and long-term loading, so can be termed a „moisture insusceptible adhesive".
- Despite of the completely different behaviour of the PUR and EP vs. moisture, and despite of very different short-term temperature modification factors k_T, both adhesive types revealed very low glass transition temperature ranges; both adhesive types are termed „low T_g adhesives". Note: „high" and „low" short-term temperature modification factors may be associated with comparably „low" T_g values, i.e. k_T and T_g values in general show very little or no correlation.

The following alternatives are considered to be realistic ways of handling the duration of load aspects in the design of glued in rods:

Alternative 1

The basis here is the assumption that no additional k_{mod} values beyond those specified today in EC 5 for solid wood and glulam should be introduced in the design analysis for sake of simplicity. The DOL behaviour is controlled by creep rupture tests on the adhesive as described under Step 2 below. This alternative was the basis when the GIROD-project was planned. It could be argued that the results from WP 2 and WP 5 do not fully support that the DOL behaviour can be controlled by a simple creep rupture test on small specimens. On the other hand, this test (WP 2) appears to be very capable of separating adhesives with respect to the creep rupture behaviour.

Alternative 2

The basis here is the same as in Alternative 1, namely the assumption that no additional k_{mod} values beyond those specified today in EC 5 for solid wood and glulam should be introduced in the design analysis for sake of simplicity. In this case, the difference between the effective

k_{mod} values of the specific adhesive (group) and the settled / prescribed k_{mod} values in EC 5 could be accounted for in a fictive reduction of the short-term bond shear strength of the specific adhesive.

Alternative 3

Appropriate testing of the DOL behaviour of the respective adhesive based on sufficient ramp load / temperature testing for determination of the modification factors k_{mc}, k_T and of the glass transition temperature T_g. Use of the adhesive specific bond properties (short-term bond strength **and** k_{mod} values) on the basis of a building certificate (eventually ETA) in the analysis.

5.2.5 Fatigue

It has been demonstrated that fatigue performance is a significant factor in the performance of bonded-in rods and recommendations are made as to how further work, beyond the scope of GIROD, could improve understanding and design treatment of the fatigue behaviour of these types of connection. In relation to the stated objectives of the study, the experimental study has indicated that the fatigue behaviour of glued-in rods may limit their use in certain applications.

5.3 Step 2 – Tests methods for adhesives

The following can be concluded:

5.3.1 Durability of adhesives

A test method for the durability of the adhesive for glued-in rods based on an existing one for ordinary wood-to-wood adhesives has been developed. The method is capable of ranking adhesives in an efficient way.

5.3.2 Creep and creep rupture

A test method for creep-rupture testing of small glued-in rod specimens has been developed. The method is based on ASTM D 4680. The results obtained with the method are linked to the duration of load behaviour of the glued-in rods. Using the creep rupture testing in the assessment of adhesives would correspond to Alternative 1 under *Duration of load effects* in the previous section.

The results from the work carried out here should be sufficient to draft standards on a test method and on requirements by CEN/TC193/SC1.

5.4 Step 3 – Test methods for production control

The following can be concluded:

o   A method for production control of glued-in rods has been developed and it has been demonstrated that the method is capable of detecting a number of gluing errors that may occur.

o   The results from the work carried out here should be sufficient to draft standards on a test method and on requirements by CEN/TC124.

6. References

Aicher, S. 2001a: WP 1.3 – Tests for calibration and verification, Technical Report for work package 1.3. Otto-Graf-Institute, University of Stuttgart.

Aicher, S. 2001b: Characteristic axial resistance of threaded rods glued-in spruce dependant on adhesive type, a complementary database for the GIROD project. Research Report, Otto-Graf-Institute, University of Stuttgart.

Aicher, S. 2001c: WP 5 – Duration of load tests on full-sized glued-in rod specimen; Technical Report for work package 5, workpart by FMPA. Otto-Graf-Institute, University of Stuttgart.

Aicher, S. 2001d: WP 4 – Effect of moisture conditions, Technical Report for work package 4. Otto-Graf-Institute, University of Stuttgart.

Aicher, S. 2002: WP 5 – Duration of load tests on full-sized glued-in rod specimen; Technical Report (consolidated) for work package 5. Otto-Graf-Institute, University of Stuttgart.

Aicher, S., Dill-Langer, G. 2001: Influence of moisture, temperature and load duration on performance of glued-in rods. Joints in timber stryctures, RILEM Proceedings PRO 22, pp. 383-392, Cachan Cedex.

Aicher, S., Gustafsson, P.J. and Wolf, M. 1999: Load-displacement and bond strength of glued-in rods in timber influenced by adhesive, wood density, rod slenderness and diameter. In Proceedings of the 1st RILEM symposium on Timber Engineering, Stockholm, Sweden, pp 369-378.

Ansell, M.P. (1995): Fatigue Design for Timber & Wood Based Materials. STEP Lecture E22, Timber Engineering STEP 2, STEP, EUROFORTECH, Centrum Hout, Almere.

ASTM D 4680: Standard test method for creep and time to failure of adhesives in static shear by compression loading (wood-to-wood).

ASTM D 4065

Bainbridge, R.J., Mettem, C.J. 1999a: GIROD - Glued-in Rods For Timber Structures, WP 6 - Effect Of Fatigue, 12th Month Progress Report. Report Number GIROD/TTL PR1, TRADA Technology, High Wycombe, UK.

Bainbridge, R.J., Mettem, C.J. 1999b: GIROD - Glued-in Rods For Timber Structures, WP 6 - Effect Of Fatigue, Mid-Term Progress Report. Report Number GIROD/TTL PR3, TRADA Technology, High Wycombe, UK.

Bainbridge, R.J., Mettem, C.J. 1999c: GIROD - Glued-in Rods For Timber Structures, WP 8 -Draft Design Rules For Eurocode 5, 12th Month Progress Report. Report Number GIROD/TTL PR2, TRADA Technology, High Wycombe, UK.

Bainbridge, R.J., Mettem, C.J. 1999d: GIROD - Glued-in Rods For Timber Structures, WP 8 -Draft Design Rules For Eurocode 5, Mid Term Progress Report. Report Number GIROD/TTL PR4, TRADA Technology, High Wycombe, UK.

Bainbridge, R.J., Mettem, C.J. 2000a.: GIROD - Glued-in Rods For Timber Structures, WP 6 - Effect Of Fatigue, 24th Month Progress Report. Report Number GIROD/TTL PR5, TRADA Technology, High Wycombe, UK.

Bainbridge, R.J., Mettem, C.J. 2000b: GIROD - Glued-in Rods For Timber Structures, WP 6 - Effect Of Fatigue, 32nd Month Progress Report. Report Number GIROD/TTL PR7, TRADA Technology, High Wycombe, UK.

Bainbridge, R.J., Mettem, C.J. 2000c: GIROD - Glued-in Rods For Timber Structures, WP 8 -Draft Design Rules For Eurocode 5, 24th Month Progress Report. Report Number GIROD/TTL PR6, TRADA Technology, High Wycombe, UK.

Bainbridge, R.J., Mettem, C.J. 2000d: GIROD - Glued-in Rods For Timber Structures, WP 8 -Draft Design Rules For Eurocode 5, 32nd Month Progress Report. Report Number GIROD/TTL PR8, TRADA Technology, High Wycombe, UK.

Bainbridge, R.J., Mettem, C.J. 2001a: GIROD - Glued-in Rods For Timber Structures, WP 6 - Effect Of Fatigue, Final Progress Report. Report Number GIROD/TTL PR9, TRADA Technology, High Wycombe, UK.

Bainbridge, R.J., Mettem, C.J. 2001b: GIROD - Glued-in Rods For Timber Structures, WP 8 -Draft Design Rules For Eurocode 5, Final Progress Report. Report Number GIROD/TTL PR10, TRADA Technology, High Wycombe, UK.

Bainbridge, R.J., Mettem, C.J. 2001c: WP 5 – Duration of load tests on full-sized glued-in rod specimen, Final Progress Report of work by TTL.

Bainbridge, R.J., Mettem, C.J., Ansell, M.P. 1999: An Overview Of Research To Assess Fatigue Performance Of Bonded-In Rods For Timber Structures Using Three Adhesive Types. Cost Action E8 Workshop - Damage In Wood - Mechanical Performance Of Wood And Wood Products, Bordeaux, 27-28 May.

Bainbridge, R.J., Harvey, K., Mettem, C.J., Ansell, M.P. 2000: Fatigue Performance of Bonded-in Rods in Glulam, Using Three Adhesive Types. CIB-W18/33-7-12, Proceedings of International Council For Building Research Studies And Documentation, Working Commission W18 - Timber Structures, Meeting Thirty-Three, Delft, Netherlands, August.

Bengtsson C. 2001: Technical report, Glued-in rods for timber structures, WP 2 - Test methods for adhesives, Report Nr SP-TR-2, SP Swedish National Testing and Research Institute, Borås, Sweden.

Blaß, H.J., Laskewitz, B. 1999: Effect of Spacing and Edge Distance on the Axial Strength of Glued-In Rods. CIB-W18A, proceedings, Graz, Austria.

Blaß, H.J., Laskewitz, B. 2001: Effect of distance between rods and between rods and timber edge on the axial strength. Technical report for WP 3. Versuchsanstalt für Stahl, Holz und Steine, Universität Fridericiana, Karlsruhe, Germany.

Bonfield, P.W., Ansell, M.P., Dinwoodie, J.M. 1994: Fatigue Testing of Wood : A Detailed Guide For The Development of Life-Prediction Formulae From Fatigue Data. Proceedings of IUFRO S5.02 - Timber Engineering, Sydney, Australia.

Clarke, J.L. (Editor). 1996: Structural Design of Polymer Composites - EUROCOMP Design Code and Handbook. E & FN Spon, London.

Draft of DIN 1052, May, 2000

DD ENV 1995-1-1 1994: Eurocode 5 Design of Timber Structures - Part 1.1: General Rules & Rules for Buildings.

DD ENV 1995-2 1997: Eurocode 5 Design of Timber Structures - Part 2: Bridges.

DD ENV 1991-1 1994: Eurocode 1 Basis of Design And Actions On Structures - Part 1: Basis Of Design.

DIN 53765-A-20

Ehlbeck, J., Görlacher, R., Werner, H. 1989: Determination of perpendicular-to-grain tensile stresses in joints with dowel-type fasteners; a draft proposal for design rules.CIB-W18A, proceedings, Berlin, GDR 1989

EN 338: Structural timber – Strength classes

Gustafsson, P. J. 1987: Analysis of Volkersen-joints in terms of non-linear fracture mechanics. In Mechanical Behaviour of Adhesive Joints, PLURALIS 1987, pp. 323-328.

Gustafsson, P. J., Serrano, E. 2002: Glued-in Rods: Local Bond Line Fracture Properties and a Strength Design Equation. Proc. of The International Symposium on "Wood Based Materials - Wood Composites and Chemistry", COST E13 and Wood KPlus, September 2002, Vienna, Austria.

Hausmann, K. Reil, N. 1999: Test methods for production control of glued-in rods for timber structures. Master´s thesis, Technical University of Karlsruhe, Fakultät für Bauingenieurwesen, 208 pages.

Hingwe, A.K. 1982: Quality Control Source Book - Threaded Steel Fasteners, American Society for Metals, Metals Park, OH, USA.

INSTA 142: Visual strength grading rules for timber.

Johansson, C.J. 1995: Glued-in Bolts. STEP Lecture C14, STEP 1, Centrum Hout, Almere.

Johansson, C.J. 2000: GIROD – Glued in rods for timber structures. WP 7 – Test methods for production control. Technical Report Nr SP-TR-1, SP, Borås, Sweden.

Kemmsies, M. 1999: Comparison of pull-out strengths of 12 adhesives for glued-in rods for timber structures, Swedish National Testing and Research Institute, Building Technology, SP Report 1999:20, 26 pages.

Wernersson, H. 1994: Fracture characterization of wood adhesive joints. Report TVSM–1006, Lund University, Division of Structural Mechanics.

7. List of publications

7.1 Conference papers and journal articles

Aicher, S., Höfflin, L., Wolf, M. 1998: Influence of specimen geometry on stress distributions in pull-out tests of glued-in steel rods in wood. Otto-Graf-Journal, Vol. 9, pp. 205 - 217, University of Stuttgart.

Aicher, S., Gustafsson, P.J., Wolf, M. 1999: Load-displacement and bond strength of glued-in rods in timber influenced by adhesive, wood density, rod slenderness and diameter. In Proc. of the 1st RILEM symposium on Timber Engineering, September, Stockholm, Sweden, pp. 369-378

Bainbridge, R.J., Mettem, C.J. 1999: Bonded-In Rods For Timber Structures - Towards A European Basis For Structural Design. Adhesives In Timber Systems, Society Of Chemical Industry, Belgrave Square, London, 13th May 1999.

Bainbridge, R.J., Mettem, C.J. 1999: Bonded-In Rods For Timber Structures -A Versatile Method For Achievement Of Structural Connections. The Structural Engineer, 77, No.15, 1999, IStructE, London.

Bainbridge, R.J., Mettem, C.J. 2000: Bonded-In Rod Connections For Timber Structures – Test Observations With Impact Upon Development of Design Practice. 38th Annual Conference on Adhesion and Adhesives. Joining Technology Research Centre, Oxford Brookes University.

Bainbridge, R.J., Mettem, C.J., Ansell, M.P. 1999: An Overview Of Research To Assess Fatigue Performance Of Bonded-In Rods For Timber Structures Using Three Adhesive Types. Cost Action E8 Workshop - Damage In Wood - Mechanical Performance Of Wood And Wood Products, Bordeaux, 27-28/5/99.

Bainbridge, R.J., Harvey, K., Mettem, C.J., Ansell, M.P. 2000: Fatigue Performance of Bonded-in Rods in Glulam, Using Three Adhesive Types. CIB-W18/33-7-12, Proceedings of International Council For Building Research Studies And Documentation, Working Commission W18 - Timber Structures, Meeting Thirty-Three, Delft, Netherlands, August 2000.

Bainbridge, R.J., Harvey, K., Mettem, C.J., Ansell, M.P. 2001: Fatigue Performance Of Structural Timber Connections. Proceedings of the IABSE Conference - Innovative Wooden Structures and Bridges, Lahti, Finland, 29-31 August.

Bainbridge, R.J., Mettem, C.J., Harvey, K., Ansell, M.P. 2000: Bonded-In Rods For Timber Structures - Development of Design Methods and Test Observations. International Journal of Adhesion and Adhesives, Vol. 20, Elsevier Science Limited, Oxford, UK. (Publication Pending)

Bengtsson, C., Johansson, C-J. 2000 Test methods for glued-in rods for timber structures, paper 33-7-13 in proceedings of CIB-W18, 28-30/8 2000, Delft, Netherlands.

Bengtsson, C., Kemmsies, M., Johansson, C-J. 2000 Production Control Methods for Glued-in Rods for Timber Structures, Proceedings (published on a CD) of World Conference on Timber Engineering, 31/7-3/8 2000, Whistler, Canada.

Bengtsson, C., Johansson, C-J. 2001: GIROD – Glued-in rods for timber structures, to be published in proceedings of CIB-W18, Venice, Italy

Bengtsson, C., Johansson, C-J. 2001: Glued-in Rods – Development of Test Methods for Adhesives, Proceedings of the RILEM Symposium on Joints in Timber, Stuttgart, September 12-14, pp. 393-402.

Blass, H. J. Laskewitz, B. 1999: Effect of spacing and edge distance on the axial strength of glued-in rods. In: Proceedings. CIB-W18 Meeting, Graz, Austria, Paper 32-7-12.

Blass, H. J. Laskewitz, B. 2001: Load-carrying capacity of axially loaded rods glued-in perpendicular to the grain, Proceedings of the RILEM Symposium on Joints in Timber, Stuttgart, September 12-14, pp. 363-372.

Gustafsson, P.J., Serrano, E. 2000: Predicting the Pull-Out Strength of Glued-in Rods, In Proc. of 6th World Conference on Timber Engineering, Whistler, B.C., Canada, August, pp. 7.4.4.1 -7.4.4.8.

Gustafsson, P.J., Serrano, E. 2002: Glued-in Rods: Local Bond Line Fracture Properties and a Strength Design Equation. Proc. of The International Symposium on "Wood Based Materials - Wood Composites and Chemistry", COST E13 and Wood KPlus, September, Vienna, Austria.

Gustafsson, P.J., Serrano, E., Aicher, S., Johansson, C-J. 2001: A Strength Design Equation for Glued-in Rods, Proceedings of the RILEM Symposium on Joints in Timber, Stuttgart, September 12-14, pp. 323-332.

Harvey, K., Ansell, M.P., Mettem, C.J., Bainbridge, R.J. 2000: The Strength of Moment Resisting Joints in LVL Connected With Bonded-in GRP Rods. CIB-W18/33-7-11, Proceedings of International Council For Building Research Studies And Documentation, Working Commission W18 - Timber Structures, Meeting Thirty-Three, Delft, Netherlands, August 2000.

Hausmann, K. Reil, N. 1999: Test methods for production control of glued-in rods for timber structures. Master's thesis, Technical University of Karlsruhe, Fakultät für Bauingenieurwesen, 208 pages.

Johansson, C-J., Bengtsson, C. 2002: Glued-in rods for timber structures – presentation of results from a European project, proceedings of International Symposium on Wood Based materials, final conference of COST E13, Vienna Austria, September 19-20.

Mettem, C.J., Bainbridge, R.J., Ansell, M.P., Harvey, K., Hutchinson, A., Broughton, J. 1999: Evaluation of Material Combinations for Bonded In Rods to Achieve Improved Timber Connections. CIB-W18/32-7-13, Proceedings of International Council For Building Research Studies And Documentation, Working Commission W18 - Timber Structures, Meeting Thirty-Two, Graz, Austria, August 1999.

Mettem, C.J., Bainbridge, R.J., Harvey, K., Ansell, M.P., Broughton, J.G., Hutchinson, A.R. 2000: Improved Timber Connections - Evaluation of Material Combinations For Bonded In Rods. Paper TEP1-BRods, Timber Engineering Papers, Vol.1, TRADA Technology, High Wycombe, UK.

Serrano, E. 2000: Adhesive Joints in Timber Engineering. Modelling and Testing of Fracture Properties." Doctoral Thesis. Report TVSM-1012. Lund University, Department of Mechanics and Materials, Structural Mechanics. Lund, Sweden.

Serrano, E. 2001: Glued-in Rods for Timber Structures – A 3D Model and Finite Element Parameter Studies". International Journal of Adhesion and Adhesives. 21(2) pp.115-127.

Serrano, E. 2001: Glued-in Rods for Timber Structures – An Experimental Study of Softening Behaviour". Materials and Structures, 34 (238) pp.228 – 234. RILEM Publications.

7.2 Technical reports

WP 1

"Theoretical work". GIROD - Glued-in Rods for Timber Structures. Technical report for work package 1.1." ULUND-TR-1. Lund University, Division of Structural Mechanics. Lund, Sweden, 1999.

"Bond Line Tests. GIROD - Glued-in Rods for Timber Structures. Technical report for work package 1.2." ULUND-TR-2. Lund University, Division of Structural Mechanics. Lund, Sweden, 2000.

"Development of a Calculation model. GIROD - Glued-in Rods for Timber Structures. Final report for work package 1." Lund University, Division of Structural Mechanics, Lund Sweden, 2001.

Gustafsson, P.J., Serrano, E. 2001: Glued-in Rods for Timber Structures – Development of a Calculation Model. Report TVSM-3056, Div. of Structural Mechanics, Lund University, Sweden.

Aicher,S. 2001: WP 1.3 – Tests for calibration and verification, Technical Report for work package 1.3. Otto-Graf-Institute, University of Stuttgart.

WP 2

Bengtsson C. 2001: Technical report, Glued-in rods for timber structures, WP 2 - Test methods for adhesives, Report Nr SP-TR-2, SP Swedish National Testing and Research Institute, Borås, Sweden. (Includes the Technical report for WP 2.1)

WP 3

Blaß, H.J., Laskewitz, B. 2001: Effect of distance between rods and between rods and timber edge on the axial strength. Technical report for WP 3. Versuchsanstalt für Stahl, Holz und Steine, Universität Fridericiana, Karlsruhe, Germany.

WP 4

Aicher,S. 2001: WP 4 – Effect of moisture conditions, Technical Report for work package 4. Otto-Graf-Institute, University of Stuttgart.

WP 5

Bainbridge, R.J., Mettem, C.J. 2001: WP 5 – Duration of load tests on full-sized glued-in rod specimen, Final Progress Report of work by TTL.

Aicher,S. 2001: WP 5 – Duration of load tests on full-sized glued-in rod specimen; Technical Report for work package 5, workpart by FMPA. Otto-Graf-Institute, University of Stuttgart.

Aicher,S. 2002: WP 5 – Duration of load tests on full-sized glued-in rod specimen; Technical Report (consolidated) for work package 5. Otto-Graf-Institute, University of Stuttgart.

WP 6

Bainbridge, R.J., Mettem, C.J. 2001: GIROD - Glued-in Rods For Timber Structures, WP 6 - Effect Of Fatigue, Final Progress Report. Report Number GIROD/TTL PR9, TRADA Technology, High Wycombe, UK.

WP 7

Johansson, C.J. 2000: GIROD – Glued in rods for timber structures. WP 7 – Test methods for production control. Technical Report Nr SP-TR-1, SP, Borås, Sweden. (Includes Technical Reports for WP 7.1 and WP 7.2.)

WP 8

Bainbridge, R.J., Mettem, C.J. 2001: GIROD - Glued-in Rods For Timber Structures, WP 8 -Draft Design Rules For Eurocode 5, Final Progress Report. Report Number GIROD/TTL PR10, TRADA Technology, High Wycombe, UK.

8. Details of the partners

1) Institutes and universities – Contractors

Institute	Contact persons	E-mail	Telephone	Fax
1) **SP - BTt** Box 857 S-50115 Borås SWEDEN	Carl-Johan Johansson Charlotte Bengtsson	carl-johan.johansson@sp.se charlotte.bengtsson@sp.se	+46-33-165117 (direct) +46-33-165491 (direct) Exchange: +46-33-165 000	+46-33-134516
2) ULUND Lund Tek. Högskola Avd. Byggnadsmekanik Box 118 S-221 00 Lund SWEDEN	Per-Johan Gustafsson	bmpjg@byggmek.lth.se	+46-46-222 4922	+46-46-2224420
3) **FMPA** Referat 14 - Abt. Holz Pfaffenwaldring 4 D-70569 Stuttgart GERMANY	Simon Aicher	simon.aicher@po.uni-stuttgart.de	+49-711-685 2287 (direct) Exchange: +49-711-685-1	+49-711-6856829
4) **TTL** TRADA Stocking Lane Hughenden Valley High Wycombe Bucks HP14 4ND GREAT BRITAIN	Christopher Mettem Vic Kearley Rob Bainbridge	cjmettem@ttlchiltern.co.uk vckearley@ttlchiltern.co.uk rjbainbridge@ttlchiltern.co.uk	Exchange: +44-1494-563 091	+44-1494-565487
5) **UKLIB** Univ. Karlsruhe (TH) Lehrstuhl f. Ingenieurholzbau & Baukonstruktionen D-76126 Karlsruhe GERMANY	Hans Blaß Rainer Görlacher Bernd Laskewitz	Hans.Blass@bau-verm.uni-karlsruhe.de Rainer.Gorlacher@bau-verm.uni-karlsruhe.de Bernd.Laskewitz@bau-verm.uni-karlsruhe.de	+49-721-608 2211 (direct) +49-721-608 3646 (direct) Exchange: +49-721-608-2710	+49-721-698116

2) Industry - Associated Contractors

Company	Contact persons	E-mail	Telephone	Fax
6) **MOELVEN** Moelven Töreboda Limträ AB Box 49 545 21 TÖREBODA	Lennart Axelsson	-	+46-506-48100	+46-506-16263
7) **CASCO** Casco Products AB Box 11538 100 61 STOCKHOLM	Niclas Wallin Sven-Erik Andersson	niclas.wallin@nacka.casco.se	+46-8-743 4373 +46-8-743 4196	+46-8-643 1607
8) **HOLZLEIMBAU** Studiengemeinschaft Holzleimbau e.V. Füllenbachstraße 6 40474 Düsseldorf GERMANY	Holger Conrad Herr Wiegand	argeholz@argeholz.de	+49-211-478 180	+49-211-452314
9) **GLTA** Glued Laminated Timber Association - Secretariat Chiltern House, Stocking Lane Hughenden Valley High Wycombe Bucks HP14 4ND GREAT BRITAIN	Frank Hall	pmwpresland@ttlchiltern.co.uk	+44-1494-565 180	+44-1494-565180
10) **KLEIBERIT** Klebchemie M.G. Becker GmbH Rudolf-Diesel Straße 34 76356 Weingarten GERMANY	Karin Wanzl-Dacho	-	+49-7244-62300	+49-7244-700350
11) **WEVO** Chemie GmbH Mergenthaler Straße 13 73760 Ostfildern GERMANY	Gustav Neidlinger Herr Speil	-	+49-711-167 6113 +49-711-16761-0 (exchange)	+49-711-4569169